# Optimization of sensitivity to disease-associated cortical metabolic abnormality by evidence-based quantification of in vivo $^{1}$H MRS data from 3 T and 7 T

Kelley M. Swanberg, M.Sc.[1]
Advisor: Professor Christoph Juchem, Ph.D.[1,2]

[1]Biomedical Engineering, Columbia University School of Engineering and Applied Science, New York, NY, USA
[2]Radiology, Columbia University Vagelos College of Physicians and Surgeons, New York, NY, USA

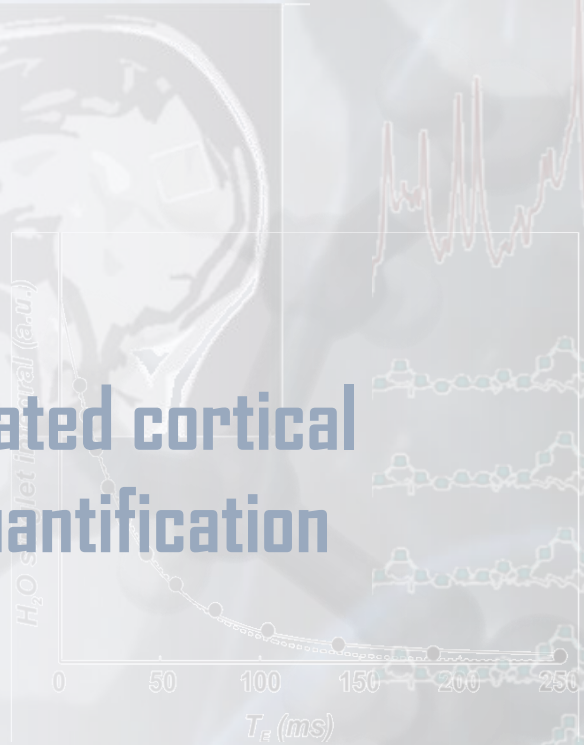



*Doctoral Dissertation Defense*
*3 February 2022*

COLUMBIA | ENGINEERING
The Fu Foundation School of Engineering and Applied Science

## The Big Picture:

$^1$H MRS is a potential but currently untapped source of clinical diagnostic biomarkers.

Chapter I

## Spectral Quantification:

What are the effects of spectral quality and baseline on the precision and accuracy of relative metabolite concentrations drawn from $^1$H MRS data, and how do we minimize them?

Chapter II

## Absolute Quantification:

Can disease-related differences in metabolite $T_2$ introduce systematic errors to the derivation of absolute from relative metabolite concentrations, and how do we minimize them?

Chapter III

## Statistical Analysis:

Can single- or multivariate analysis of metabolite concentrations derived from optimized quantification of $^1$H MRS data alone classify disease states (case application multiple sclerosis)?

Chapter IV

## Generalization:

Can a quantification and statistics pipeline optimized for classification of multiple sclerosis via $^1$H MRS-derived metabolite concentrations be generalized to identification of PTSD and MDD?

Chapter V

## Back to the Big Picture:

General conclusions and outlook

Chapter VI

# $^1$H MRS: Potential

## Chapter 1: Introduction

### *Noninvasive small-molecule metabolic profiling of tissue*

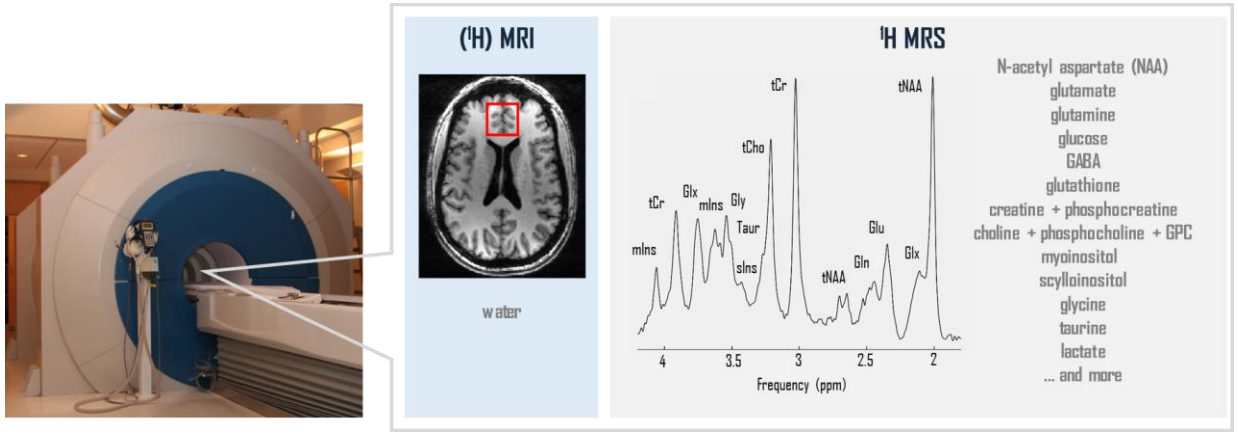


Swanberg, Prinsen, Bailey, Destefano, Pitt, Fulbright, and Juchem. *Proc Int Soc Magn Reson Med* 2017, 2970.

### *Magnet field strength ↑ ⟶ data quality ceiling ↑*

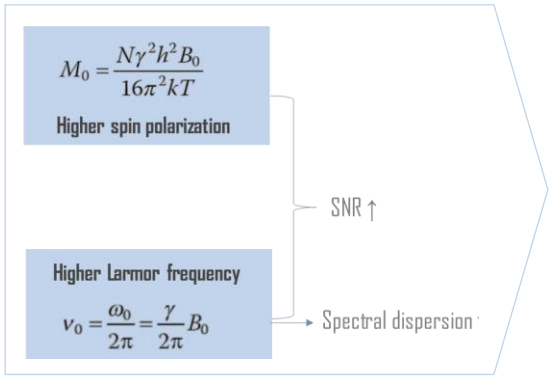


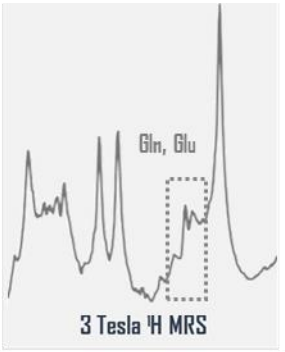


MR SCIENCE Laboratory (2021) *NMR Biomed* 34(6): e4486.

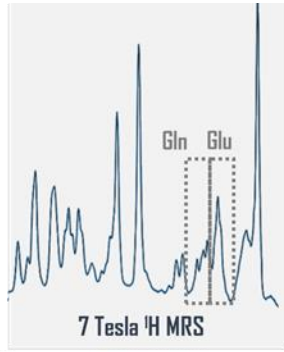


MR SCIENCE Laboratory (2016)

### *Multiple time points*

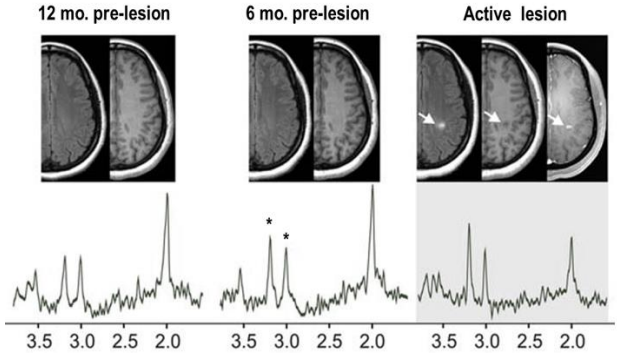


Kirov, Liu, Tal, Wu, Davitz, Babb, Rusinek, Herbert, and Gonen. *Human Brain Mapping* 2017; 38: 4047-63.

### *Multiple voxels*

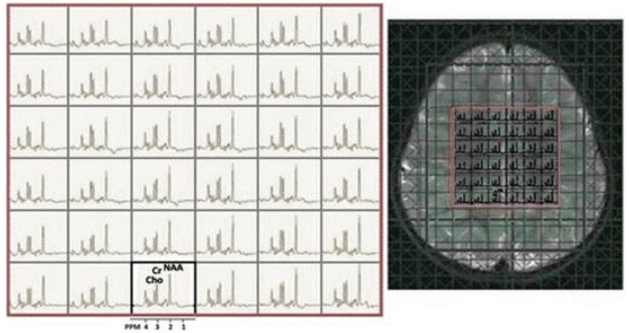


Zhu and Barker. *Methods Mol Biol* 2011; 711: 203-26.

### *Multiple metabolites*

**TABLE 4 |** F1-scores for all nine classification tasks (rows) after training LDA using only metabolic ratios.

| | NAA/Cho | NAA/Cre | Cho/Cre | All 3 metabolic ratios |
|---|---|---|---|---|
| HC vs. CIS | 35 | 33 | 43 | 36 |
| HC vs. RR | 6 | 16 | – | 14 |
| HC vs. PP | 47 | 45 | 19 | 49 |
| HC vs. RR+SP | 8 | 19 | – | 16 |
| HC vs. PP+SP | 21 | 26 | – | 28 |
| CIS vs. RR | 15 | – | – | 21 |
| CIS vs. RR+SP | 3 | – | – | 19 |
| RR vs. PP | 75 | 78 | 75 | 74 |
| RR vs. SP | 60 | 67 | 58 | 69 |

*Values above 75 are colored in light gray.*

Ion-Margineau, Kocevar, Stamile, Sima, Durand-Dubief, Huffel, and Sappey-Marinier. *Front Neurosci.* 2017; 11:398.

## Chapter 1: Introduction

UnitedHealthcare

January 2020

**policy update bulletin**

UnitedHealthcare West Medical Management Guideline Updates

| | | |
|---|---|---|
| Magnetic Resonance Spectroscopy (MRS) | Aug. 1, 2018 | • Updated non-coverage rationale:<br>o Replaced language indicating "[the listed service] is unproven *and* not medically necessary" with "[the listed service] is unproven *and/or* not medically necessary"<br>o Replaced reference to "patients" with "individuals"<br>• Updated supporting information to reflect the most current clinical evidence, FDA information, and references |

BlueCross BlueShield of North Carolina

An independent licensee of the Blue Cross and Blue Shield Association

Corporate Medical Policy

### Magnetic Resonance Spectroscopy

| | |
|---|---|
| **File Name:** | magnetic_resonance_spectroscopy |
| **Origination:** | 12/1997 |
| **Last CAP Review:** | 5/2020 |
| **Next CAP Review:** | 5/2021 |
| **Last Review:** | 5/2020 |

**Policy**

**Magnetic Resonance Spectroscopy is considered investigational. BCBSNC does not provide coverage for investigational services or procedures.**

aetna™

Aetna considers magnetic resonance spectroscopy (MRS) (also known as NMR spectroscopy) experimental and investigational for all other indications, including the following (not an all-inclusive list) because there is a lack of evidence of its efficacy in the medical literature.

- Adrenoleukodystrophy
- Breast cancer
- Cerebrovascular diseases/disorders/injuries
- Dementia and movement disorders (e.g., Alzheimer's disease, dementia with Lewy bodies, frontotemporal dementia, Huntington disease, motor neuron disease, normal-pressure hydrocephalus, Parkinson disease/Parkinsonian syndromes, vascular dementia)
- Dermatomyositis
- Detection and quantification of hepatic steatosis in living liver donors
- Detection of esophageal squamous cell carcinoma
- Differentiatiation of primary central nervous system lymphoma (PCNSL) from other focal brain lesions
- Epilepsy (including juvenile myoclonic epilepsy, and temporal lobe epilepsy)
- Evaluation of migraine pathophysiology and identification of biomarkers in migraine
- Head trauma
- Low back pain
- Lyme neuroborreliosis
- Metabolic and mitochondrial diseases
- Monitoring hepatocellular carcinoma and liver cirrhosis development
- Mucopolysaccharidosis
- Multiple sclerosis
- Polymyositis
- Prognosis of consciousness recovery in individuals with vegetative state
- Prostate cancer
- Psychiatric disorders (e.g., attention-deficit/hyperactivity disorder, autism spectrum disorders, bipolar disorder, depression, emotional dysregulation, obsessive-compulsive disorder, and schizophrenia)
- Radiation encephalopathy
- Sport-related concussion
- Substance use disorders
- Traumatic brain injury

**Policy**

Aetna considers magnetic resonance spectroscopy (MRS) (also known as NMR spectroscopy) medically necessary for the following indications:

- Assessing prognosis in hypoxic ischemic encephalopathy
- Distinguishing low grade from high grade gliomas
- Evaluate a brain lesion of indeterminate nature when the MRS findings will be used to determine whether biopsy/resection can be safely postponed
- Distinguishing recurrent brain tumor from radiation-induced tumor necrosis.

## Chapter 1: Introduction

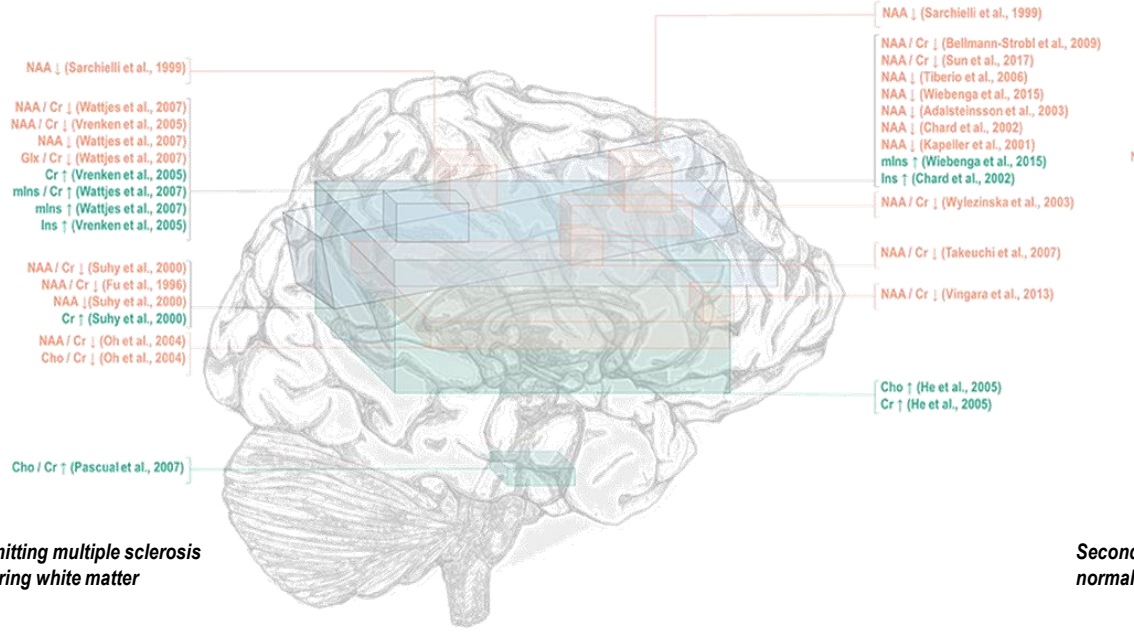


***Relapsing-remitting multiple sclerosis normal-appearing white matter***

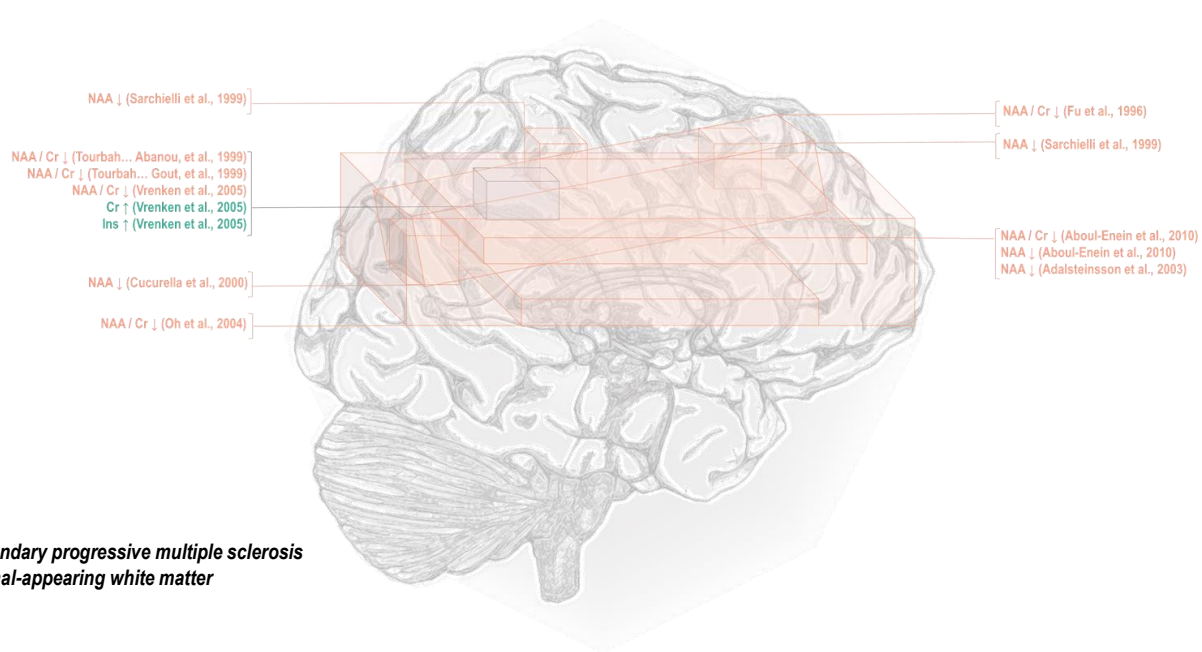


***Secondary progressive multiple sclerosis normal-appearing white matter***

Swanberg, Landheer, Pitt, and Juchem. *Frontiers in Neurology* 10 (2019): 1173.

Classification of multiple sclerosis by single $^{1}$H-MRS-visible metabolites lacks diagnostically useful sensitivity and especially specificity.

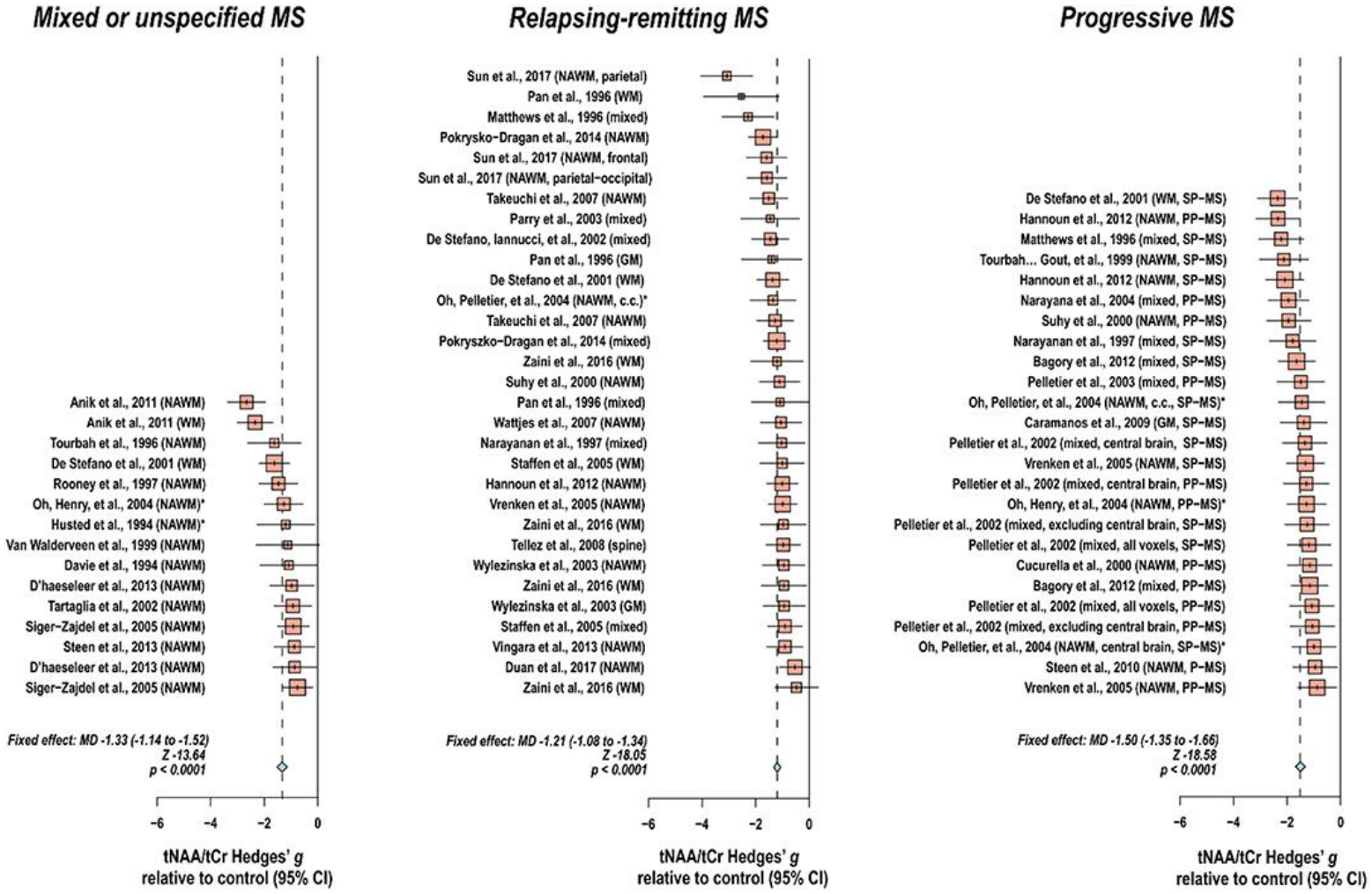


Swanberg, Landheer, Pitt and Juchem. *Frontiers in Neurology* 10 (2019): 1173.

Classification of multiple sclerosis by single $^{1}$H-MRS-visible metabolites lacks diagnostically useful sensitivity and especially specificity.

| References | MS | Tissue | Effect |
|---|---|---|---|
| Aboul-Enein et al. (80) | SP | NAWM | ↓ in MS |
| Aboul-Enein et al. (80) | R | NAWM | NS |
| Anik et al. (41) | M | WM | ↓ in MS |
| Anik et al. (41) | M | NAWM | ↓ in MS |
| Arnold et al. (47) | M | mixed | ↓ in MS |
| Bagory et al. (84) | SP | mixed | ↓ in MS |
| Bagory et al. (84) | PP | mixed | ↓ in MS |
| Bagory et al. (84) | R | mixed | NS |
| Bellmann-Strobl et al. (65) | R | NAWM | ↓ in MS |
| Brass et al. (43) | M | NAWM | ↓ in MS |
| Caramanos et al. (83) | SP | GM | ↓ in MS |
| Caramanos et al. (83) | R | GM | NS |
| Casanova et al. (204) | R | NAWM, peduncles | NS |
| Casanova et al. (204) | R | NAWM, pons | NS |
| Cucurella et al. (78) | SP | NAWM | NS |
| Cucurella et al. (78) | PP | NAWM | ↓ in MS |
| Davie et al. (24) | M | NAWM | ↓ in MS |
| De Stefano et al. (86) | RP | mixed | ↓ in MS* |
| De Stefano et al. (36) | M | WM | ↓ in MS |
| De Stefano et al. (36) | R | WM | ↓ in MS |
| De Stefano et al. (36) | SP | WM | ↓ in MS |
| De Stefano et al. (72) | R | mixed | ↓ in MS |
| De Stefano et al. (61) | R | WM | ↓ in MS |
| D'Haeseleer et al. (42) | M | NAWM | ↓ in MS |
| Duan et al. (64) | R | WM | ↓ in MS |
| Fu et al. (52) | SP | NAWM | ↓ in MS |
| Fu et al. (52) | R | NAWM | ↓ in MS |
| Fu et al. (60) | SP | WM | ↓ in MS |
| Fu et al. (60) | R | WM | ↓ in MS |
| Hannoun et al. (62) | SP | WM | ↓ in MS |
| Hannoun et al. (62) | PP | WM | ↓ in MS |
| Hannoun et al. (62) | R | WM | ↓ in MS |
| Husted et al. (30) | M | NAWM | ↓ in MS |
| Kimura et al. (32) | M | NAWM | NS |
| Leary et al. (82) | PP | NAWM | ↓ in MS |
| Maffei et al. (76) | R | spine | ↓ in MS* |
| Maffei et al. (76) | SP | spine | NS* |
| Mathiesen et al. (144) | R | GM | NS |
| Mathiesen et al. (144) | R | mixed | NS |
| Mathiesen et al. (144) | R | NAWM | NS |
| Matthews et al. (55) | M | NAWM | NS |
| Matthews et al. (71) | SP | mixed | ↓ in MS |
| Matthews et al. (71) | R | mixed | ↓ in MS |
| Narayanan et al. (73) | SP | mixed | ↓ in MS |
| Narayanan et al. (73) | R | mixed | ↓ in MS |
| Narayana et al. (87) | PP | mixed | ↓ in MS |
| Obert et al. (172) | SP | NAWM | NS |
| Obert et al. (172) | R | NAWM | NS |
| Oguz et al. (148) | R | NAWM | NS |
| Oh et al. (45) | M | NAWM | ↓ in MS |
| Oh et al. (45) | PP | NAWM | ↓ in MS |
| Oh et al. (66) | SP | NAWM, c.c. | ↓ in MS |
| Oh et al. (66) | SP | NAWM, central | ↓ in MS |
| Oh et al. (66) | SP | NAWM, not c.c. | NS |
| Oh et al. (66) | R | NAWM, c.c. | ↓ in MS |
| Oh et al. (66) | R | NAWM, central | NS |
| Oh et al. (66) | R | NAWM, not c.c. | NS |
| Pan et al. (54) | R | GM | ↓ in MS |
| Pan et al. (54) | R | WM | ↓ in MS |
| Parry et al. (74) | R | mixed | ↓ in MS |
| Pascual et al. (141) | R | NAWM | NS |
| Pelletier et al. (85) | PP | mixed, supratentorial | ↓ in MS |
| Pelletier et al. (85) | PP | mixed, excluding central | ↓ in MS |
| Pelletier et al. (85) | PP | mixed, central | ↓ in MS |
| Pelletier et al. (85) | SP | mixed, supratentorial | ↓ in MS |
| Pelletier et al. (85) | SP | mixed, excluding central | ↓ in MS |
| Pelletier et al. (85) | SP | mixed, central | ↓ in MS |
| Pelletier et al. (85) | R | mixed, supratentorial | NS |
| Pelletier et al. (85) | R | mixed, excluding central | NS |
| Pelletier et al. (85) | R | mixed, central | NS |
| Pelletier et al. (89) | PP | mixed | ↓ in MS |
| Pokryszko-Dragan et al. (63) | R | mixed | ↓ in MS |
| Pokryszko-Dragan et al. (63) | R | WM | ↓ in MS |
| Reddy et al. (59) | R | WM | ↓ in MS* |
| Rooney et al. (37) | M | NAWM | ↓ in MS |
| Ruiz-Peña et al. (143) | R | NAWM | NS |
| Sarchielli et al. (53) | R | NAWM | NS |
| Sarchielli et al. (88) | SP | mixed | ↓ in MS |
| Siger-Zajdel et al. (44) | $M_{sp}$ | NAWM | ↓ in MS |
| Siger-Zajdel et al. (44) | $M_f$ | NAWM | ↓ in MS |
| Staffen et al. (58) | R | mixed | ↓ in MS |
| Staffen et al. (58) | $R_{nl}$ | NAWM | NS |
| Staffen et al. (58) | $R_l$ | WM | ↓ in MS |
| Steen et al. (81) | P | NAWM | ↓ in MS |
| Steen et al. (39) | M | NAWM | ↓ in MS |
| Suhy et al. (50) | PP | NAWM | ↓ in MS |
| Suhy et al. (50) | R | NAWM | ↓ in MS |
| Sun et al. (68) | R | NAWM, frontal | ↓ in MS |
| Sun et al. (68) | R | NAWM, parietal | ↓ in MS |
| Sun et al. (68) | R | NAWM, parietal-occipital | ↓ in MS |
| Takeuchi et al. (51) | R | NAWM | ↓ in MS |
| Tartaglia et al. (25) | M | NAWM | ↓ in MS |
| Tedeschi et al. (34) | M | NAWM | ↓ in MS |
| Téllez et al. (75) | $R_{hf}$ | mixed, lentiform nucleus | ↓ in MS |
| Téllez et al. (75) | $R_{hf}$ | WM, frontal | NS |
| Téllez et al. (75) | $R_{lf}$ | mixed, lentiform nucleus | NS |
| Téllez et al. (75) | $R_{lf}$ | WM, frontal | NS |
| Tourbah et al. (40) | M | NAWM | ↓ in MS |
| Tourbah et al. (46) | M | NAWM | ↓ in MS |
| Tourbah et al. (46) | R | NAWM | NS |
| Tourbah et al. (46) | SP | NAWM | ↓ in MS |
| Tourbah et al. (79) | R | NAWM | NS |
| Tourbah et al. (79) | SP | NAWM | ↓ in MS |
| van Walderveen et al. (22) | M | NAWM | ↓ in MS |
| Vingara et al. (48) | R | NAWM | ↓ in MS |
| Vrenken et al. (69) | PP | NAWM | ↓ in MS |
| Vrenken et al. (69) | SP | NAWM | ↓ in MS |
| Vrenken et al. (69) | R | NAWM | ↓ in MS |
| Wattjes et al. (67) | R | NAWM | ↓ in MS |
| Wood et al. (38) | M | NAWM | ↓ in MS |
| Wu et al. (145) | R | mixed | NS |
| Wylezinska et al. (70) | R | GM | ↓ in MS |
| Wylezinska et al. (70) | R | NAWM | ↓ in MS |
| Yetkin et al. (56) | R | NAWM | NS |
| Zaini et al. (57) | $R_{hf}$ | WM | ↓ in MS |
| Zaini et al. (57) | $R_{lf}$ | WM | ↓ in MS |

**Single-subject MS case report.*

*MS: multiple sclerosis; P: progressive; SP: secondary progressive; PP: primary progressive; R: relapsing-remitting; M: mixed or unspecified MS phenotype(s); c.c.: corpus callosum; $M_{sp}$: sporadic MS; $M_f$: familial MS; $R_{nl}$: relapsing-remitting with no lesions in region of interest; $R_l$: relapsing-remitting with lesions in region of interest; $R_{hf}$: relapsing-remitting with any or high fatigue; $R_{lf}$: relapsing-remitting with no or low fatigue.*

Swanberg, Landheer, Pitt, and Juchem. *Frontiers in Neurology* (2019): 10.

Classification of multiple sclerosis by single $^{1}$H-MRS-visible metabolites lacks diagnostically useful sensitivity and especially specificity.

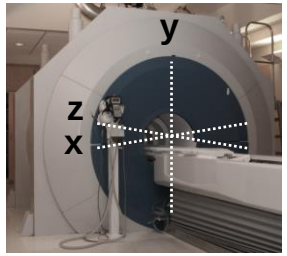


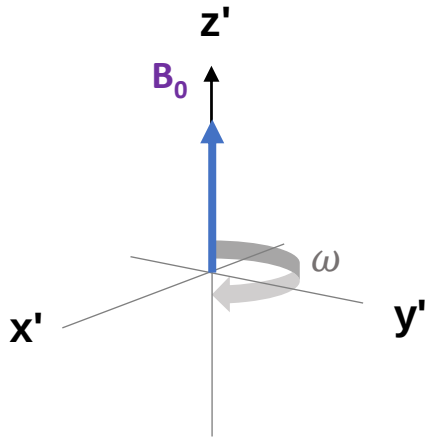


**Net magnetization vector** along z from nuclear spin **polarization** at thermal equilibrium and **precession** about z at **Larmor frequency**

$$\omega = -\gamma(B_0 + \Delta B)$$

*ω = Larmor frequency; γ = gyromagnetic ratio*
*$B_0$ = scanner field; B = local field*

$$\alpha \propto \gamma \int_0^\tau B_1(t)\,\mathrm{d}t$$

*α = net magnetization angle from z'*
*γ = gyromagnetic ratio*
*$B_1$ = RF pulse power; τ = RF pulse duration*

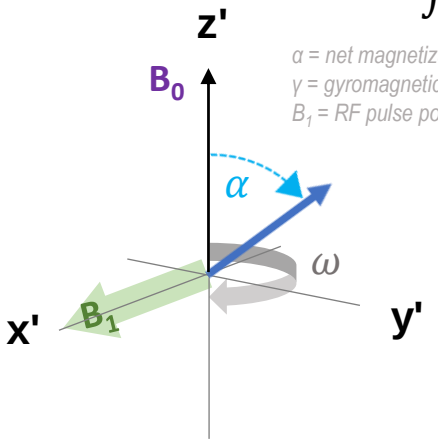


**Excitation in z** and **phasing in xy** of spins by **radiofrequency pulse** application

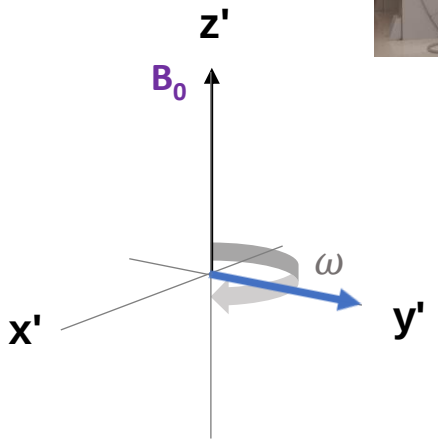


**Precession** about z on **xy plane** detected by radiofrequency **receive coils**

$^1$H-MRS signals represent radiofrequency field-induced changes in receive coil voltage, not metabolite concentration or proton density.

$\Phi_{0,1}$ = zero-, first-order phase
$N_M$ = number of metabolites
$C_l$ = Metabolite concentrations
$N_B$ = number of baseline splines
B = baseline spline
$S_n$ = metabolite basis function lineshape coefficients
ν = frequency domain value
γ = line broadening parameter
ε = frequency shift parameter

$$\widehat{Y}(\nu_k) = e^{-i(\phi_0+\nu\phi_1)}\left[\sum_{j=1}^{N_B}\beta_j B_j(\nu_k) + \sum_{l=1}^{N_M} C_l \sum_{n=-N_s}^{N_s} S_n M_l(\nu_{k-n}, \gamma_l, \epsilon_l)\right]$$

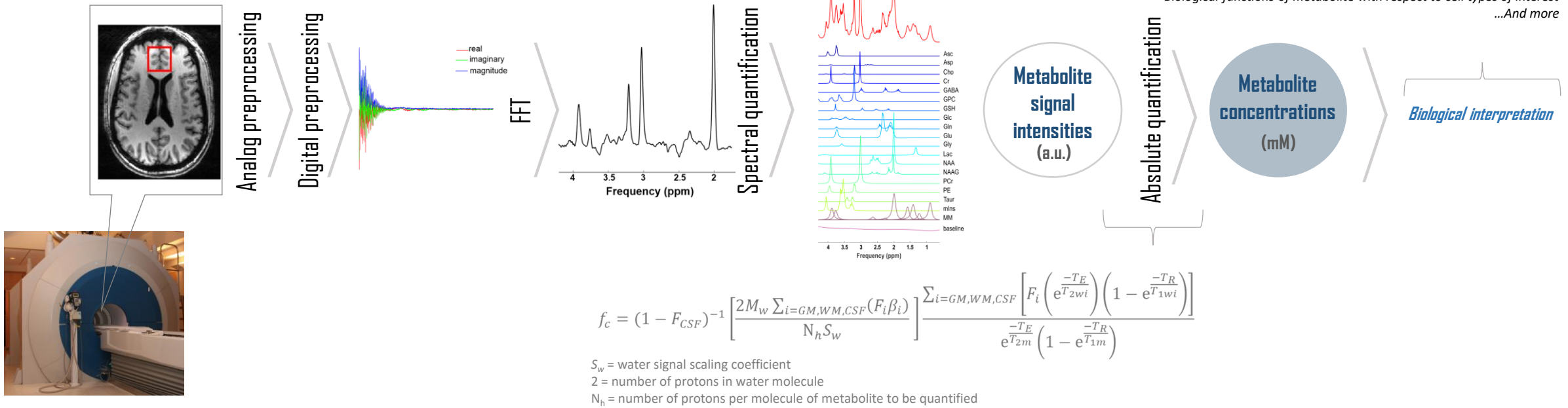


*Metabolite concentrations by tissue*
*Intracellular vs. extracellular metabolite concentration*
*Intracellular metabolite concentrations within cell types of interest*
*Biological functions of metabolite with respect to cell types of interest*
*…And more*



$$f_c = (1 - F_{CSF})^{-1}\left[\frac{2M_w \sum_{i=GM,WM,CSF}(F_i\beta_i)}{N_h S_w}\right]\frac{\sum_{i=GM,WM,CSF}\left[F_i\left(e^{\frac{-T_E}{T_{2wi}}}\right)\left(1 - e^{\frac{-T_R}{T_{1wi}}}\right)\right]}{e^{\frac{-T_E}{T_{2m}}}\left(1 - e^{\frac{-T_R}{T_{1m}}}\right)}$$

$S_w$ = water signal scaling coefficient
2 = number of protons in water molecule
$N_h$ = number of protons per molecule of metabolite to be quantified
$M_w$ = molarity of pure water
$\beta_i$ = molarity of water as a fraction of pure water in either grey matter (GM), white matter (WM), or CSF
$F_i$ = voxel fraction occupied by grey matter (GM), white matter (WM), or CSF
$T_{2wi}$ = $T_2$ of water in grey matter (GM), white matter (WM), or CSF
$T_{1wi}$ = $T_1$ of water in grey matter (GM), white matter (WM), or CSF
$T_{2m}$ = $T_2$ of metabolite
$T_{1m}$ = $T_1$ of metabolite
$T_E$ = echo time of sequence
$T_R$ = repetition time of sequence

***Chapter II***

***Spectral Quantification:*** *What are the effects of spectral quality and baseline on the precision and accuracy of relative metabolite concentrations drawn from $^1$H MRS data, and how do we minimize them?*

$\Phi_{0,1}$ = zero-, first-order phase
$N_M$ = number of metabolites
$C_l$ = Metabolite concentrations
$N_B$ = number of baseline splines
B = baseline spline
$S_n$ = metabolite basis function lineshape coefficients
ν = frequency domain value
γ = line broadening parameter
ε = frequency shift parameter

$$\widehat{Y}(\nu_k) = e^{-i(\phi_0+\nu\phi_1)}\left[\sum_{j=1}^{N_B}\beta_j B_j(\nu_k) + \sum_{l=1}^{N_M} C_l \sum_{n=-N_s}^{N_s} S_n M_l(\nu_{k-n}, \gamma_l, \epsilon_l)\right]$$

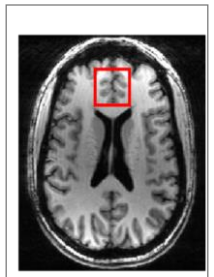

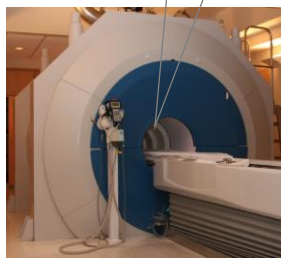

Analog preprocessing

Digital preprocessing

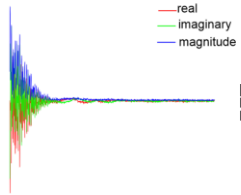


FFT

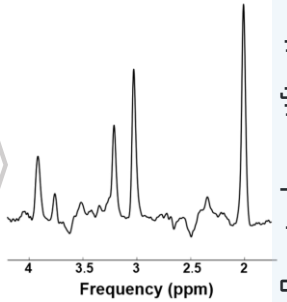


Spectral quantification

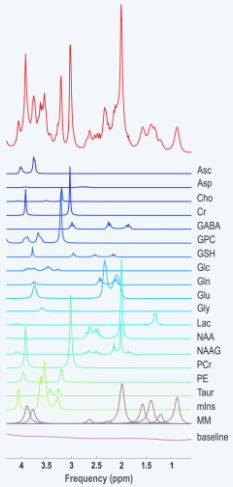


**Metabolite signal intensities (a.u.)**

Absolute quantification

**Metabolite concentrations (mM)**

*Metabolite concentrations by tissue*
*Intracellular vs. extracellular metabolite concentration*
*Intracellular metabolite concentrations within cell types of interest*
*Biological functions of metabolite with respect to cell types of interest*
*…And more*

***Biological interpretation***

$$f_c = (1 - F_{CSF})^{-1}\left[\frac{2M_w \sum_{i=GM,WM,CSF}(F_i\beta_i)}{N_h S_w}\right]\frac{\sum_{i=GM,WM,CSF}\left[F_i\left(e^{\frac{-T_E}{T_{2wi}}}\right)\left(1 - e^{\frac{-T_R}{T_{1wi}}}\right)\right]}{e^{\frac{-T_E}{T_{2m}}}\left(1 - e^{\frac{-T_R}{T_{1m}}}\right)}$$

$S_w$ = water signal scaling coefficient
2 = number of protons in water molecule
Nh = number of protons per molecule of metabolite to be quantified
$M_w$ = molarity of pure water
$\beta_i$ = molarity of water as a fraction of pure water in either grey matter (GM), white matter (WM), or CSF
$F_i$ = voxel fraction occupied by grey matter (GM), white matter (WM), or CSF
$T_{2wi}$ = $T_2$ of water in grey matter (GM), white matter (WM), or CSF
$T_{1wi}$ = $T_1$ of water in grey matter (GM), white matter (WM), or CSF
$T_{2m}$ = $T_2$ of metabolite
$T_{1m}$ = $T_1$ of metabolite
$T_E$ = echo time of sequence
$T_R$ = repetition time of sequence

$\Phi_{0,1}$ = zero-, first-order phase
$N_M$ = number of metabolites
$C_l$ = Metabolite concentrations
$N_B$ = number of baseline splines
B = baseline spline
$S_n$ = metabolite basis function lineshape coefficients
ν = frequency domain value
γ = line broadening parameter
ε = frequency shift parameter

$$\widehat{Y}(\nu_k) = e^{-i(\phi_0+\nu\phi_1)}\left[\sum_{j=1}^{N_B}\beta_j B_j(\nu_k) + \sum_{l=1}^{N_M} C_l \sum_{n=-N_s}^{N_s} S_n M_l(\nu_{k-n}, \gamma_l, \epsilon_l)\right]$$

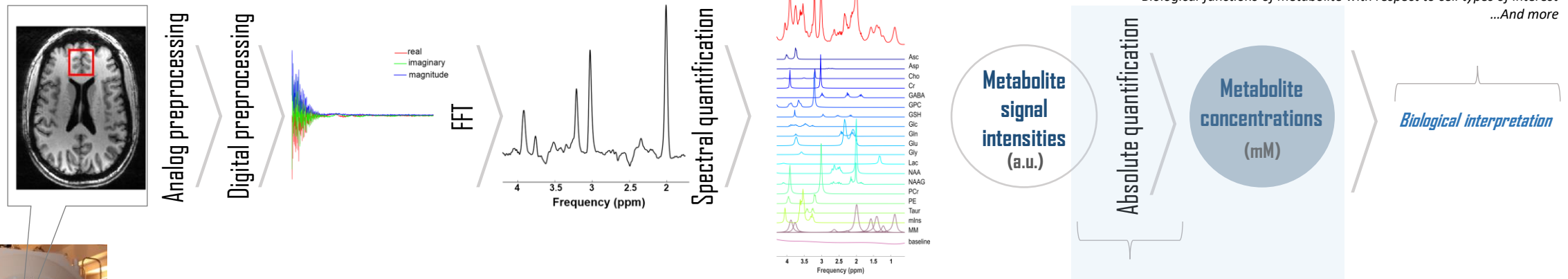


*Metabolite concentrations by tissue*
*Intracellular vs. extracellular metabolite concentration*
*Intracellular metabolite concentrations within cell types of interest*
*Biological functions of metabolite with respect to cell types of interest*
*…And more*

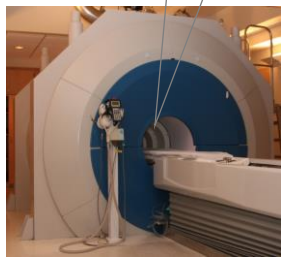

***Chapter III***

> ***Absolute Quantification:*** *Can disease-related differences in metabolite $T_2$ introduce systematic errors to the derivation of absolute from relative metabolite concentrations, and how do we minimize them?*

$$f_c = (1 - F_{CSF})^{-1}\left[\frac{2M_w \sum_{i=GM,WM,CSF}(F_i\beta_i)}{N_h S_w}\right]\frac{\sum_{i=GM,WM,CSF}\left[F_i\left(e^{\frac{-T_E}{T_{2wi}}}\right)\left(1 - e^{\frac{-T_R}{T_{1wi}}}\right)\right]}{e^{\frac{-T_E}{T_{2m}}}\left(1 - e^{\frac{-T_R}{T_{1m}}}\right)}$$

$S_w$ = water signal scaling coefficient
2 = number of protons in water molecule
Nh = number of protons per molecule of metabolite to be quantified
$M_w$ = molarity of pure water
$\beta_i$ = molarity of water as a fraction of pure water in either grey matter (GM), white matter (WM), or CSF
$F_i$ = voxel fraction occupied by grey matter (GM), white matter (WM), or CSF
$T_{2wi}$ = $T_2$ of water in grey matter (GM), white matter (WM), or CSF
$T_{1wi}$ = $T_1$ of water in grey matter (GM), white matter (WM), or CSF
$T_{2m}$ = $T_2$ of metabolite
$T_{1m}$ = $T_1$ of metabolite
$T_E$ = echo time of sequence
$T_R$ = repetition time of sequence

$\Phi_{0,1}$ = zero-, first-order phase
$N_M$ = number of metabolites
$C_l$ = Metabolite concentrations
$N_B$ = number of baseline splines
B = baseline spline
$S_n$ = metabolite basis function lineshape coefficients
ν = frequency domain value
γ = line broadening parameter
ε = frequency shift parameter

$$\widehat{Y}(\nu_k) = e^{-i(\phi_0+\nu\phi_1)}\left[\sum_{j=1}^{N_B}\beta_j B_j(\nu_k) + \sum_{l=1}^{N_M} C_l \sum_{n=-N_s}^{N_s} S_n M_l(\nu_{k-n}, \gamma_l, \epsilon_l)\right]$$

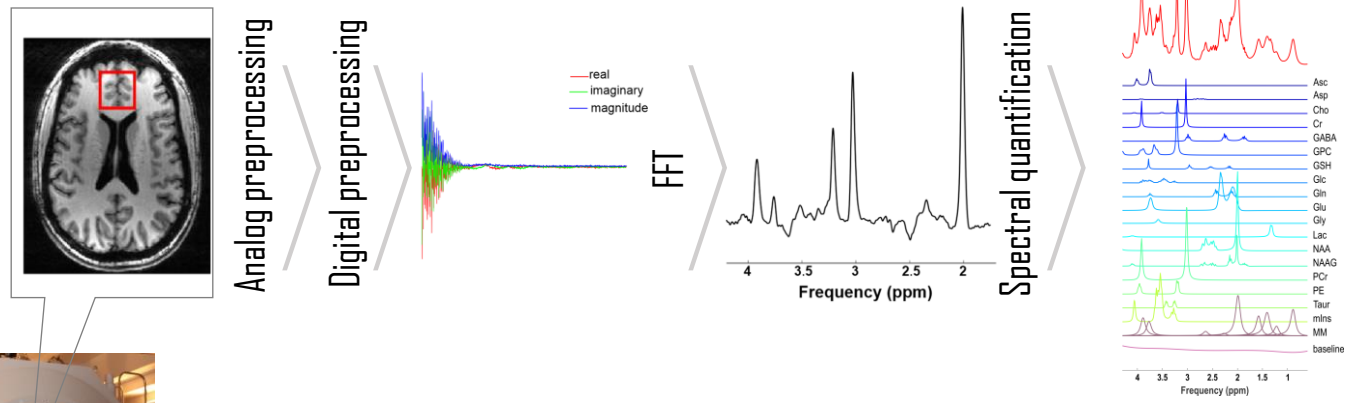


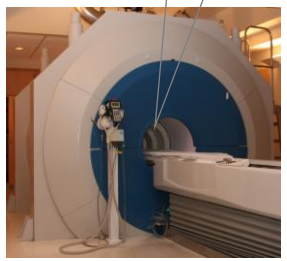

$$f_c = (1 - F_{CSF})^{-1}\left[\frac{2M_w \sum_{i=GM,WM,CSF}(F_i\beta_i)}{N_h S_w}\right]\frac{\sum_{i=GM,WM,CSF}\left[F_i\left(e^{\frac{-T_E}{T_{2wi}}}\right)\left(1 - e^{\frac{-T_R}{T_{1wi}}}\right)\right]}{e^{\frac{-T_E}{T_{2m}}}\left(1 - e^{\frac{-T_R}{T_{1m}}}\right)}$$

$S_w$ = water signal scaling coefficient
2 = number of protons in water molecule
Nh = number of protons per molecule of metabolite to be quantified
$M_w$ = molarity of pure water
$\beta_i$ = molarity of water as a fraction of pure water in either grey matter (GM), white matter (WM), or CSF
$F_i$ = voxel fraction occupied by grey matter (GM), white matter (WM), or CSF
$T_{2wi}$ = $T_2$ of water in grey matter (GM), white matter (WM), or CSF
$T_{1wi}$ = $T_1$ of water in grey matter (GM), white matter (WM), or CSF
$T_{2m}$ = $T_2$ of metabolite
$T_{1m}$ = $T_1$ of metabolite
$T_E$ = echo time of sequence
$T_R$ = repetition time of sequence

### Chapter IV

***Statistical Analysis:*** *Can single- or multivariate analysis of metabolite concentrations derived from optimized quantification of 1H MRS data alone classify disease states (case application multiple sclerosis)?*

*Metabolite concentrations by tissue*
*Intracellular vs. extracellular metabolite concentration*
*Intracellular metabolite concentrations within cell types of interest*
*Biological functions of metabolite with respect to cell types of interest*
*...And more*

## Chapter 1: Introduction

$\Phi_{0,1}$ = zero-, first-order phase
$N_M$ = number of metabolites
$C_l$ = Metabolite concentrations
$N_B$ = number of baseline splines
B = baseline spline
$S_n$ = metabolite basis function lineshape coefficients
ν = frequency domain value
γ = line broadening parameter
ε = frequency shift parameter

$$\widehat{Y}(\nu_k) = e^{-i(\phi_0+\nu\phi_1)}\left[\sum_{j=1}^{N_B}\beta_j B_j(\nu_k) + \sum_{l=1}^{N_M} C_l \sum_{n=-N_s}^{N_s} S_n M_l(\nu_{k-n}, \gamma_l, \epsilon_l)\right]$$

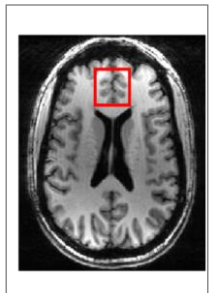

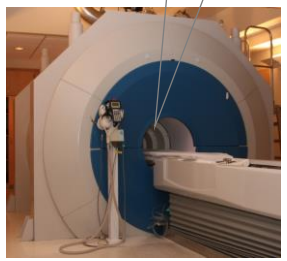

Analog preprocessing

Digital preprocessing

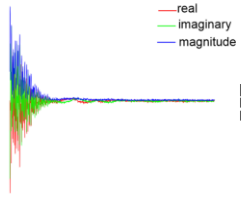


FFT

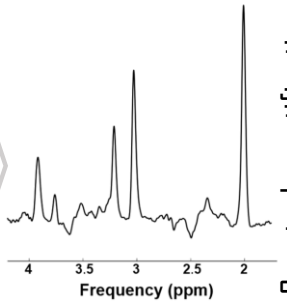


Spectral quantification

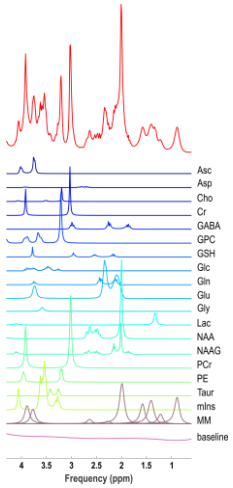


**Metabolite signal intensities (a.u.)**

Absolute quantification

**Metabolite concentrations (mM)**

*Metabolite concentrations by tissue*
*Intracellular vs. extracellular metabolite concentration*
*Intracellular metabolite concentrations within cell types of interest*
*Biological functions of metabolite with respect to cell types of interest*
*...And more*

***Biological interpretation***

$$f_c = (1 - F_{CSF})^{-1}\left[\frac{2M_w \sum_{i=GM,WM,CSF}(F_i\beta_i)}{N_h S_w}\right]\frac{\sum_{i=GM,WM,CSF}\left[F_i\left(e^{\frac{-T_E}{T_{2wi}}}\right)\left(1 - e^{\frac{-T_R}{T_{1wi}}}\right)\right]}{e^{\frac{-T_E}{T_{2m}}}\left(1 - e^{\frac{-T_R}{T_{1m}}}\right)}$$

$S_w$ = water signal scaling coefficient
2 = number of protons in water molecule
Nh = number of protons per molecule of metabolite to be quantified
$M_w$ = molarity of pure water
$\beta_i$ = molarity of water as a fraction of pure water in either grey matter (GM), white matter (WM), or CSF
$F_i$ = voxel fraction occupied by grey matter (GM), white matter (WM), or CSF
$T_{2wi}$ = $T_2$ of water in grey matter (GM), white matter (WM), or CSF
$T_{1wi}$ = $T_1$ of water in grey matter (GM), white matter (WM), or CSF
$T_{2m}$ = $T_2$ of metabolite
$T_{1m}$ = $T_1$ of metabolite
$T_E$ = echo time of sequence
$T_R$ = repetition time of sequence

***Chapter V***

***Generalization:*** *Can a quantification and statistics pipeline optimized for classification of multiple sclerosis via 1H MRS-derived metabolite concentrations be generalized to identification of PTSD and MDD?*

## The Big Picture:

$^1$H MRS is a potential but currently untapped source of clinical diagnostic biomarkers.

Chapter I

## Spectral Quantification:

What are the effects of spectral quality and baseline on the precision and accuracy of relative metabolite concentrations drawn from $^1$H MRS data, and how do we minimize them?

Chapter II

## Absolute Quantification:

Can disease-related differences in metabolite $T_2$ introduce systematic errors to the derivation of absolute from relative metabolite concentrations, and how do we minimize them?

Chapter III

## Statistical Analysis:

Can single- or multivariate analysis of metabolite concentrations derived from optimized quantification of $^1$H MRS data alone classify disease states (case application multiple sclerosis)?

Chapter IV

## Generalization:

Can a quantification and statistics pipeline optimized for classification of multiple sclerosis via $^1$H MRS-derived metabolite concentrations be generalized to identification of PTSD and MDD?

Chapter V

## Back to the Big Picture:

General conclusions and outlook

Chapter VI

***Chapter II***

***Spectral Quantification:*** *What are the effects of spectral quality and baseline on the precision and accuracy of relative metabolite concentrations drawn from $^1$H MRS data, and how do we minimize them?*

$\Phi_{0,1}$ = zero-, first-order phase
$N_M$ = number of metabolites
$C_l$ = Metabolite concentrations
$N_B$ = number of baseline splines
B = baseline spline
$S_n$ = metabolite basis function lineshape coefficients
ν = frequency domain value
γ = line broadening parameter
ε = frequency shift parameter

$$\widehat{Y}(\nu_k) = e^{-i(\phi_0+\nu\phi_1)}\left[\sum_{j=1}^{N_B}\beta_j B_j(\nu_k) + \sum_{l=1}^{N_M} C_l \sum_{n=-N_s}^{N_s} S_n M_l(\nu_{k-n}, \gamma_l, \epsilon_l)\right]$$

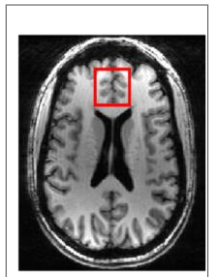

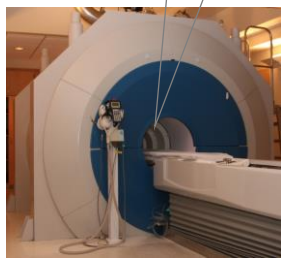

Analog preprocessing

Digital preprocessing

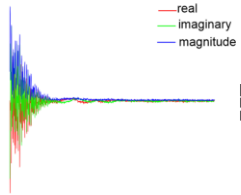


FFT

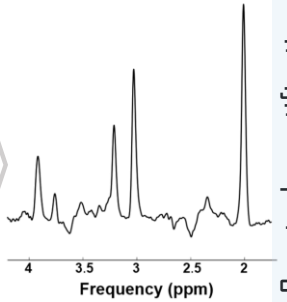


Spectral quantification

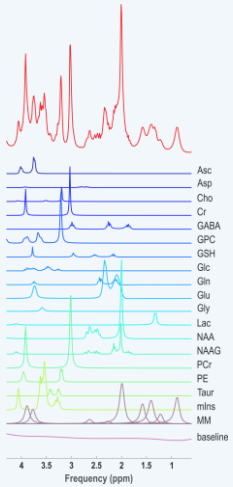


**Metabolite signal intensities (a.u.)**

Absolute quantification

**Metabolite concentrations (mM)**

*Metabolite concentrations by tissue*
*Intracellular vs. extracellular metabolite concentration*
*Intracellular metabolite concentrations within cell types of interest*
*Biological functions of metabolite with respect to cell types of interest*
*…And more*

***Biological interpretation***

$$f_c = (1 - F_{CSF})^{-1}\left[\frac{2M_w \sum_{i=GM,WM,CSF}(F_i\beta_i)}{N_h S_w}\right]\frac{\sum_{i=GM,WM,CSF}\left[F_i\left(e^{\frac{-T_E}{T_{2wi}}}\right)\left(1 - e^{\frac{-T_R}{T_{1wi}}}\right)\right]}{e^{\frac{-T_E}{T_{2m}}}\left(1 - e^{\frac{-T_R}{T_{1m}}}\right)}$$

$S_w$ = water signal scaling coefficient
2 = number of protons in water molecule
Nh = number of protons per molecule of metabolite to be quantified
$M_w$ = molarity of pure water
$\beta_i$ = molarity of water as a fraction of pure water in either grey matter (GM), white matter (WM), or CSF
$F_i$ = voxel fraction occupied by grey matter (GM), white matter (WM), or CSF
$T_{2wi}$ = $T_2$ of water in grey matter (GM), white matter (WM), or CSF
$T_{1wi}$ = $T_1$ of water in grey matter (GM), white matter (WM), or CSF
$T_{2m}$ = $T_2$ of metabolite
$T_{1m}$ = $T_1$ of metabolite
$T_E$ = echo time of sequence
$T_R$ = repetition time of sequence

Chapter 2: Spectral Quantification

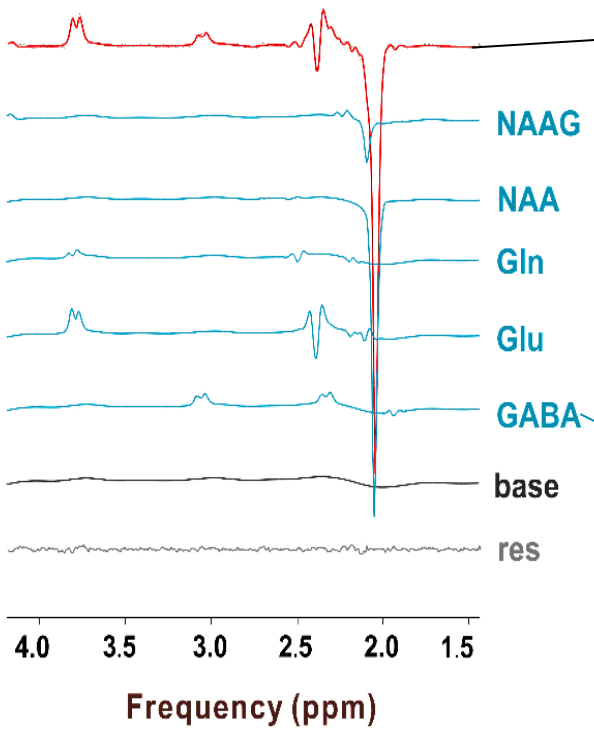


Swanberg, Prinsen, Kurada, Bailey, Destefano, Pitt, Fulbright, and Juchem. *NMR in Biomedicine* (2021); 34(11).

Zero- and first-order phase correction | Baseline term | Metabolite scalings | Metabolite basis shapes

$$\hat{Y}(\nu_k) = e^{-i(\phi_0+\nu\phi_1)}\left[\sum_{j=1}^{N_B}\beta_j B_j(\nu_k) + \sum_{l=1}^{N_M} C_l \sum_{n=-N_s}^{N_s} S_n M_l(\nu_{k-n}, \gamma_l, \epsilon_l)\right]$$

$\Phi_{0,1}$ = zero-, first-order phase
$N_M$ = number of metabolites
$C_l$ = Metabolite concentrations
$N_B$ = number of spline knots
$B$ = baseline spline
$\beta$ = spline coefficient

$S_n$ = metabolite basis function lineshape coefficients
$N_S$ = Number of signal points
$\nu$ = frequency domain value
$\gamma$ = line broadening parameter
$\epsilon$ = frequency shift parameter
$\mathbf{m}$ = simulated or measured basis metabolite FID

$M_l$ = metabolite basis function: $M_l(\nu, \gamma_l, \epsilon_l) = \mathcal{F}(m_l(t)e^{-(\gamma_l+i\epsilon_l)t})$

$\Phi_0$, $\Phi_1$, $\beta_j$, $C_l$, $S_n$, $\gamma_l$, $\epsilon_l$ adjusted to minimize regularized least-squares error between model and data

Provencher, S. *MRM* (1993); 30.

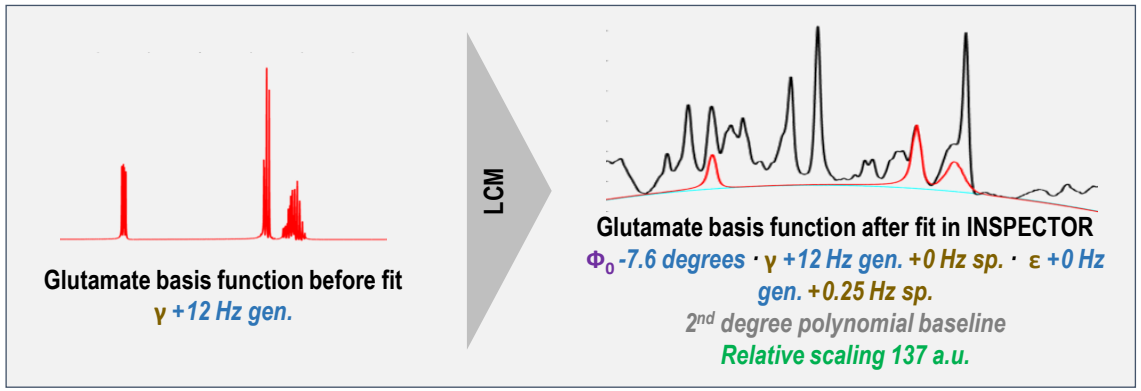

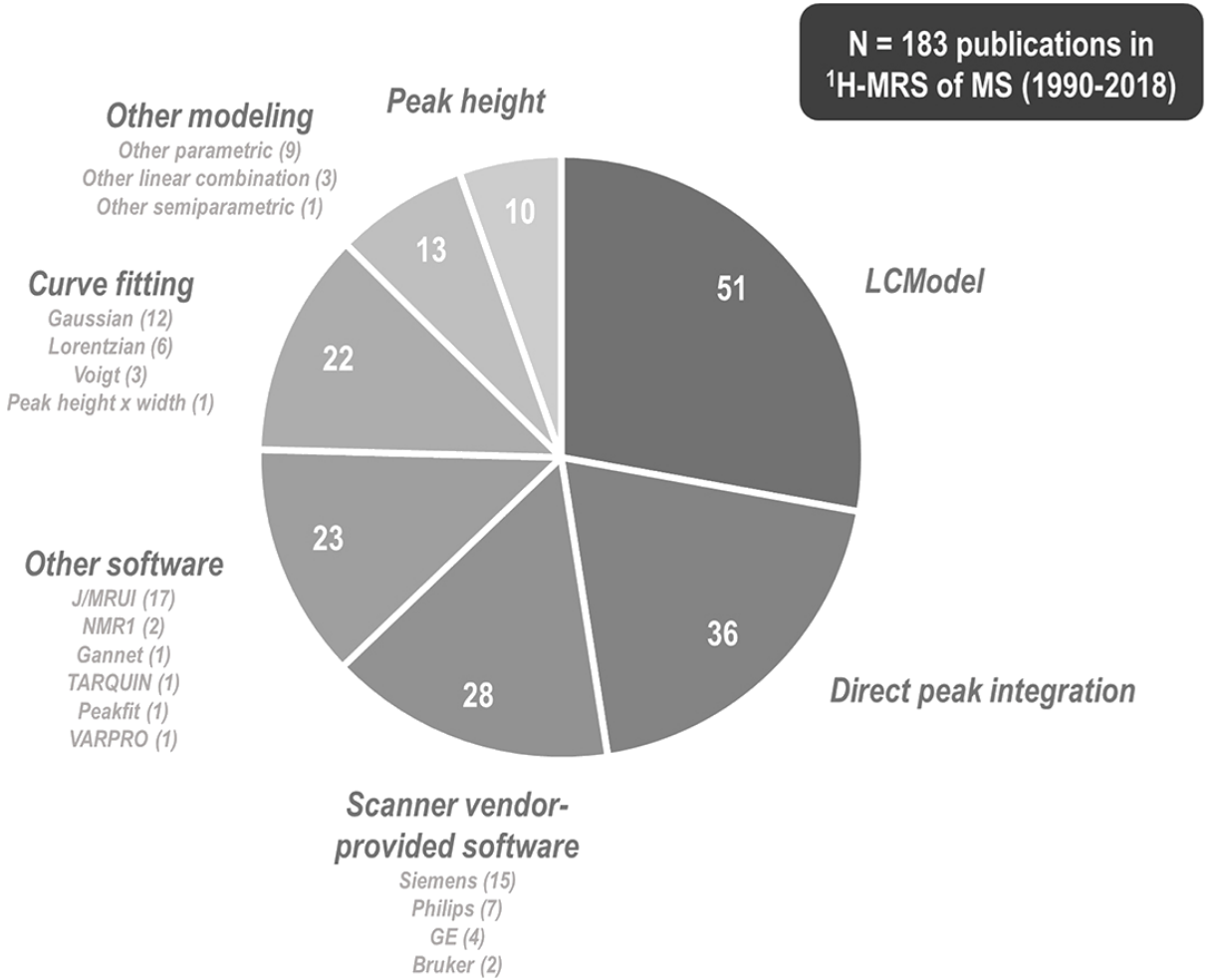


Swanberg, Landheer, Pitt, and Juchem. *Frontiers in Neurology* (2019); 1173.

Characterizing and optimizing the accuracy and precision of $^1$H MRS quantification methods is a prerequisite for standardizing them.

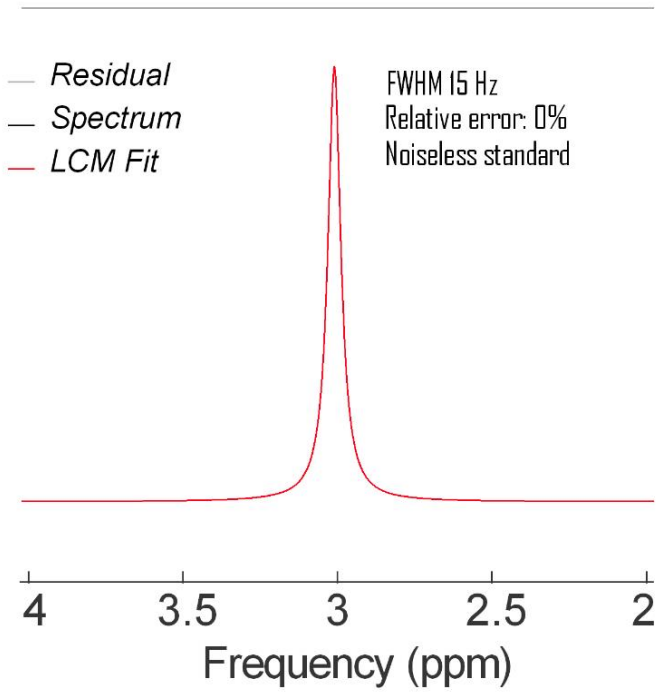


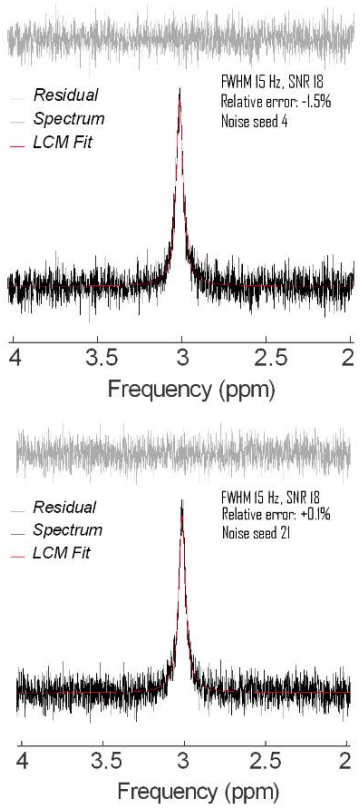


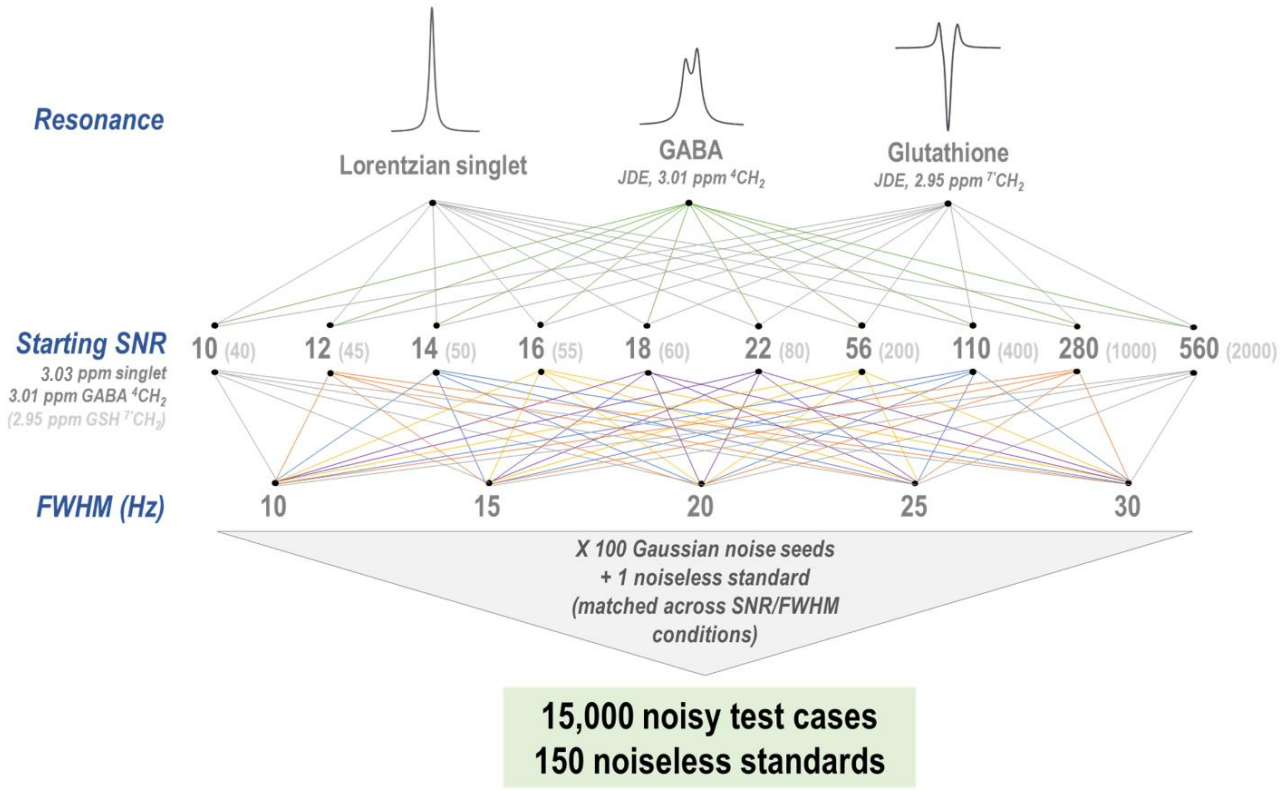


**15,000 noisy test cases**
**150 noiseless standards**

Swanberg, Prinsen, and Juchem. *Proc Intl Soc Mag Reson Med*. (2019); 4237.

Spectral quantification method is an important but testable source of inaccuracy and imprecision in $^1$H MRS data.

## Chapter 2: Spectral Quantification

**Tool 1:** *GUI-supported automated batch spectral simulation and quantification pipeline development and validation*

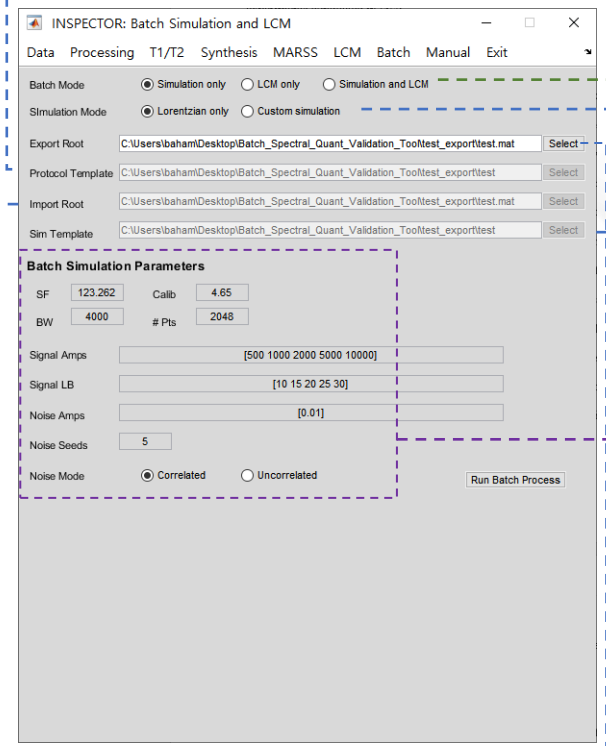


**Simulation only**

Simulated on demand

Optional input: Custom spectrum

Define Simulation

Define Quality Vectors

Batch Simulate

Spectra output to user-defined directory

**Simulation and LCM**

Input: INSPECTOR protocol template

Input: LCM basis set

Automated Protocol Generation and Data I/O

Batch LCM*

LCM results output to user-defined directory

**LCM only**

Input: Directory of spectral data to fit

Master CSV: Concentration estimates and errors for all fits

Statistical analysis pipeline of choice

*LCM functions and outputs native to INSPECTOR

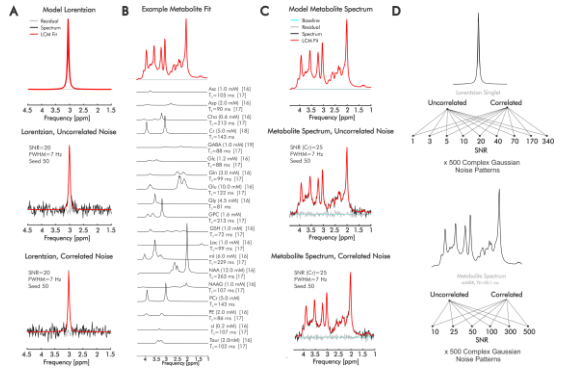

***First employment of novel GUI-accessible batch tool by another colleague in:***
Campos, Swanberg, Gajdošík, Landheer, and Juchem. Submitted to *Proc Intl Soc Mag Reson Med.* (2022).

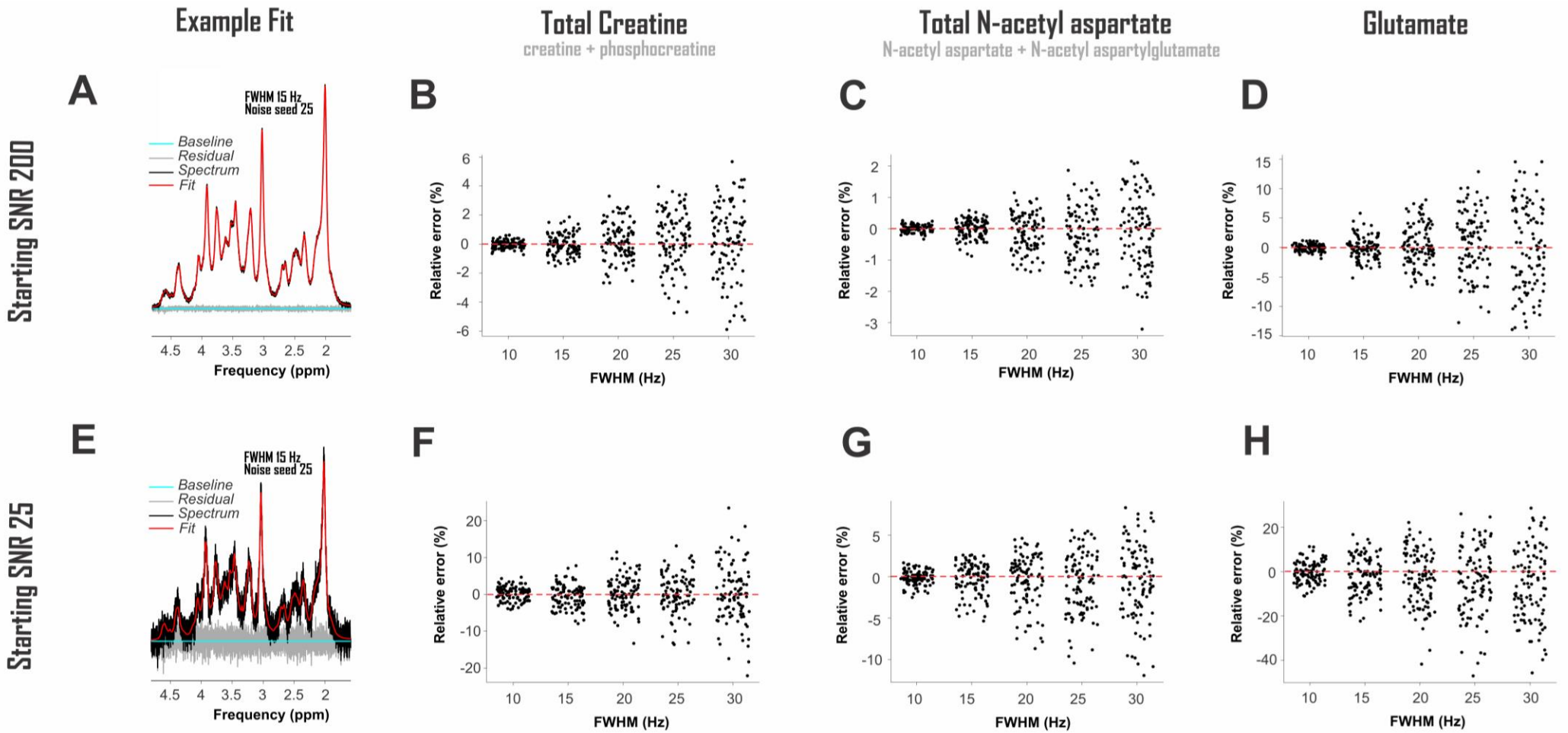


Swanberg, Prinsen, and Juchem. *Proc Intl Soc Mag Reson Med*. (2019); 4237.

Spectral line width and signal-to-noise ratio alone affect spectral quantification precision but not accuracy.

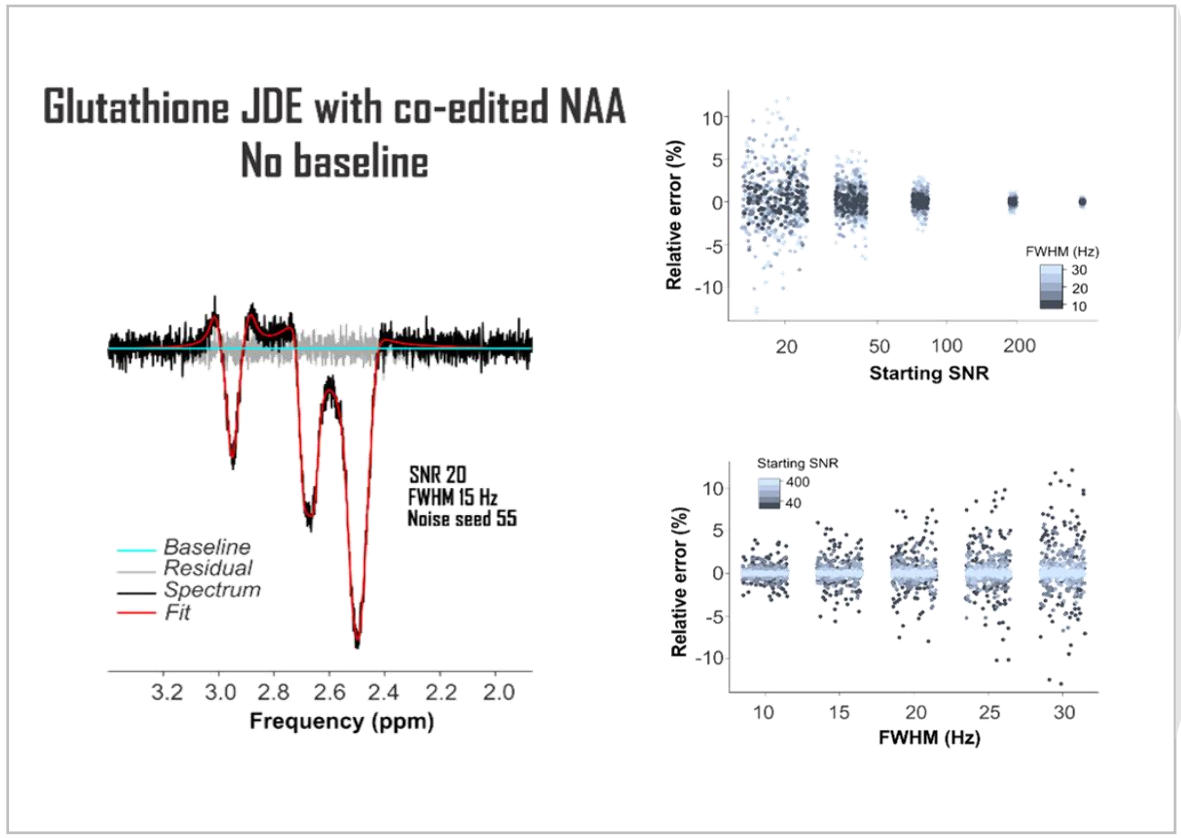


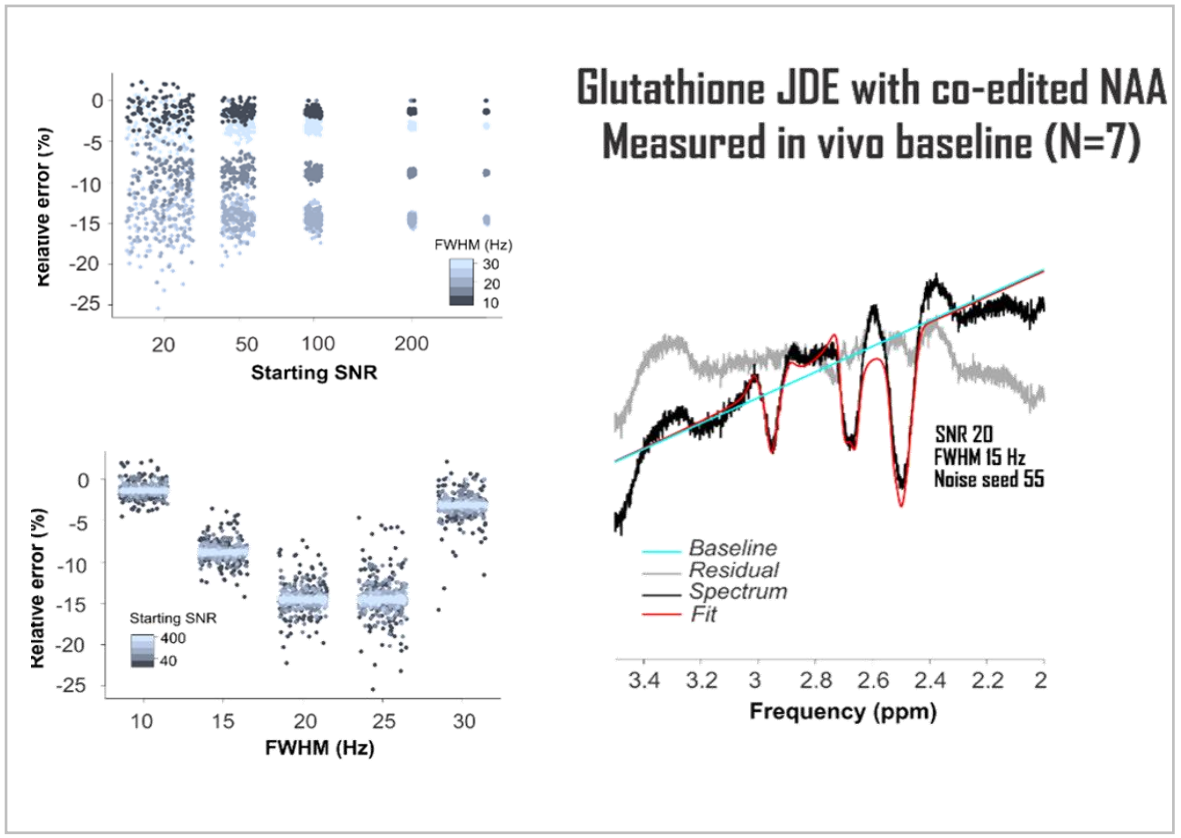


Swanberg, Prinsen, and Juchem. *Proc Intl Soc Mag Reson Med*. (2019); 4237.

Data quality can interact with spectral baselines to induce additional systematic effects on spectral fit accuracy.

*Absolute knot interval not fixed by user (DKNTMN **is not** knot interval)*
*Λ not fixed by user (determined by spectral line width)*

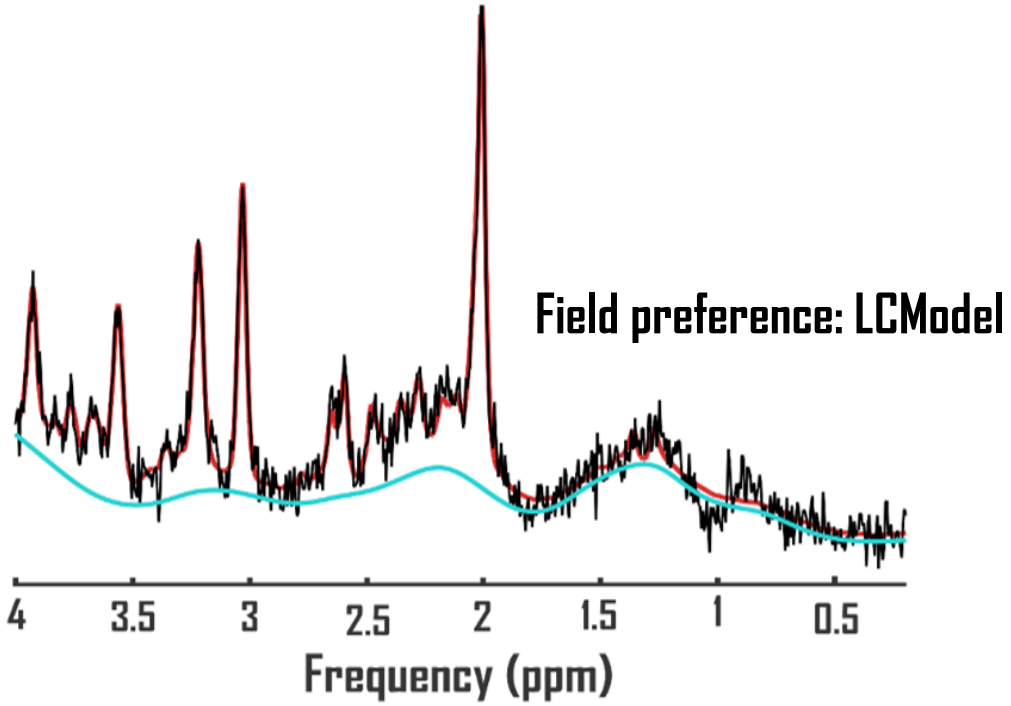


*Test data set provided by LCModel package*

*Absolute knot interval = 0.3*
*Λ = 20*

$$\left[\hat{Y}(\nu_k) - Y(\nu_k)\right]^2 + \lambda \|B''(\nu_k)\|$$

model data baseline smoothing

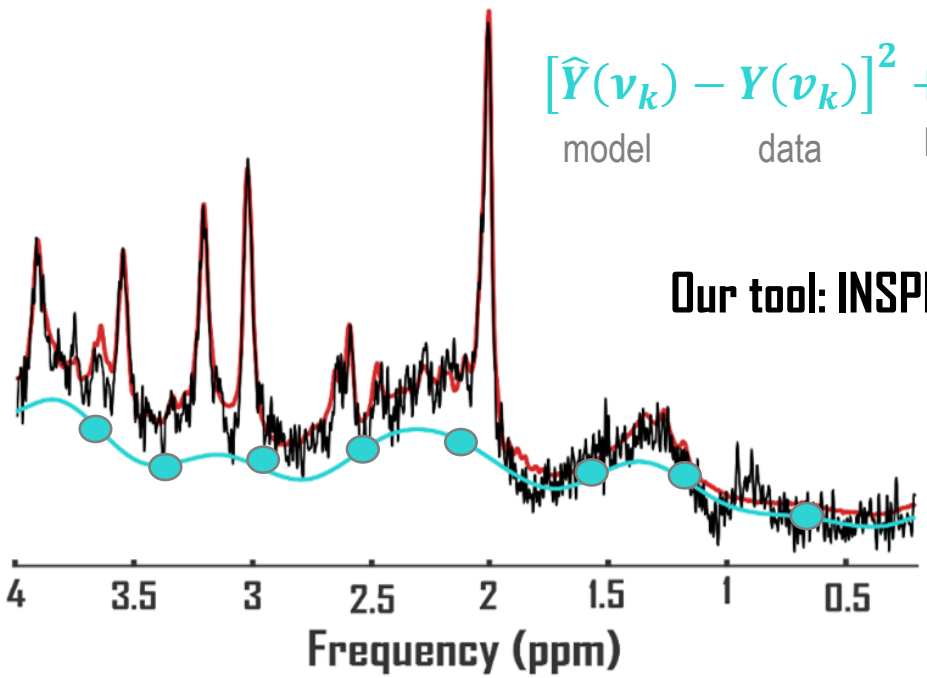


Swanberg, Landheer, Gajdošík, Treacy, and Juchem. *Proc Intl Soc Mag Reson Med*. (2020); 2856.

$^1$H MRS spectral baseline modeling by smoothed cubic splines is common but understudied, partly due to lack of available tools.

## CHAPTER 2: SPECTRAL QUANTIFICATION

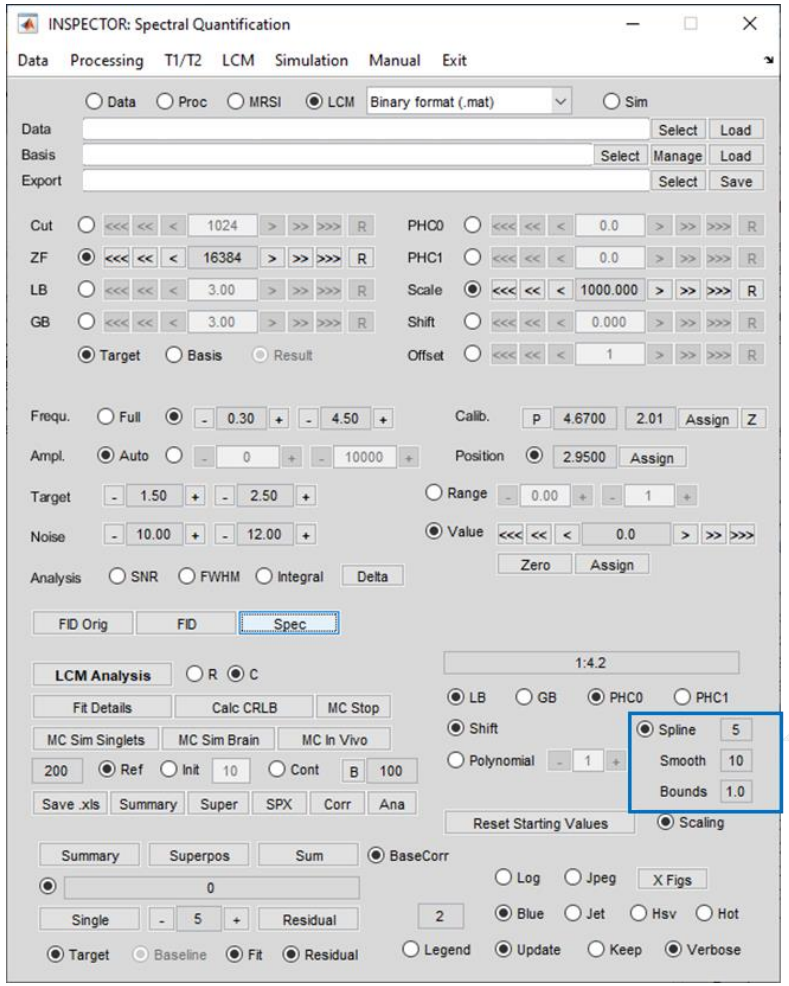


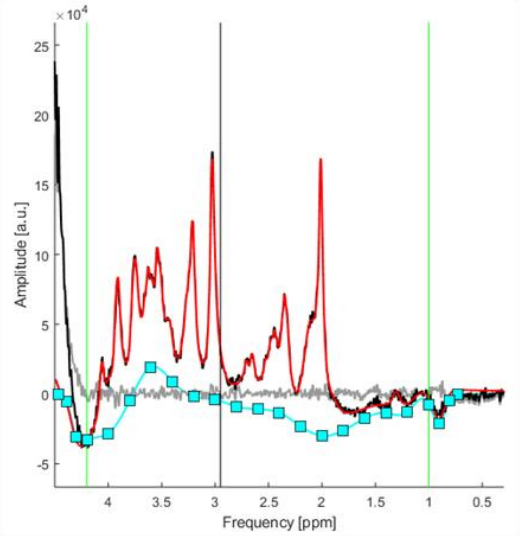


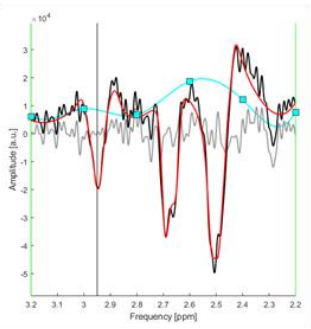


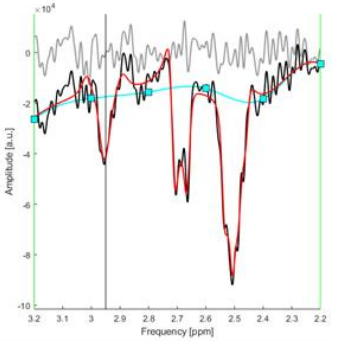


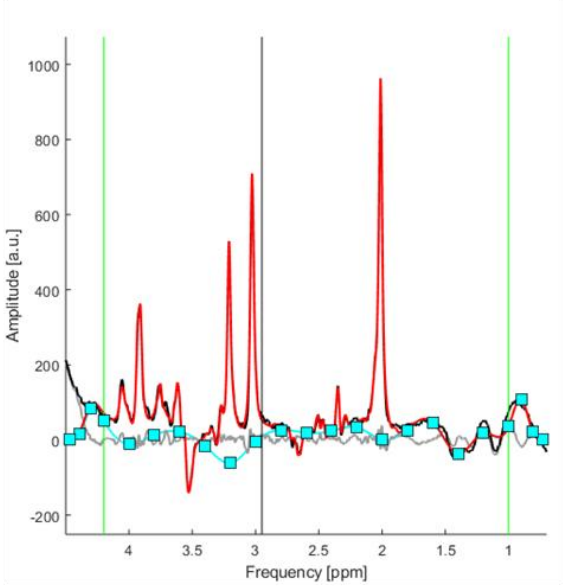


**Spline:** Number of knot points/ppm

**Smooth:** Lambda value on cost function ($l^2$ norm of spline second derivative)

**Bounds:** Upper and lower bound of spline knots (% of residual on initial $0^{th}$-degree polynomial fit)

***Tool 2:*** *GUI-supported regularized cubic spline definition for spectral baseline modeling*


scientific reports

OPEN **INSPECTOR: free software for magnetic resonance spectroscopy data inspection, processing, simulation and analysis**

***First full-length publication showing results of novel spline baseline tool as featured by a colleague in:***
Gajdošík, Landheer, Swanberg, and Juchem. *Sci Rep* (2021); 11, 2094.

# Optimizing $^1$H MRS: Spectral Quantification

## Chapter 2: Spectral Quantification

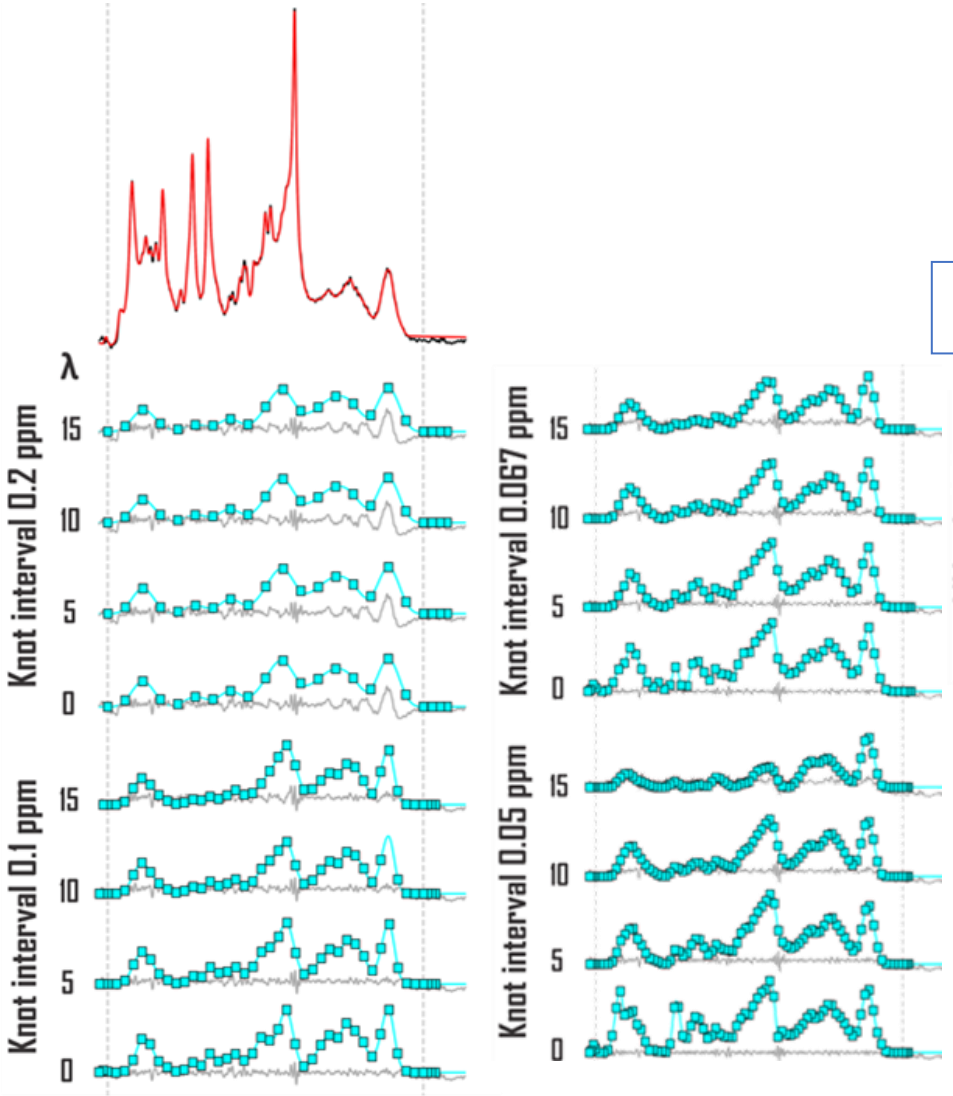


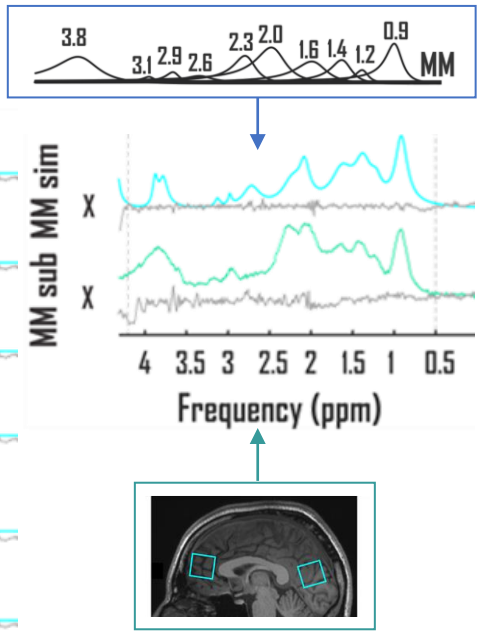


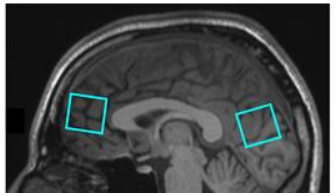

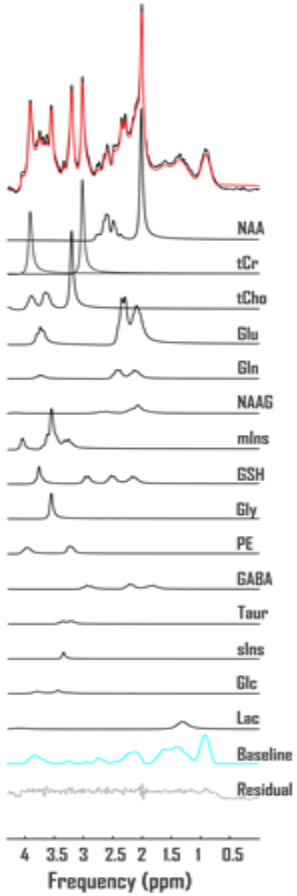


*In collaboration with:*

*Martin Gajdošík, Ph.D.*

*Karl Landheer, Ph.D.*

*Michael Treacy, B.A.*

sLASER[1] ($T_E$ 20.1 ms; $T_R$ 2 s)
DOTCOPS-optimized crushers[2]
16-step phase cycling[3]
3 T Siemens MAGNETOM Prisma

[1]Landheer et al. (2020). *NMR Biomed* e4324
[2]Landheer et al. (2020). *MRM* 81(4).
[3]Landheer et al. (2019). *MRM*. 83(2).

Swanberg, Landheer, Gajdošík, Treacy, and Juchem. *Proc Intl Soc Mag Reson Med.* (2020); 2856.

## Macromolecule prediction error

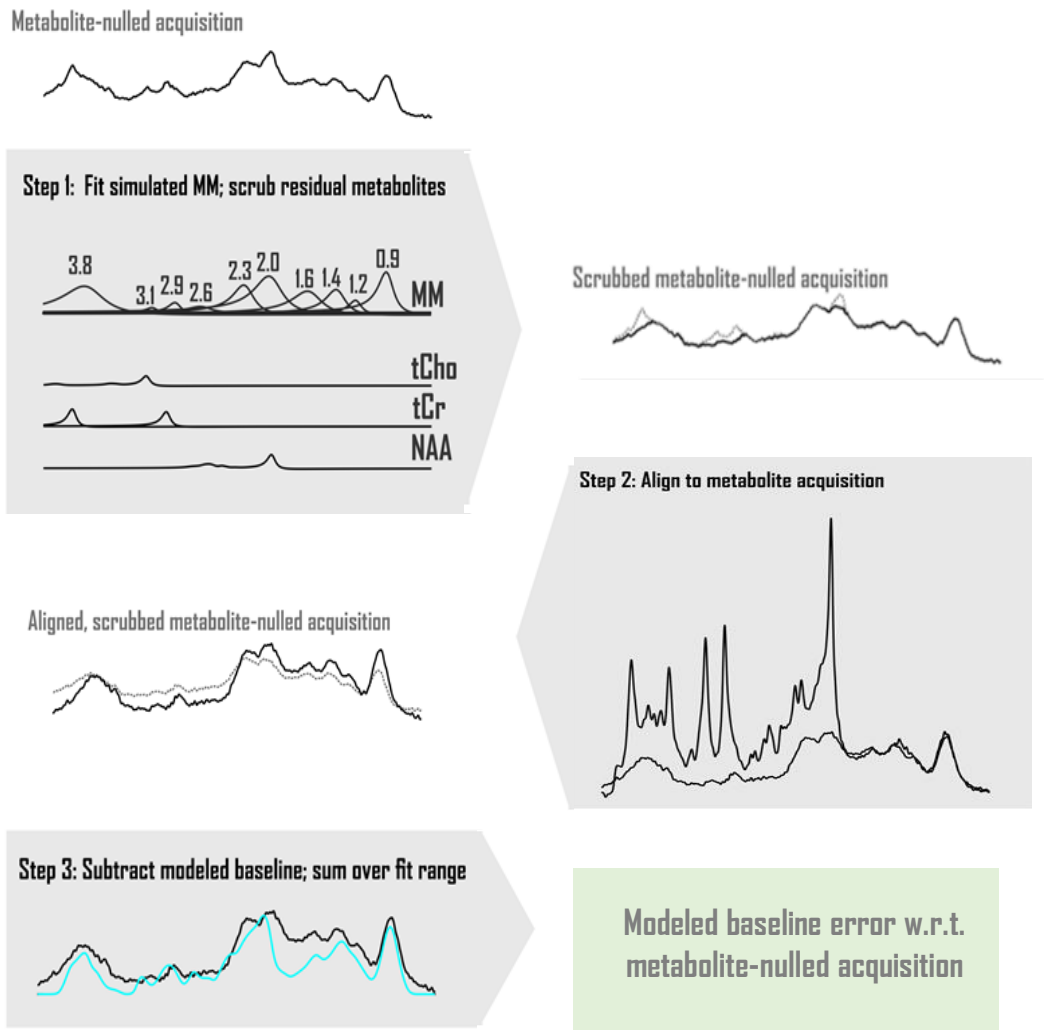


## Metabolite quantification error

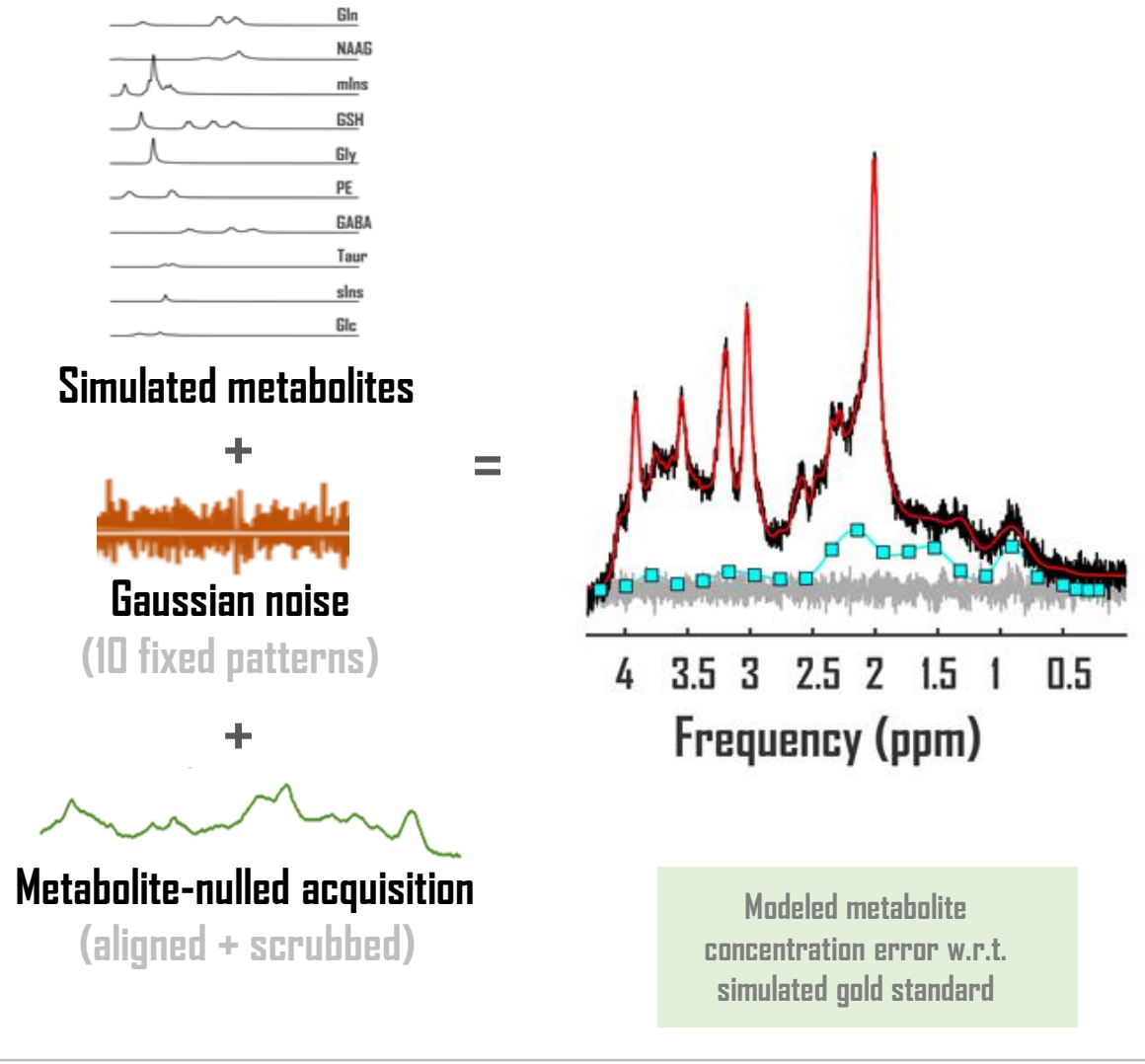


Swanberg, Landheer, Gajdošík, Treacy, and Juchem. *Proc Intl Soc Mag Reson Med.* (2020); 2856.

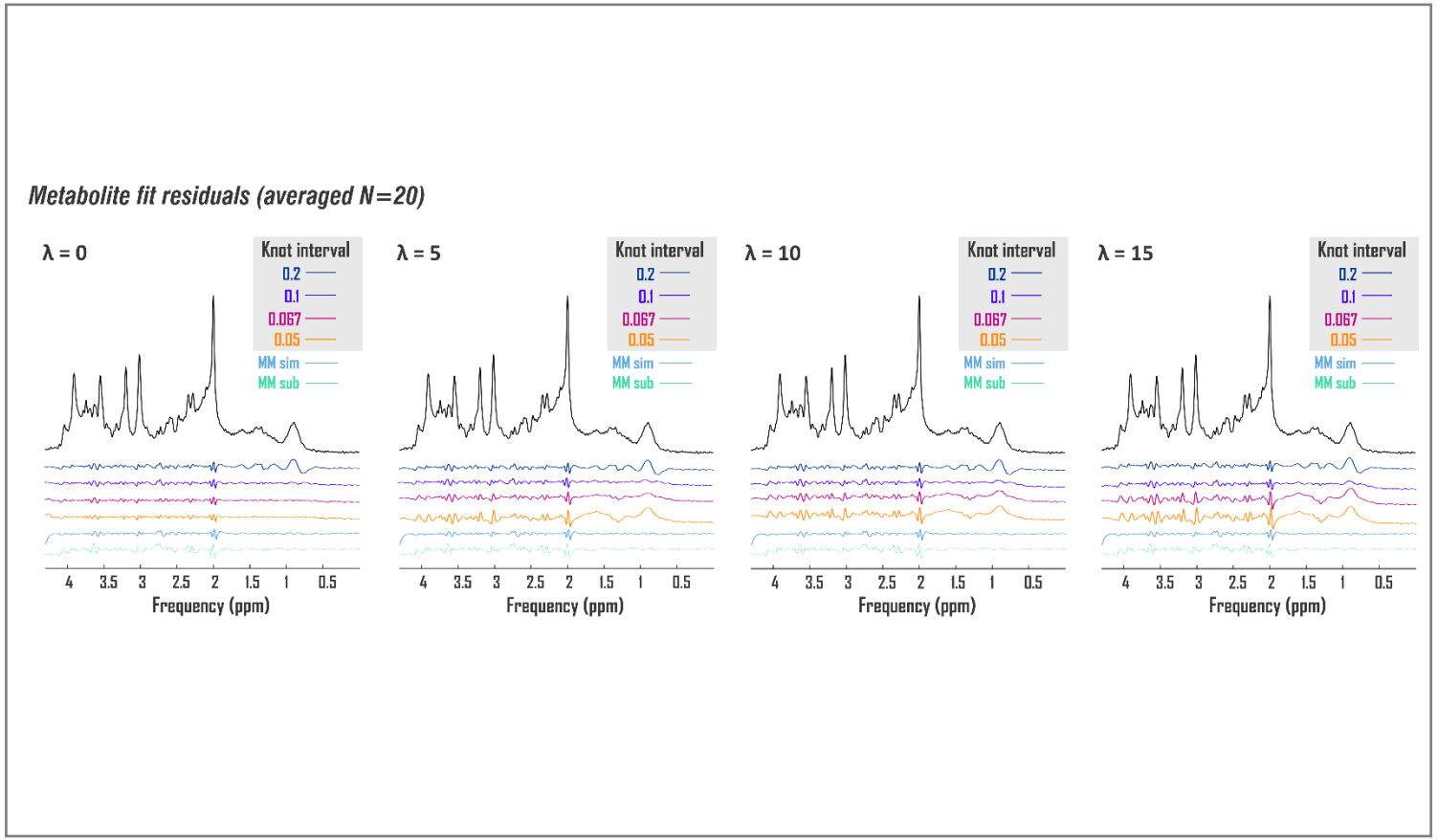


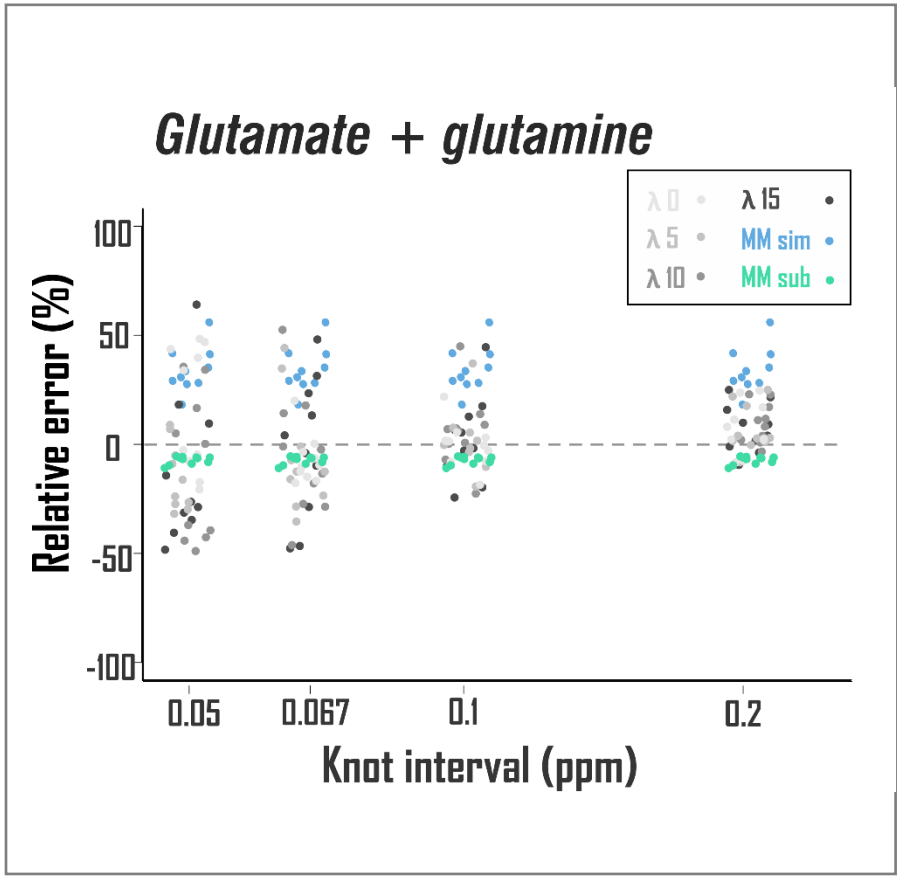


Swanberg, Landheer, Gajdošík, Treacy, and Juchem. *Proc Intl Soc Mag Reson Med*. (2020); 2856.

Fit residual is not a reliable proxy for metabolite quantification accuracy.

Chapter 2: Spectral Quantification

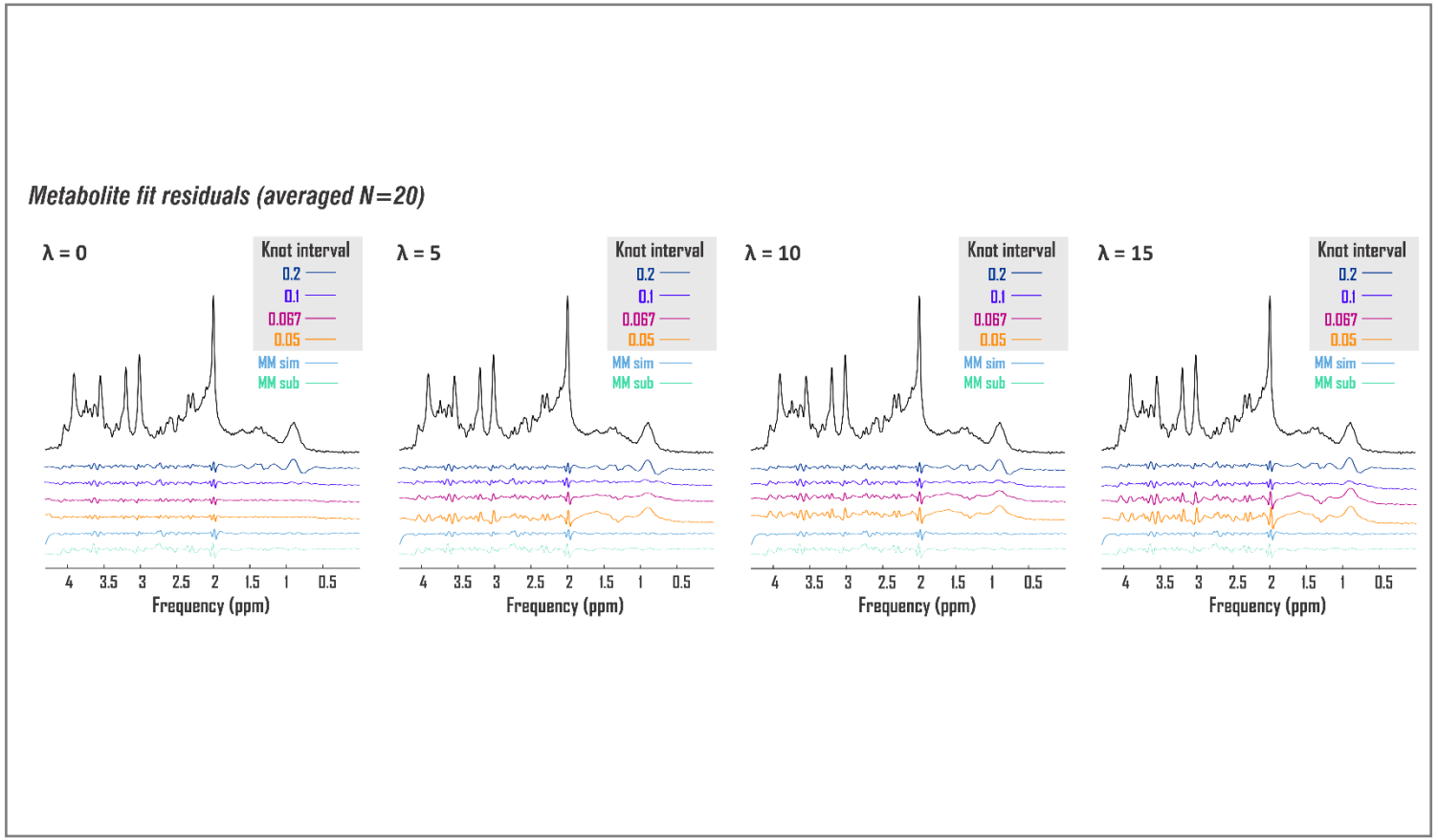


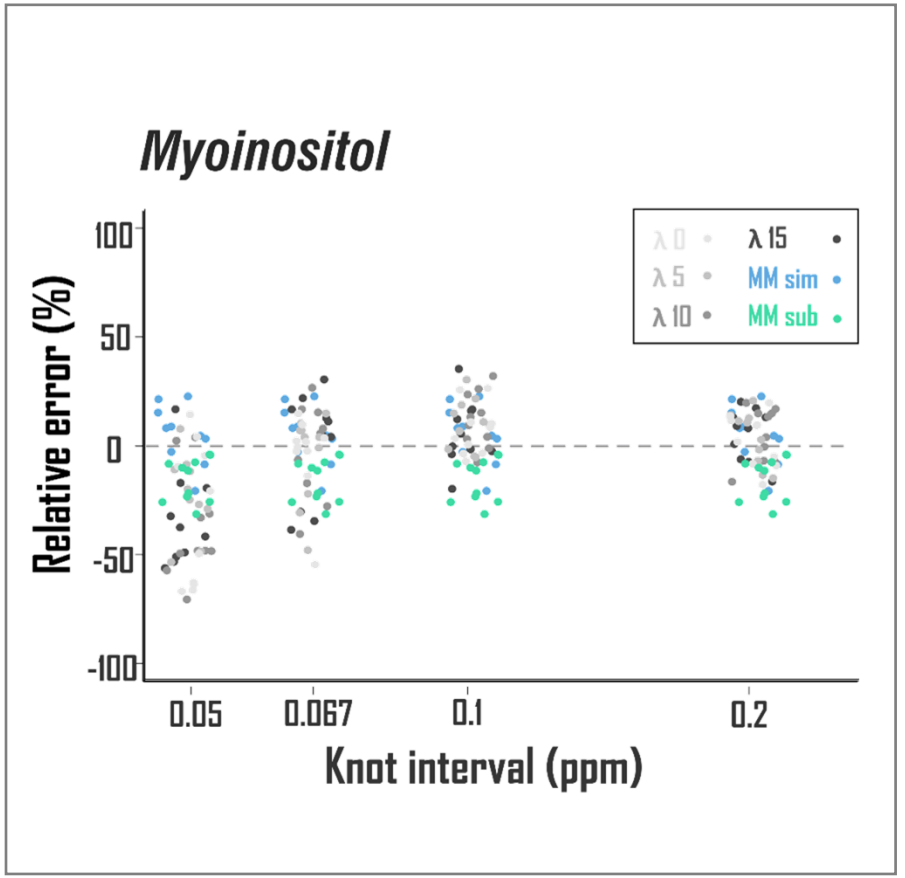


Swanberg, Landheer, Gajdošík, Treacy, and Juchem. *Proc Intl Soc Mag Reson Med*. (2020); 2856.

Fit residual is not a reliable proxy for metabolite quantification accuracy.

$$\sigma_{p_l} \geq \mathrm{CRB}_{p_l}$$

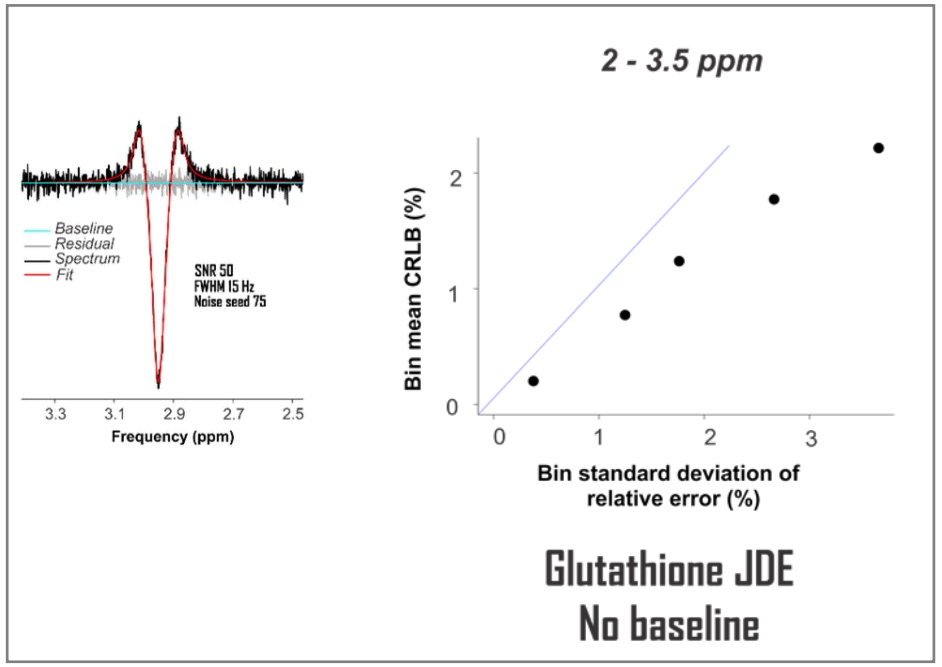


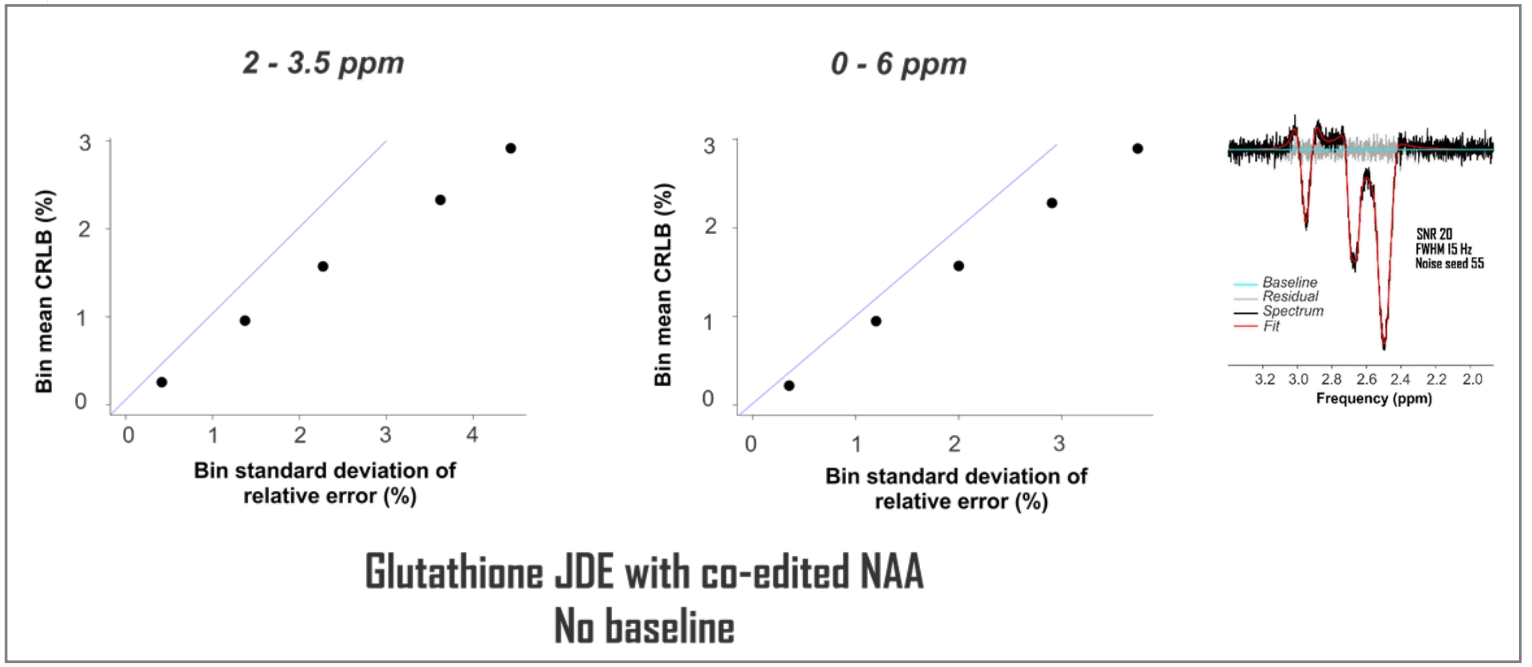


Swanberg, Prinsen, and Juchem. *Proc Intl Soc Mag Reson Med*. (2019); 4237.

In the absence of a gold standard, the Cramér-Rao Lower Bound can help to approximate in vivo fit errors.

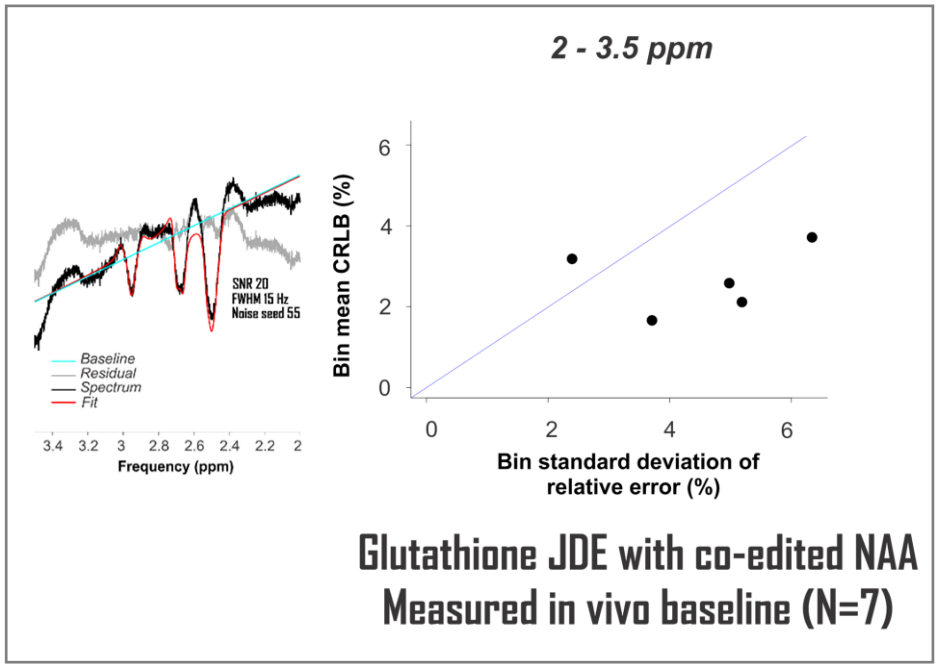


Swanberg, Prinsen, and Juchem. *Proc Intl Soc Mag Reson Med*. (2019); 4237.

| Metabolite | $a_m^{true}$ (a.u.) | $a_m^{est}$ (a.u.) | $2 \times CRB_{a_m}^{est}$ (a.u.) | $2 \times CRB_{a_m,\theta}^{est}$ (a.u.) |
|---|---|---|---|---|
| NAA | 13.00 | 12.00 | 0.77 | 1.10 |
| Cr_PCr | 6.00 | 5.95 | 0.46 | 0.59 |
| Cho | 2.00 | 1.82 | 0.48 | 0.52 |
| mI | 5.50 | 6.10 | 2.20 | 2.31 |
| Glx | 13.50 | 16.89 | 2.70 | 3.20 |

Ratiney et al. *MAGMA* 16 (2004); 284.

But this relationship between Cramér-Rao Lower Bound and fit error depends on inclusion of baseline terms.

$$\sigma_{p_l} \geq \mathrm{CRB}_{p_l} = \sqrt{(F^{-1})_{ll}} \longleftarrow F = \frac{1}{\sigma^2}\Re(P^{\mathrm{T}}D^{\mathrm{H}}DP)$$

- $\sigma$ S.D. of noise amplitude
- $D$ Partial derivative of model w.r.t. each parameter
- $P$ Prior knowledge matrix

## $D$ (example columns for spline baseline amplitudes; real part shown)

2.4-2.6 ppm

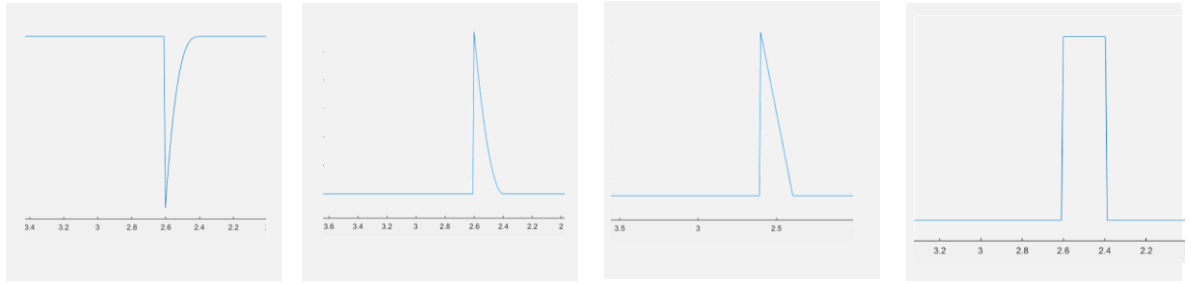

Model P.D. w.r.t. degree 3 baseline component amplitude | Model P.D. w.r.t. degree 2 baseline component amplitude | Model P.D. w.r.t. degree 1 baseline component amplitude | Model P.D. w.r.t. degree 0 baseline component amplitude

2.6-2.8 ppm

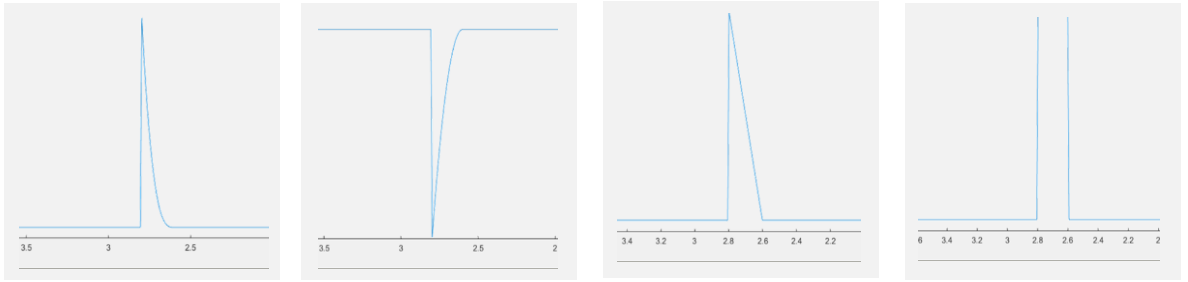

Model P.D. w.r.t. degree 3 baseline component amplitude | Model P.D. w.r.t. degree 2 baseline component amplitude | Model P.D. w.r.t. degree 1 baseline component amplitude | Model P.D. w.r.t. degree 0 baseline component amplitude

## $P$ (incorporating baseline terms)

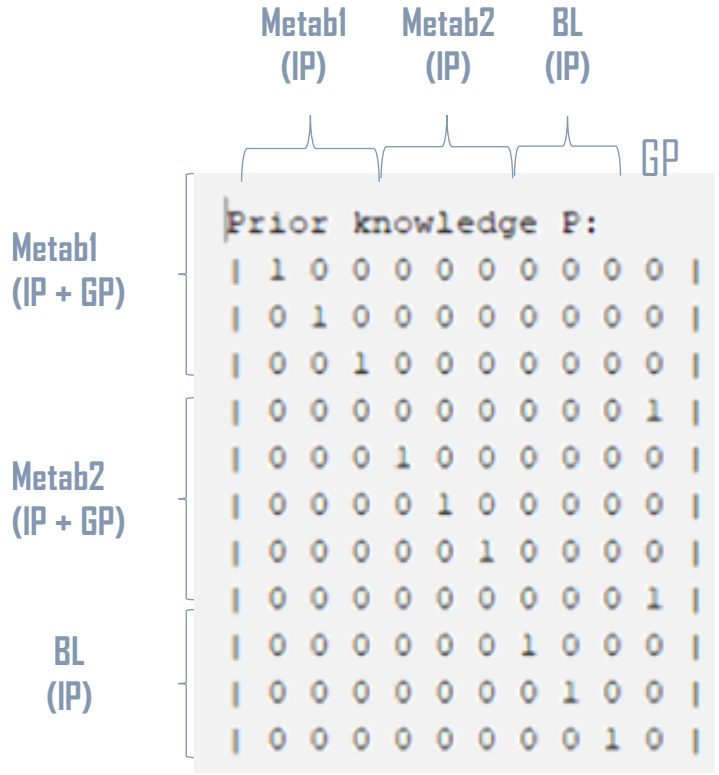


Baseline terms can be included in Cramér-Rao Lower Bound calculations as scaled polynomial shapes.

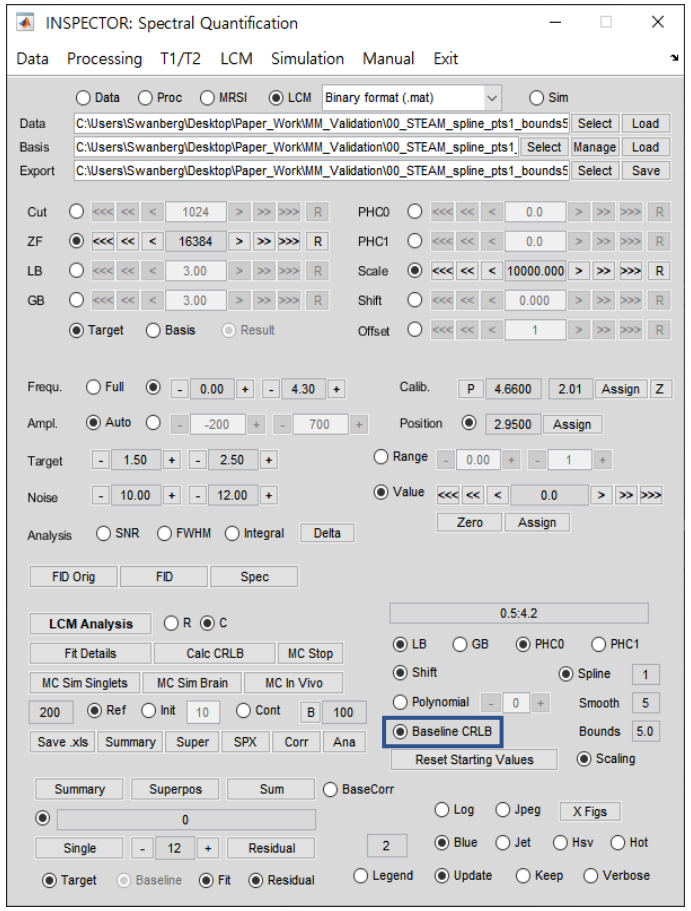


```
Full D:  2 metabs * 4 metab-specific pars + 41 polynomial baseline coefficients = 49
After P: 2 metabs * 3 metab-specific pars + 1 global pars + 41 polynomial baseline coefficients = 48 fit pars (CRLB)

Summary of amplitude CRLBs:
GSH:  4.610%
NAA:  1.092%

CRLB(amplitude)                 = [4.609992 1.091928]%
CRLB(LB)                        = [0.549687 0.124653] Hz
CRLB(Shift)                     = [0.143785 0.060952] Hz
CRLB(PHC0)                      = 0.629687 deg
CRLB(Spline, 1.97 - 2.03 ppm)   = [29.645544]%
CRLB(Spline, 2.03 - 2.10 ppm)   = [47.097105 53.157634 43.573187 32.961269]%
CRLB(Spline, 2.10 - 2.20 ppm)   = [47.024316 22.876282 9.182262 2.528464]%
CRLB(Spline, 2.20 - 2.40 ppm)   = [37.387031 26.199661 36.470409 0.793382]%
CRLB(Spline, 2.40 - 2.60 ppm)   = [79.686996 55.116961 50.446840 0.972640]%
CRLB(Spline, 2.60 - 2.80 ppm)   = [219.076590 122.924176 85.723342 0.869879]%
CRLB(Spline, 2.80 - 3.00 ppm)   = [643.838396 519.757889 134.353913 0.800714]%
CRLB(Spline, 3.00 - 3.20 ppm)   = [336.323145 728.388733 168.856288 0.793278]%
CRLB(Spline, 3.20 - 3.30 ppm)   = [14.314476 151.906508 38.210219 1.333068]%
CRLB(Spline, 3.30 - 3.37 ppm)   = [50.064434 35.881835 13.488720 2.995382]%
CRLB(Spline, 3.37 - 3.43 ppm)   = [379.114049 211.640147 101.542109 40.847510]%

LCMODEL ANALYSIS SUMMARY:
(errors as CRLB / Hessian of LSQ)
GSH:  2.36 mM (3.845, 4.6/9.5%) / LB 11.9 Hz (0.5/1.2 Hz) / Shift -3.58 Hz (0.1/0.3 Hz)
NAA:  10.00 mM (16.316, 1.1/2.2%) / LB 7.2 Hz (0.1/0.3 Hz) / Shift -1.06 Hz (<0.1/0.1 Hz)
PHC0: 5.9 deg (0.6/1.2 deg)
```

***Tool 3:*** *GUI-supported polynomial and cubic spline baseline error definitions by geometry-based calculation of Cramer-Rao Lower bound*

Baseline terms can be included in Cramér-Rao Lower Bound calculations as scaled polynomial shapes.

## Chapter 2: Spectral Quantification

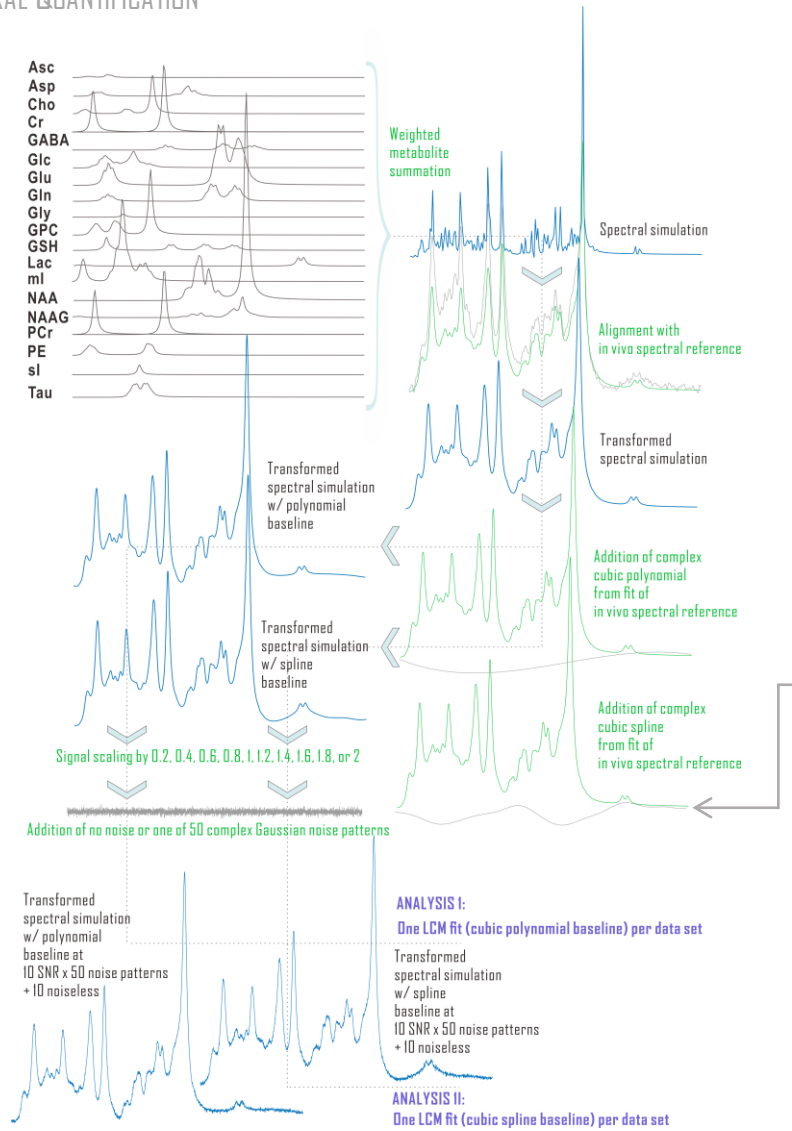


*Sample baselines and residuals for representative prefrontal cortex spectrum (N=1) by spline baseline definition*

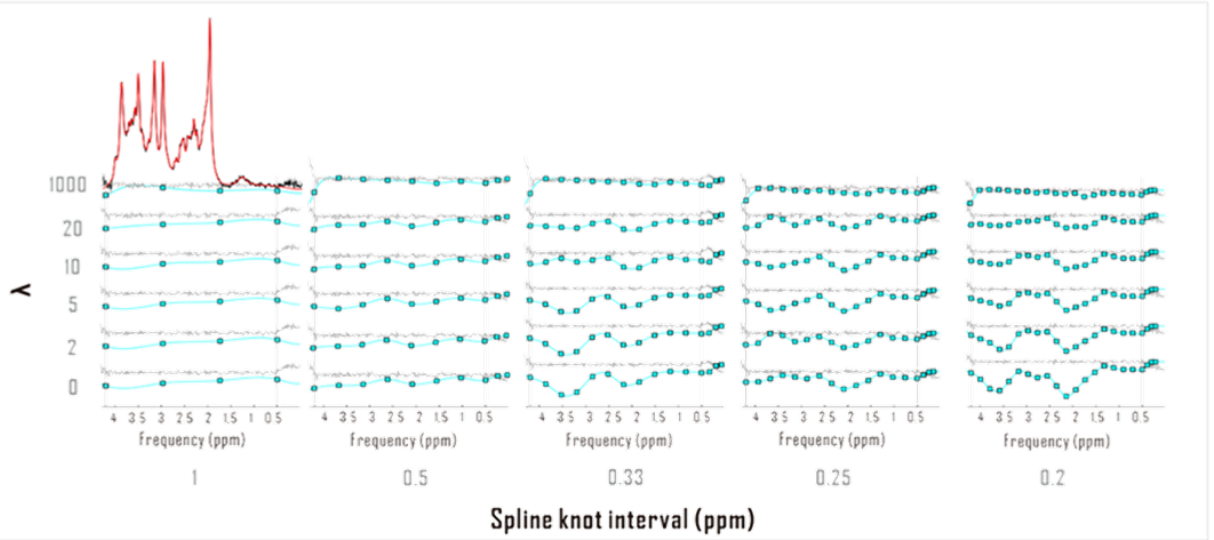


*Prefrontal cortex metabolite between-subjects (N=10) coefficients of variation by spline baseline definition*

**tNAA : tCr**

| Spline λ \ Spline knot interval (ppm) | 1 | 0.5 | 0.33 | 0.25 | 0.2 |
|---|---|---|---|---|---|
| 1000 | 11.4 | 11.2 | 12.4 | 11.9 | 11.9 |
| 20 | 12.3 | 8.2 | 9.3 | 6.7 | 11.0 |
| 10 | 11.5 | 9.8 | 10.9 | 7.6 | 9.9 |
| 5 | 12.1 | 9.4 | 10.5 | 6.4 | 10.6 |
| 2 | 12.6 | 11.4 | 11.4 | 6.6 | 16.7 |
| 0 | 11.3 | 10.9 | 11.6 | 12.0 | 19.4 |

**Glx : tCr**

| Spline λ \ Spline knot interval (ppm) | 1 | 0.5 | 0.33 | 0.25 | 0.2 |
|---|---|---|---|---|---|
| 1000 | 12.5 | 12.0 | 13.6 | 12.5 | 12.7 |
| 20 | 12.9 | 13.4 | 15.8 | 16.3 | 11.5 |
| 10 | 11.2 | 13.2 | 21.8 | 31.5 | 28.1 |
| 5 | 14.1 | 13.5 | 16.4 | 24.5 | 36.3 |
| 2 | 13.6 | 14.0 | 20.9 | 33.0 | 33.1 |
| 0 | 10.5 | 13.1 | 25.6 | 36.2 | 29.3 |

Swanberg, Gajdošík, Landheer, and Juchem. *Proc Intl Soc Mag Reson Med*. (2021); 2010.

## Cubic polynomial baselines

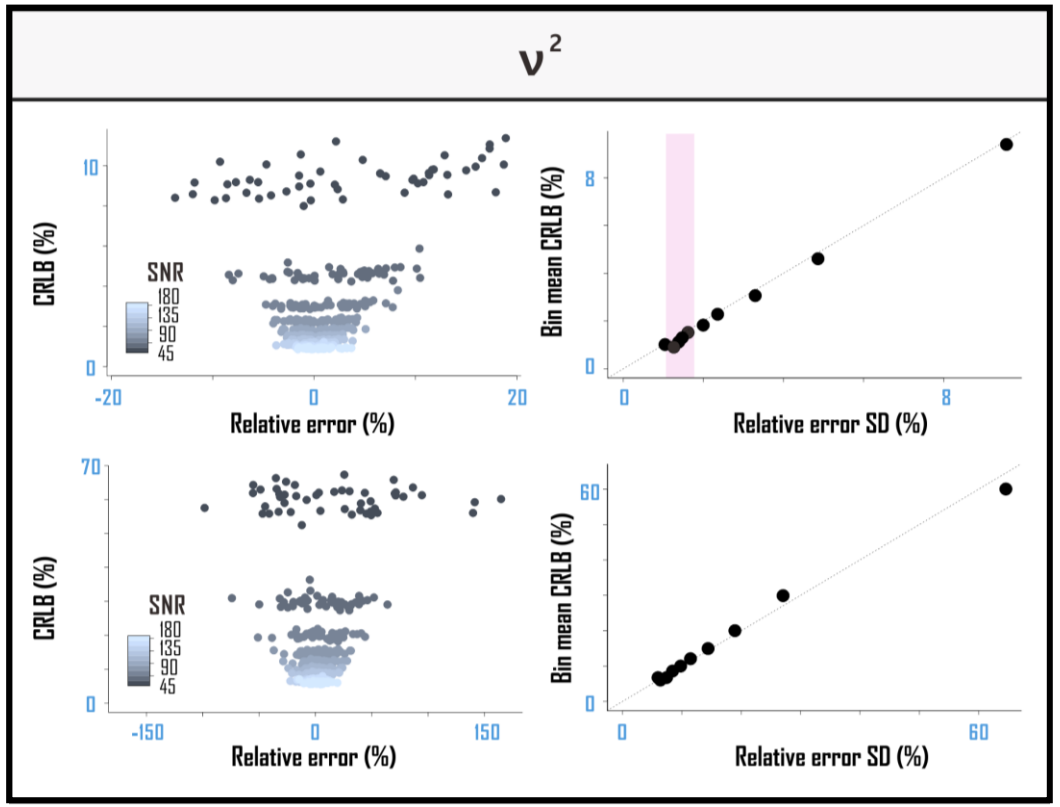


*Shapiro-Wilk test indicates that fit error distribution significantly differs from normality*

## Cubic spline baselines (2.35-2.61 ppm shown)

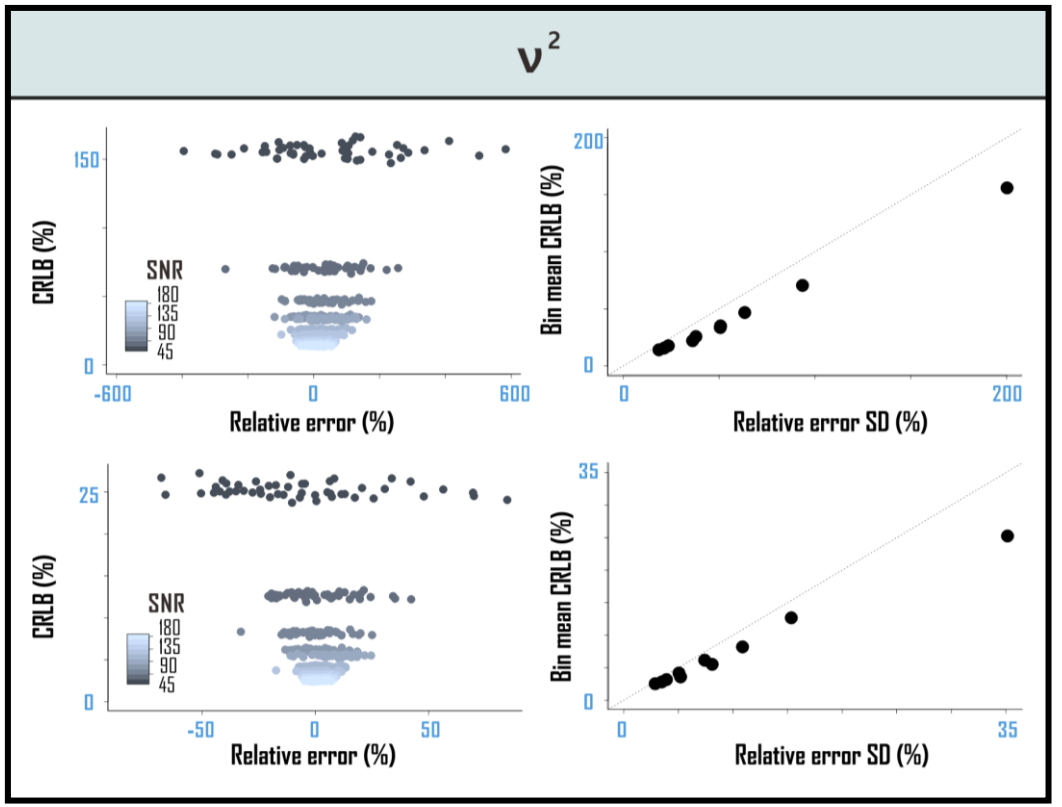


Swanberg, Gajdošík, Landheer, and Juchem. *Proc Intl Soc Mag Reson Med*. (2021); 2010.

Inclusion of baseline terms in Cramér-Rao Lower Bound calculations as scaled polynomial shapes provides estimates of baseline fit error.

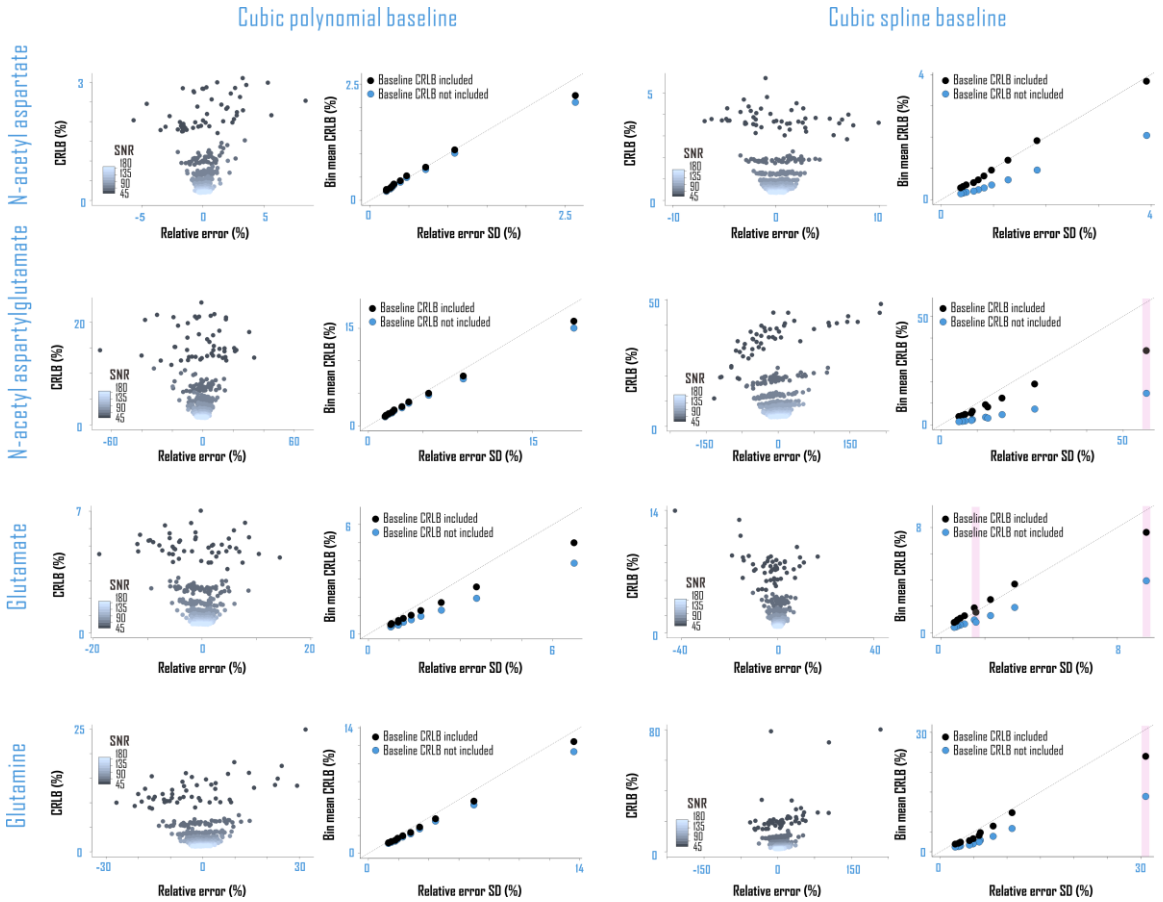


*Shapiro-Wilk test indicates that fit error distribution significantly differs from normality*

Swanberg, Gajdošík, Landheer, and Juchem. *Proc Intl Soc Mag Reson Med*. (2021); 2010.

Inclusion of baseline terms in Cramér-Rao Lower Bound calculations as scaled polynomial shapes improves CRLB estimates of metabolite fit error.

## The Big Picture:

$^1$H MRS is a potential but currently untapped source of clinical diagnostic biomarkers.

Chapter I

## Spectral Quantification:

Data quality (FWHM and SNR) interacts with spectral baselines to affect metabolite fit accuracy.

Fit residual can be misleading when deciding whether a spectral baseline model supports accurate metabolite estimates.

Incorporating baseline terms to the Fisher information matrix improves utility of CRLB as a proxy for metabolite fit precision.

Chapter II

## Absolute Quantification:

Can disease-related differences in metabolite $T_2$ introduce systematic errors to the derivation of absolute from relative metabolite concentrations, and how do we minimize them?

Chapter III

## Statistical Analysis:

Can single- or multivariate analysis of metabolite concentrations derived from optimized quantification of $^1$H MRS data alone classify disease states (case application multiple sclerosis)?

Chapter IV

## Generalization:

Can a quantification and statistics pipeline optimized for classification of multiple sclerosis via $^1$H MRS-derived metabolite concentrations be generalized to identification of PTSD and MDD?

Chapter V

## Back to the Big Picture:

General conclusions and outlook

Chapter VI

$\Phi_{0,1}$ = zero-, first-order phase
$N_M$ = number of metabolites
$C_l$ = Metabolite concentrations
$N_B$ = number of baseline splines
B = baseline spline
$S_n$ = metabolite basis function lineshape coefficients
ν = frequency domain value
γ = line broadening parameter
ε = frequency shift parameter

$$\widehat{Y}(\nu_k) = e^{-i(\phi_0+\nu\phi_1)}\left[\sum_{j=1}^{N_B}\beta_j B_j(\nu_k) + \sum_{l=1}^{N_M} C_l \sum_{n=-N_s}^{N_s} S_n M_l(\nu_{k-n}, \gamma_l, \epsilon_l)\right]$$

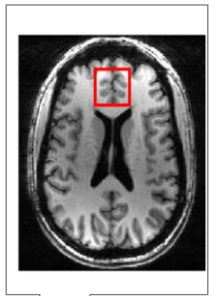

Analog preprocessing

Digital preprocessing

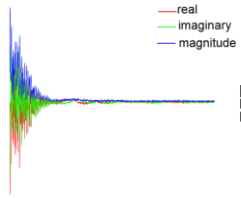


FFT

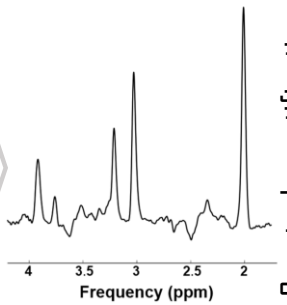


Spectral quantification

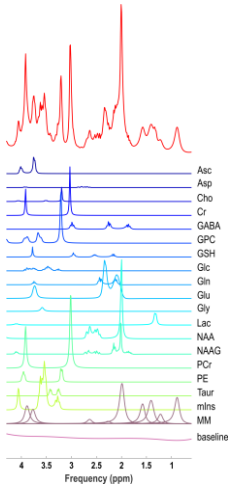


**Metabolite signal intensities (a.u.)**

Absolute quantification

**Metabolite concentrations (mM)**

*Metabolite concentrations by tissue*
*Intracellular vs. extracellular metabolite concentration*
*Intracellular metabolite concentrations within cell types of interest*
*Biological functions of metabolite with respect to cell types of interest*
*…And more*

***Biological interpretation***

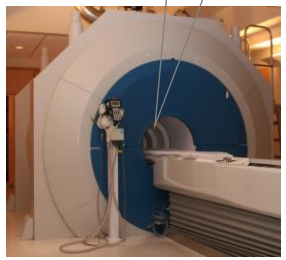

***Chapter III***

***Absolute Quantification:*** *Can disease-related differences in metabolite $T_2$ introduce systematic errors to the derivation of absolute from relative metabolite concentrations, and how do we minimize them?*

$$f_c = (1-F_{CSF})^{-1}\left[\frac{2M_w\sum_{i=GM,WM,CSF}(F_i\beta_i)}{N_h S_w}\right]\frac{\sum_{i=GM,WM,CSF}\left[F_i\left(e^{\frac{-T_E}{T_{2wi}}}\right)\left(1-e^{\frac{-T_R}{T_{1wi}}}\right)\right]}{e^{\frac{-T_E}{T_{2m}}}\left(1-e^{\frac{-T_R}{T_{1m}}}\right)}$$

$S_w$ = water signal scaling coefficient
2 = number of protons in water molecule
Nh = number of protons per molecule of metabolite to be quantified
$M_w$ = molarity of pure water
$\beta_i$ = molarity of water as a fraction of pure water in either grey matter (GM), white matter (WM), or CSF
$F_i$ = voxel fraction occupied by grey matter (GM), white matter (WM), or CSF
$T_{2wi}$ = $T_2$ of water in grey matter (GM), white matter (WM), or CSF
$T_{1wi}$ = $T_1$ of water in grey matter (GM), white matter (WM), or CSF
$T_{2m}$ = $T_2$ of metabolite
$T_{1m}$ = $T_1$ of metabolite
$T_E$ = echo time of sequence
$T_R$ = repetition time of sequence

CHAPTER 3: ABSOLUTE QUANTIFICATION

$$f_c = (1 - F_{CSF})^{-1} \left[ \frac{2M_w \sum_{i=GM,WM,CSF}(F_i \beta_i)}{N_h S_w} \right] \frac{\sum_{i=GM,WM,CSF} \left[ F_i \left( e^{\frac{-T_E}{T_{2wi}}} \right) \left( 1 - e^{\frac{-T_R}{T_{1wi}}} \right) \right]}{e^{\frac{-T_E}{T_{2m}}} \left( 1 - e^{\frac{-T_R}{T_{1m}}} \right)}$$

Final result

| | |
|---|---|
| $f_c$ | conversion factor from spectral quantification scaling coefficient to absolute concentration |

Accounting for proton number and estimating water molarity in voxel

| | |
|---|---|
| $S_w$ | water signal scaling coefficient |
| 2 | number of protons in water molecule |
| Nh | number of protons per molecule of metabolite to be quantified |
| $M_w$ | molarity of pure water |
| $\beta_i$ | molarity of water as a fraction of pure water in either grey matter (GM), white matter (WM), or CSF |
| $F_i$ | voxel fraction occupied by grey matter (GM), white matter (WM), or CSF |

Accounting for relaxation differences between water and metabolite

| | |
|---|---|
| $T_{2wi}$ | $T_2$ of water in grey matter (GM), white matter (WM), or CSF |
| $T_{1wi}$ | $T_1$ of water in grey matter (GM), white matter (WM), or CSF |
| $T_{2m}$ | $T_2$ of metabolite |
| $T_{1m}$ | $T_1$ of metabolite |
| $T_E$ | echo time of sequence |
| $T_R$ | repetition time of sequence |

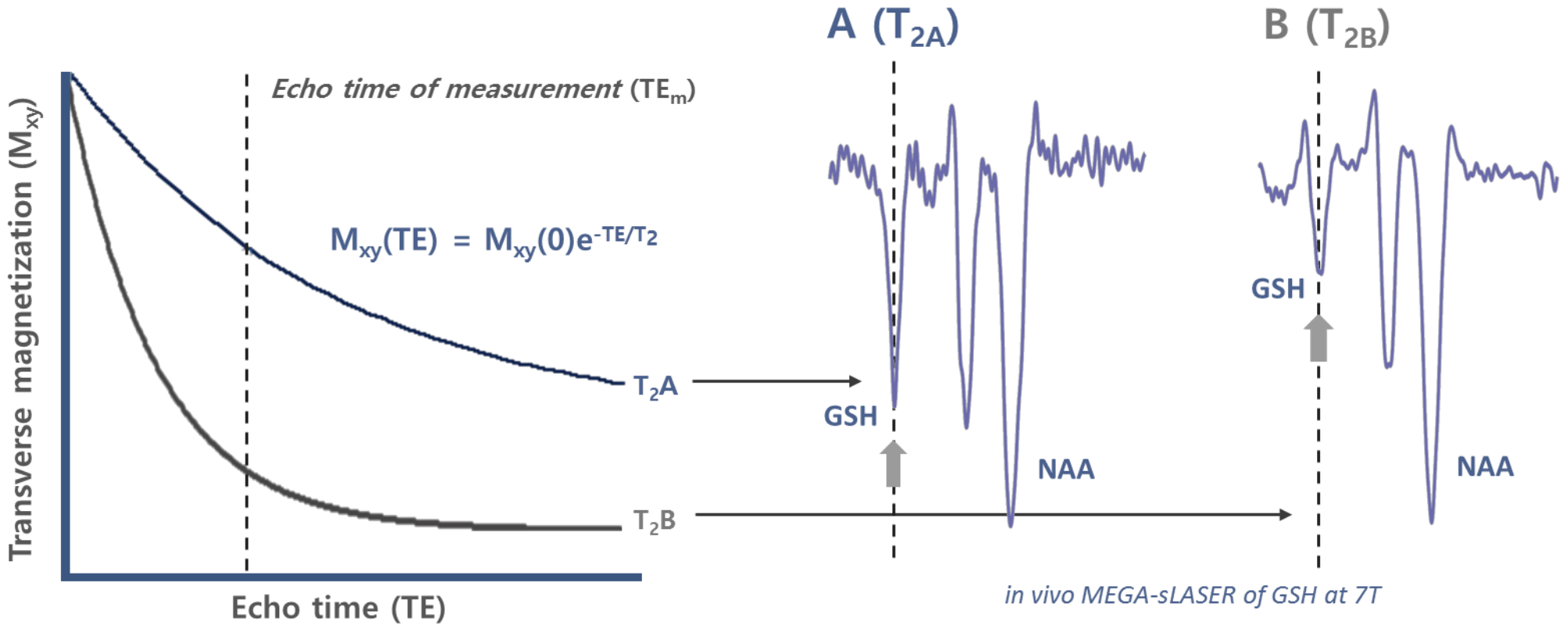


**[A] = [B], but $T_{2A} > T_{2B}$, so at $TE_M$ $M_{xy}A > M_{xy}B$**

# Optimizing $^1$H MRS: Absolute Quantification



**MS → increases in water $T_2$ for:**

- normal-appearing white matter
- non-enhancing lesions
- contrast-enhancing lesions
- dirty-appearing white matter
- $T_1$-hypointense lesions

**MS → decreases in metabolite $T_2$ for:**

- normal-appearing white matter
- normal-appearing grey matter
- white-matter lesions

Swanberg, Landheer, Pitt, and Juchem. *Frontiers in Neurology* 10 (2019): 1173.

A review has shown that water $T_2$ relaxation may change with multiple sclerosis disease state.

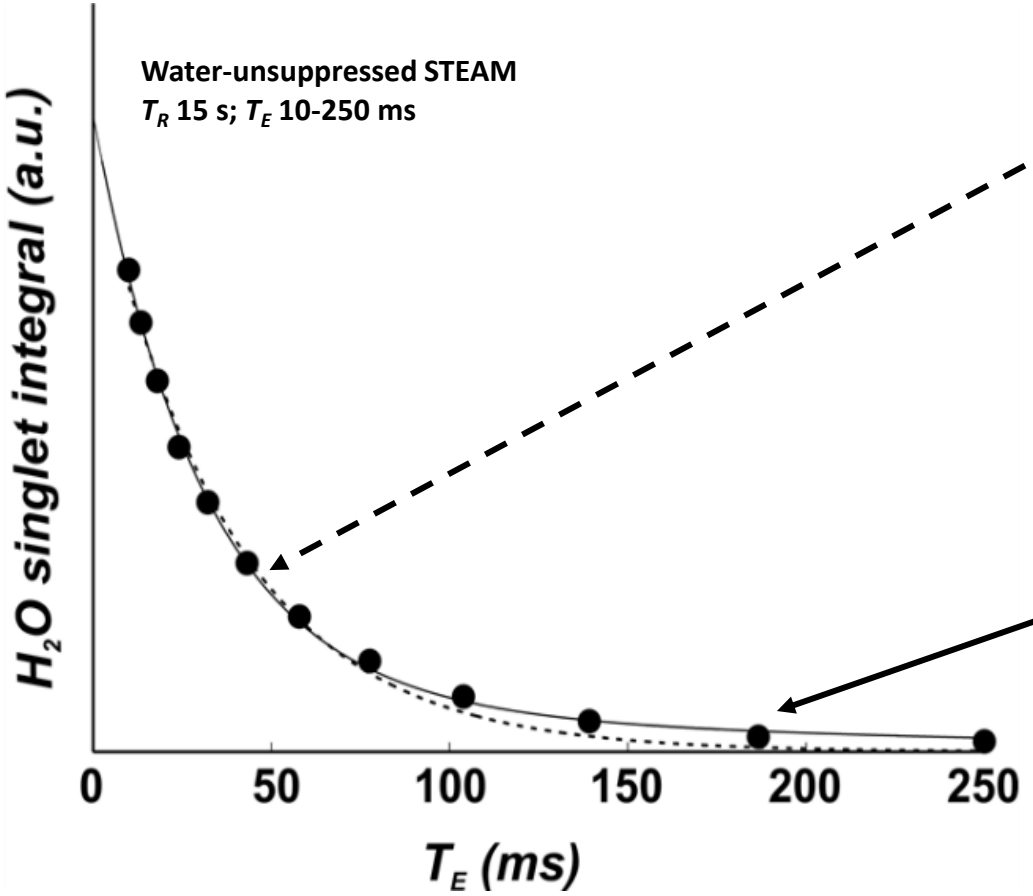


## Monoexponential

$$M_{TE} = M_0 e^{\frac{-T_E}{T_2}}$$

## Biexponential with fixed coefficients

$$M_{TE} = M_0 \left( \chi_t e^{\frac{-T_E}{T_{2t}}} + \chi_f e^{\frac{-T_E}{T_{2f}}} \right)$$

$$\chi_t = \frac{PV_{gm}[H_2O]_{gm} + PV_{wm}[H_2O]_{wm}}{PV_{gm}[H_2O]_{gm} + PV_{wm}[H_2O]_{wm} + PV_{csf}[H_2O]_{csf}}$$

$$\chi_f = \frac{PV_{csf}[H_2O]_{csf}}{PV_{gm}[H_2O]_{gm} + PV_{wm}[H_2O]_{wm} + PV_{csf}[H_2O]_{csf}}$$

Swanberg, Prinsen, Kurada, Destefano, Bailey, Pitt, Fulbright, and Juchem. *Proc. Intl. Soc. Mag. Reson. Med.* (2018); 0161.

We first assessed voxel water $T_2$ using monoexponential modeling.

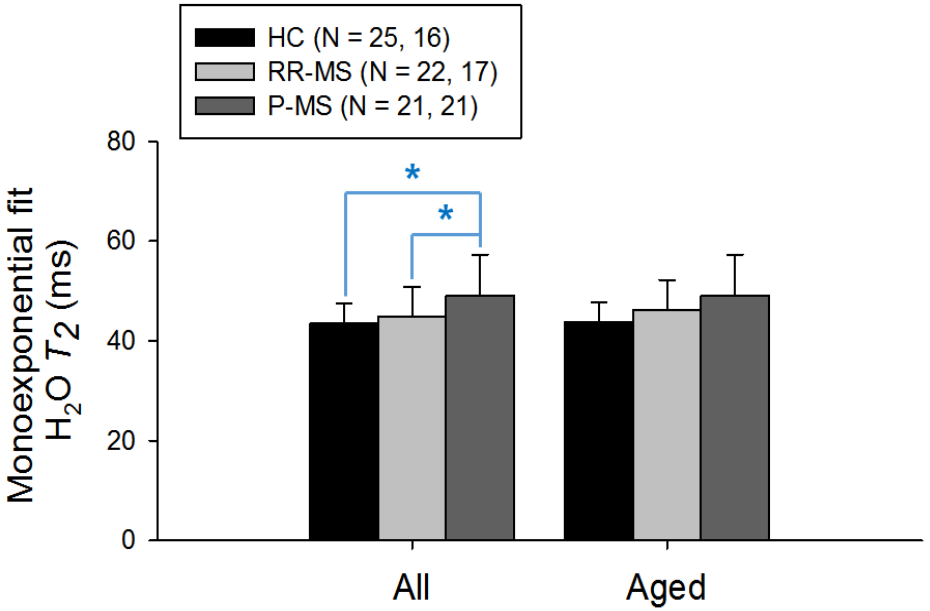


Mann-Whitney test $^*p < 0.05$

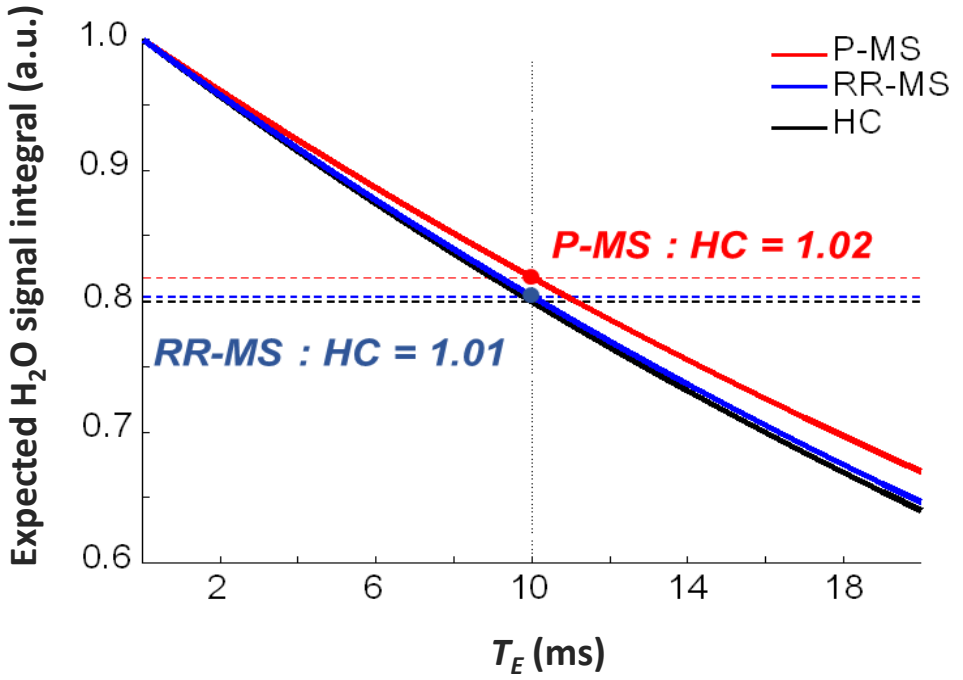


Swanberg, Prinsen, Kurada, Destefano, Bailey, Pitt, Fulbright, and Juchem. *Proc. Intl. Soc. Mag. Reson. Med.* (2018); 0161.

Monoexponentially modeled water $T_2$ was higher in the aged progressive MS group than the other two groups.

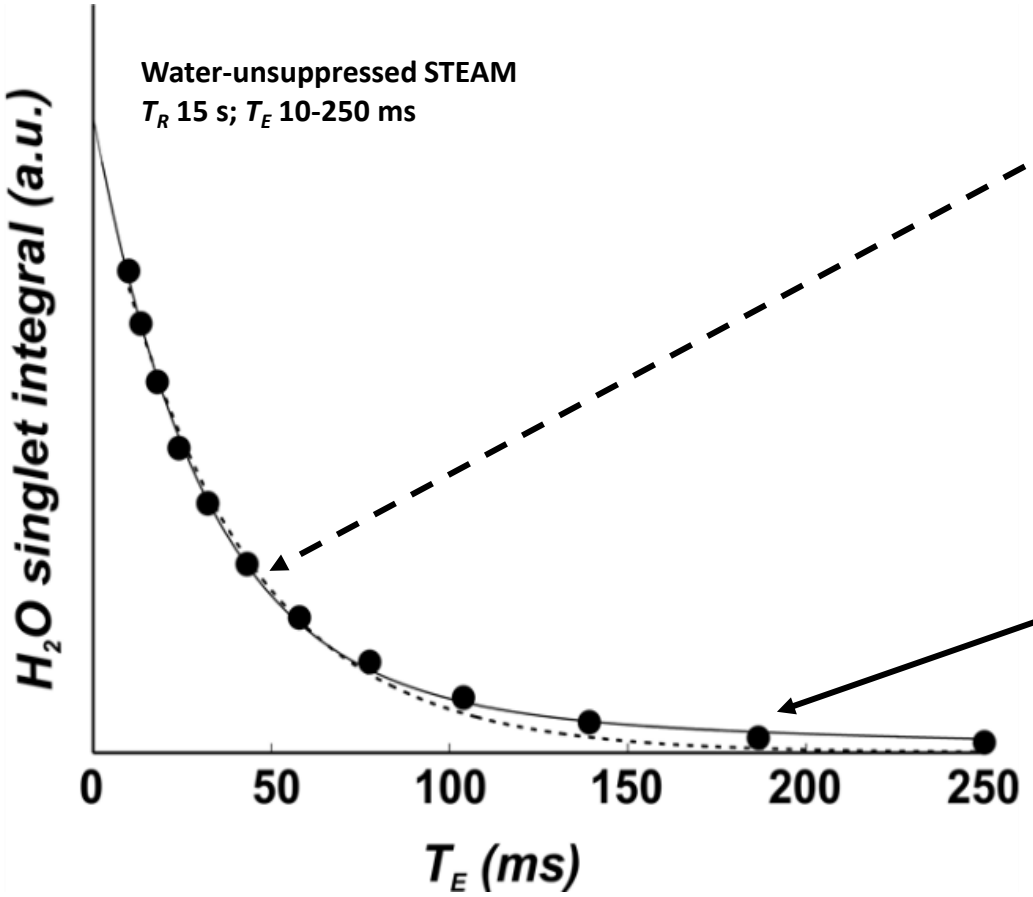


**Monoexponential**

$$M_{TE} = M_0 e^{\frac{-T_E}{T_2}}$$

**Biexponential with fixed coefficients**

$$M_{TE} = M_0 \left( \chi_t e^{\frac{-T_E}{T_{2t}}} + \chi_f e^{\frac{-T_E}{T_{2f}}} \right)$$

$$\chi_t = \frac{PV_{gm}[H_2O]_{gm} + PV_{wm}[H_2O]_{wm}}{PV_{gm}[H_2O]_{gm} + PV_{wm}[H_2O]_{wm} + PV_{csf}[H_2O]_{csf}}$$

$$\chi_f = \frac{PV_{csf}[H_2O]_{csf}}{PV_{gm}[H_2O]_{gm} + PV_{wm}[H_2O]_{wm} + PV_{csf}[H_2O]_{csf}}$$

Swanberg, Prinsen, Kurada, Destefano, Bailey, Pitt, Fulbright, and Juchem. *Proc. Intl. Soc. Mag. Reson. Med.* (2018); 0161.

We then assessed voxel water $T_2$ using biexponential modeling.

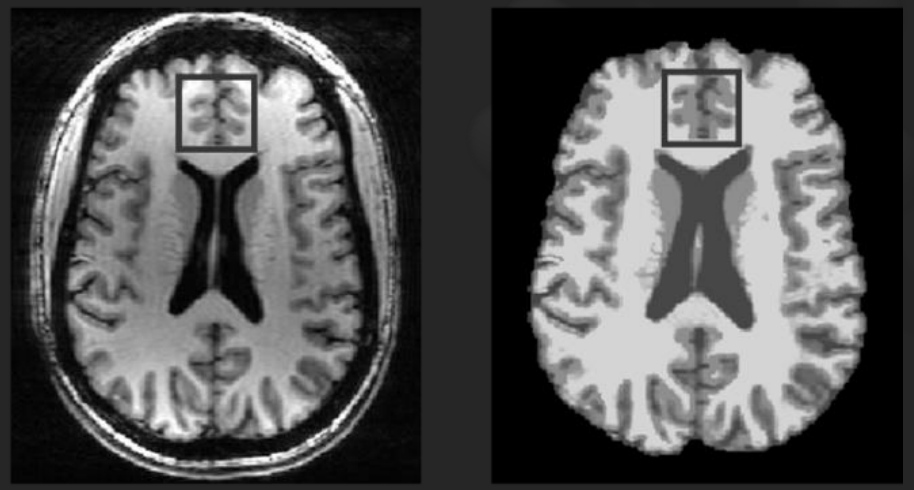

**Skull-stripping (FMRIB Brain Extraction Tool; BET) + segmentation (BrainSuite)**

Smith SM. *Human Brain Mapping* 2002; 17(3): 143-155
Shattuck D, Leahy RM. *Medical Image Analysis* 2002; 6(2): 129-142

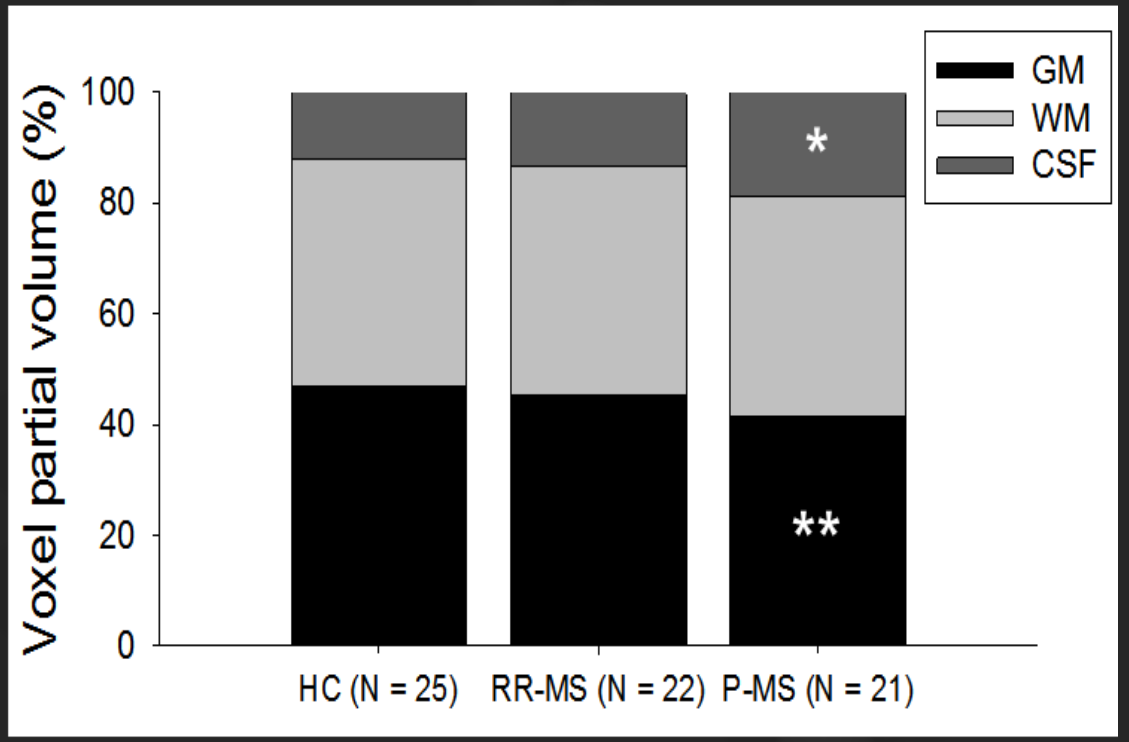


Mann-Whitney test v. HC $*p < 0.05$, $**p < 0.01$

*In collaboration with Abhinav Kurada, B.Sc.*

Swanberg, Prinsen, Kurada, Destefano, Bailey, Pitt, Fulbright, and Juchem. *Proc. Intl. Soc. Mag. Reson. Med.* (2018); 0161.

We controlled $T_2$ fits for voxel composition differences in relapsing-remitting, progressive, and no MS.

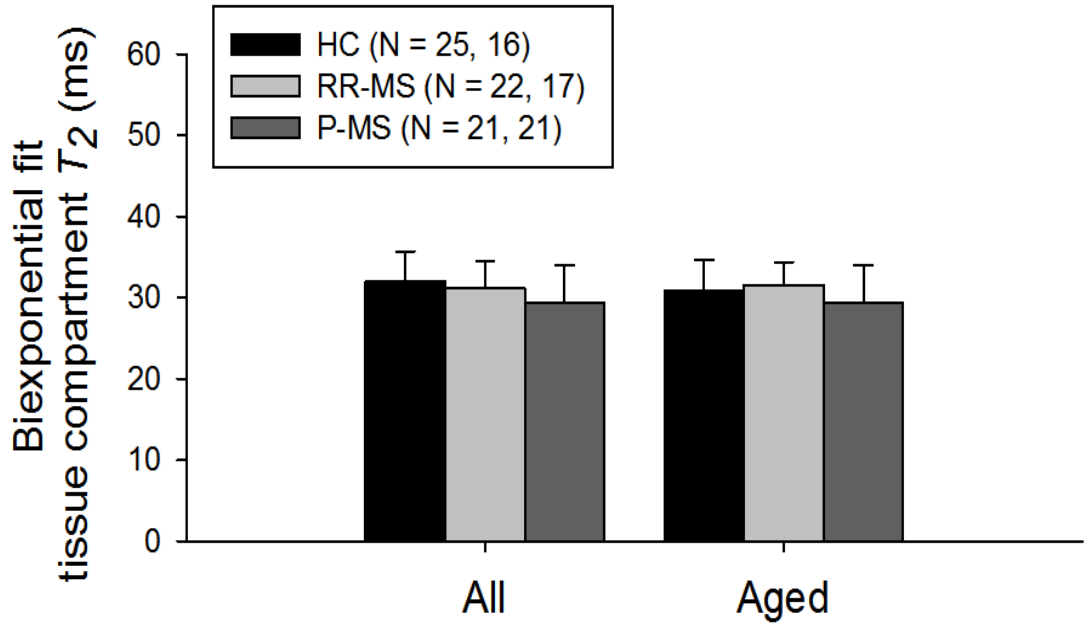


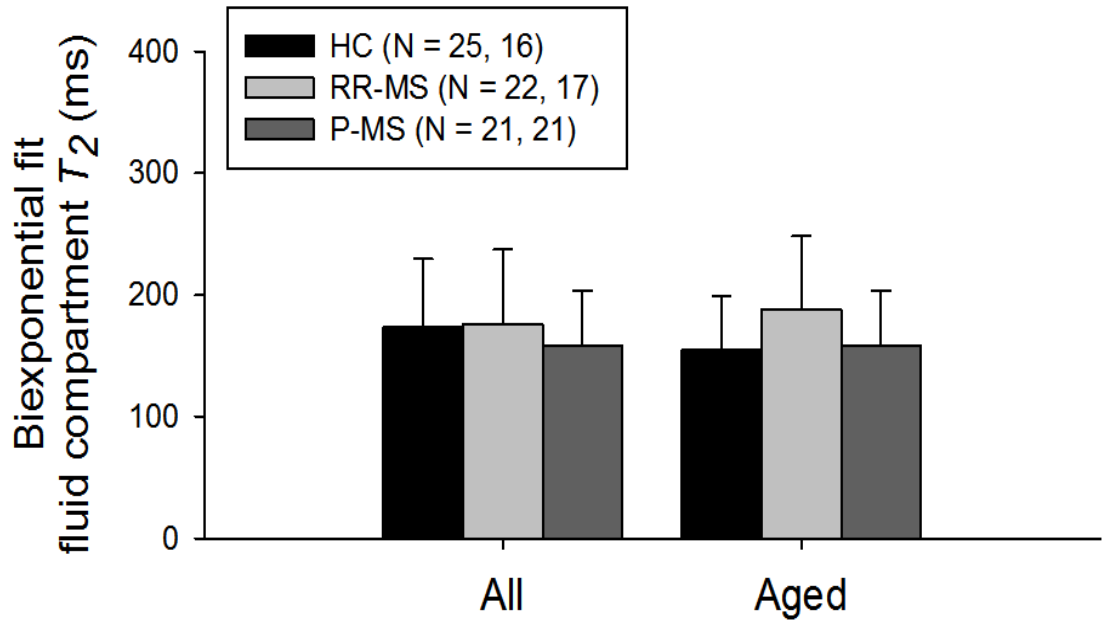


Swanberg, Prinsen, Kurada, Destefano, Bailey, Pitt, Fulbright, and Juchem. *Proc. Intl. Soc. Mag. Reson. Med.* (2018); 0161.

Biexponentially modeled water $T_2$ controlled for voxel composition displayed no between-group differences.

## The Big Picture:

$^1$H MRS is a potential but currently untapped source of clinical diagnostic biomarkers.

Chapter I

## Spectral Quantification:

Data quality (FWHM and SNR) interacts with spectral baselines to affect metabolite fit accuracy.

Fit residual can be misleading when deciding whether a spectral baseline model supports accurate metabolite estimates.

Incorporating baseline terms to the Fisher information matrix improves utility of CRLB as a proxy for metabolite fit precision.

Chapter II

## Absolute Quantification:

Water $T_2$ was shown to differ between individuals with and without progressive multiple sclerosis, emphasizing the utility of group-specific corrections for this variable when employed in cross-sectional $^1$H MRS studies of disease.

Chapter III

## Statistical Analysis:

Can single- or multivariate analysis of metabolite concentrations derived from optimized quantification of $^1$H MRS data alone classify disease states (case application multiple sclerosis)?

Chapter IV

## Generalization:

Can a quantification and statistics pipeline optimized for classification of multiple sclerosis via $^1$H MRS-derived metabolite concentrations be generalized to identification of PTSD and MDD?

Chapter V

## Back to the Big Picture:

General conclusions and outlook

Chapter VI

**Chapter IV**

***Statistical Analysis:*** *Can single- or multivariate analysis of metabolite concentrations derived from optimized quantification of 1H MRS data alone classify disease states (case application multiple sclerosis)?*

$\Phi_{0,1}$ = zero-, first-order phase
$N_M$ = number of metabolites
$C_l$ = Metabolite concentrations
$N_B$ = number of baseline splines
B = baseline spline
$S_n$ = metabolite basis function lineshape coefficients
ν = frequency domain value
γ = line broadening parameter
ε = frequency shift parameter

$$\widehat{Y}(\nu_k) = e^{-i(\phi_0+\nu\phi_1)}\left[\sum_{j=1}^{N_B}\beta_j B_j(\nu_k) + \sum_{l=1}^{N_M} C_l \sum_{n=-N_s}^{N_s} S_n M_l(\nu_{k-n}, \gamma_l, \epsilon_l)\right]$$

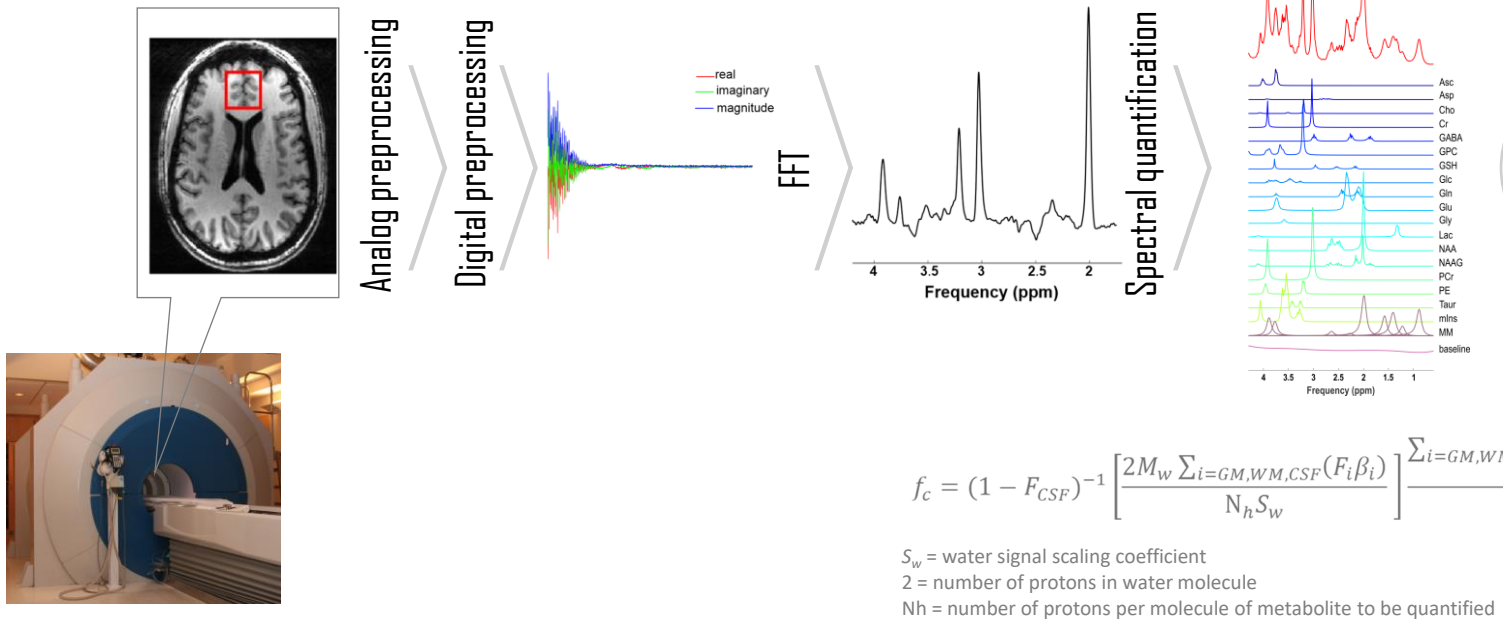


*Metabolite concentrations by tissue*
*Intracellular vs. extracellular metabolite concentration*
*Intracellular metabolite concentrations within cell types of interest*
*Biological functions of metabolite with respect to cell types of interest*
*...And more*

$$f_c = (1 - F_{CSF})^{-1}\left[\frac{2M_w \sum_{i=GM,WM,CSF}(F_i\beta_i)}{N_h S_w}\right]\frac{\sum_{i=GM,WM,CSF}\left[F_i\left(e^{\frac{-T_E}{T_{2wi}}}\right)\left(1 - e^{\frac{-T_R}{T_{1wi}}}\right)\right]}{e^{\frac{-T_E}{T_{2m}}}\left(1 - e^{\frac{-T_R}{T_{1m}}}\right)}$$

$S_w$ = water signal scaling coefficient
2 = number of protons in water molecule
Nh = number of protons per molecule of metabolite to be quantified
$M_w$ = molarity of pure water
$\beta_i$ = molarity of water as a fraction of pure water in either grey matter (GM), white matter (WM), or CSF
$F_i$ = voxel fraction occupied by grey matter (GM), white matter (WM), or CSF
$T_{2wi}$ = $T_2$ of water in grey matter (GM), white matter (WM), or CSF
$T_{1wi}$ = $T_1$ of water in grey matter (GM), white matter (WM), or CSF
$T_{2m}$ = $T_2$ of metabolite
$T_{1m}$ = $T_1$ of metabolite
$T_E$ = echo time of sequence
$T_R$ = repetition time of sequence

Chapter 4: Statistical Analysis

## Neurological symptoms

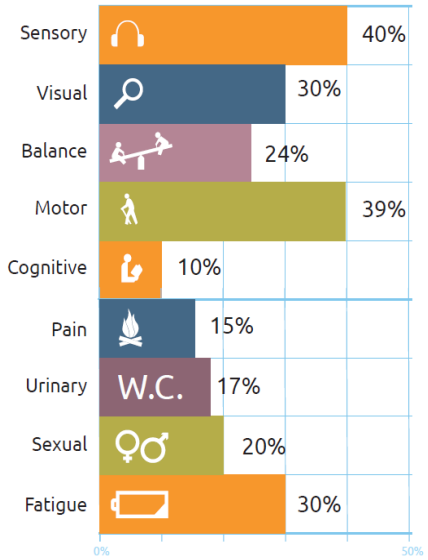


World MS Federation, *Atlas of MS 2013*

## Radiological abnormality

***Relapsing-remitting (RR-MS)***

Brief et al. (2010). *NMR Biomed* 23.

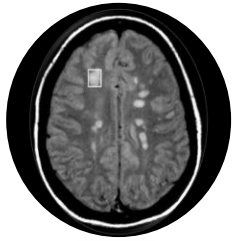

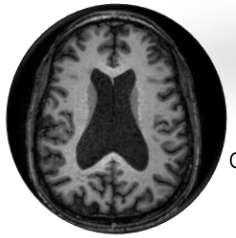

***Secondary progressive (SP-MS)***

Gordon-Lipkin et al. (2007). *Neurology* 69 (16).

## CNS immune activity

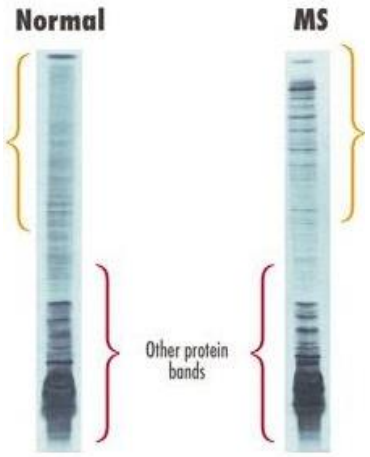


MSTrust.org

| | Number of lesions with objective clinical evidence | Additional data needed for a diagnosis of multiple sclerosis |
|---|---|---|
| ≥2 clinical attacks | ≥2 | None* |
| ≥2 clinical attacks | 1 (as well as clear-cut historical evidence of a previous attack involving a lesion in a distinct anatomical location†) | None* |
| ≥2 clinical attacks | 1 | Dissemination in space demonstrated by an additional clinical attack implicating a different CNS site or by MRI‡ |
| 1 clinical attack | ≥2 | Dissemination in time demonstrated by an additional clinical attack or by MRI§ OR demonstration of CSF-specific oligoclonal bands¶ |
| 1 clinical attack | 1 | Dissemination in space demonstrated by an additional clinical attack implicating a different CNS site or by MRI‡<br>AND<br>Dissemination in time demonstrated by an additional clinical attack or by MRI§ OR demonstration of CSF-specific oligoclonal bands¶ |

Thompson et al., (2018). *Lancet Neurol* 17: 162-73.

Multiple sclerosis is an autoimmune disease with multiple heterogeneous physical manifestations and diagnostic uncertainty.

Chapter 4: Statistical Analysis

*In collaboration with Hetty Prinsen, Ph.D.*

| | |
|---|---|
| 12♀ 13♂ 43 ± 15 y.* | Non-MS control |
| 18♀ 8♂ 44 ± 13 y. | Relapsing-remitting MS |
| 12♀ 9♂ 55 ± 8 y. | Progressive MS |

*mean ± standard deviation

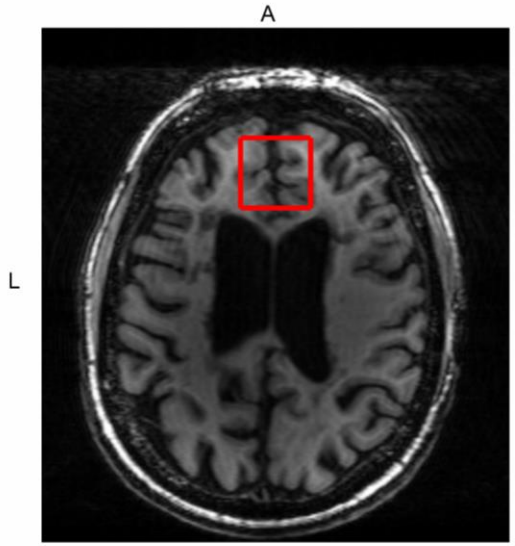


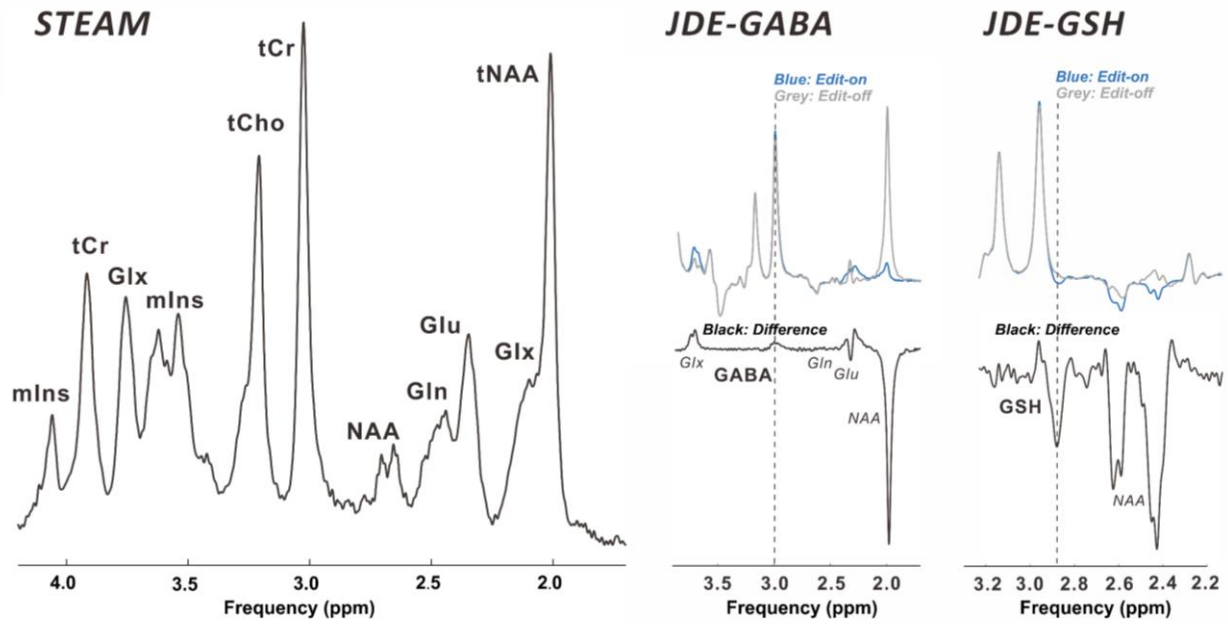


Swanberg, Prinsen, Kurada, Bailey, Destefano, Pitt, Fulbright, and Juchem, *NMR in Biomedicine* (2021); 34(11): e4590.

We used 7-Tesla $^{1}$H MRS to characterize the prefrontal cortex metabolic signatures of two multiple sclerosis phenotypes.

Chapter 4: Statistical Analysis

## Spectral Quantification:

Data quality (FWHM and SNR) can interact with spectral baselines to induce systematic effects on spectral fit accuracy. Fit residual is a misleading proxy for spectral baseline model's support of accurate metabolite estimates.

Chapter 2: Spectral Quantification

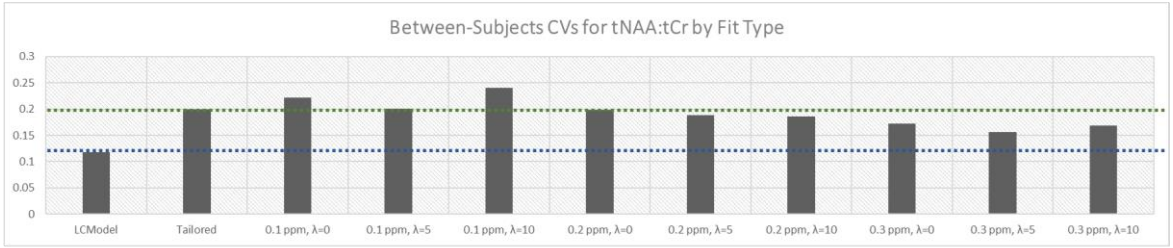


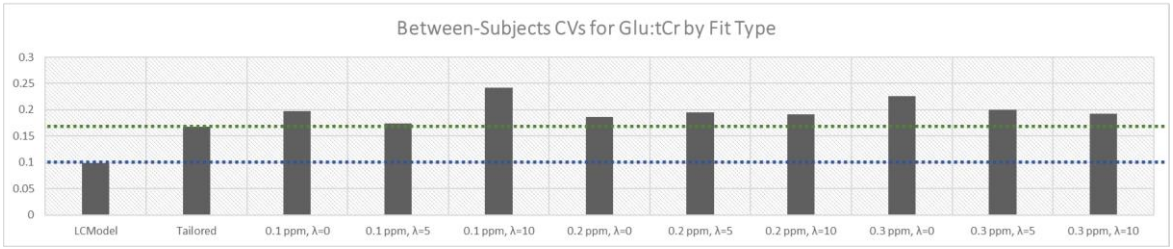


Empirically supported spectral quantification method

## Absolute Quantification:

Water $T_2$ was shown to differ between individuals with and without progressive multiple sclerosis, emphasizing the utility of group-specific corrections for this variable when employed in cross-sectional $^1$H MRS studies of disease.

Chapter 3: Absolute Quantification

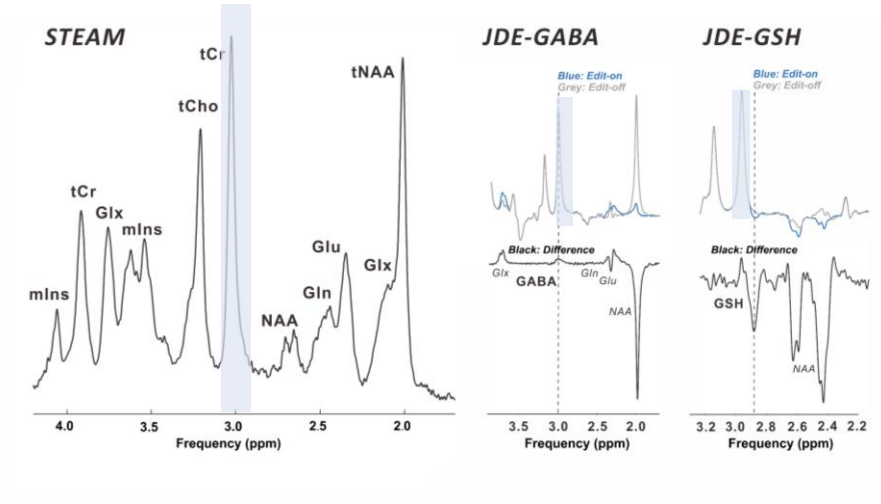


Empirically supported absolute quantification method

## Chapter 4: Statistical Analysis

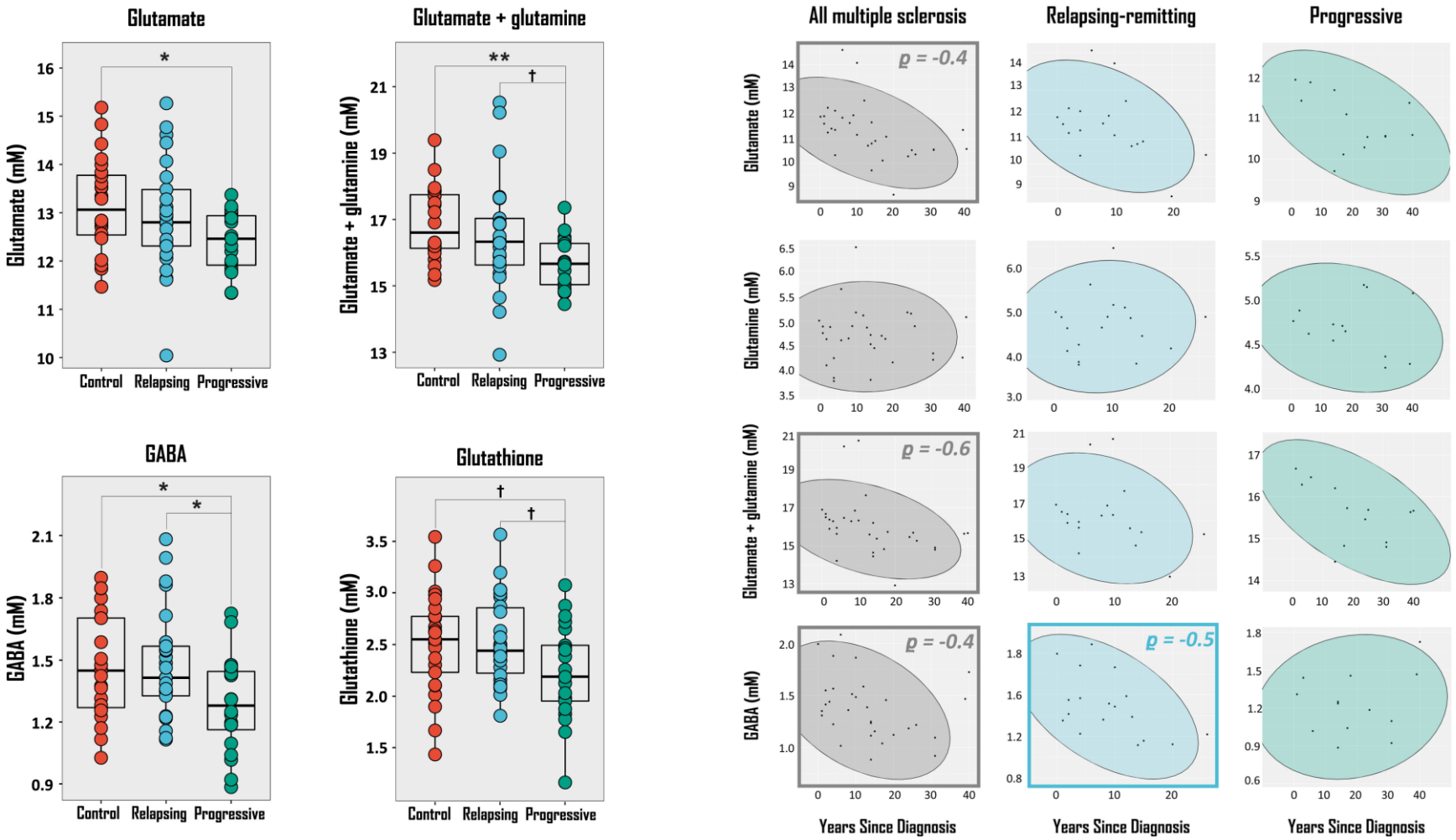


Tukey's honest significant difference test post hoc to analysis of variance *$p \leq 0.05$, **$p < 0.01$, †$p < 0.1$
Metabolite concentrations corrected for age when regression coefficient significant in control

Boxes indicate Spearman's ρ $p < 0.05$

Swanberg, Prinsen, Kurada, Bailey, Destefano, Pitt, Fulbright, and Juchem, *NMR in Biomedicine* (2021); 34(11): e4590.

## Chapter 4: Statistical Analysis

***Relapsing-remitting MS***
*17 women, 8 men*
*45 ± 13 y.o.*

***Progressive MS***
***(6 primary; 13 secondary)***
*11 women, 8 men*
*55 ± 8.3 y.o.*

***No MS***
*15 women, 9 men*
*43 ± 15 y.o.*

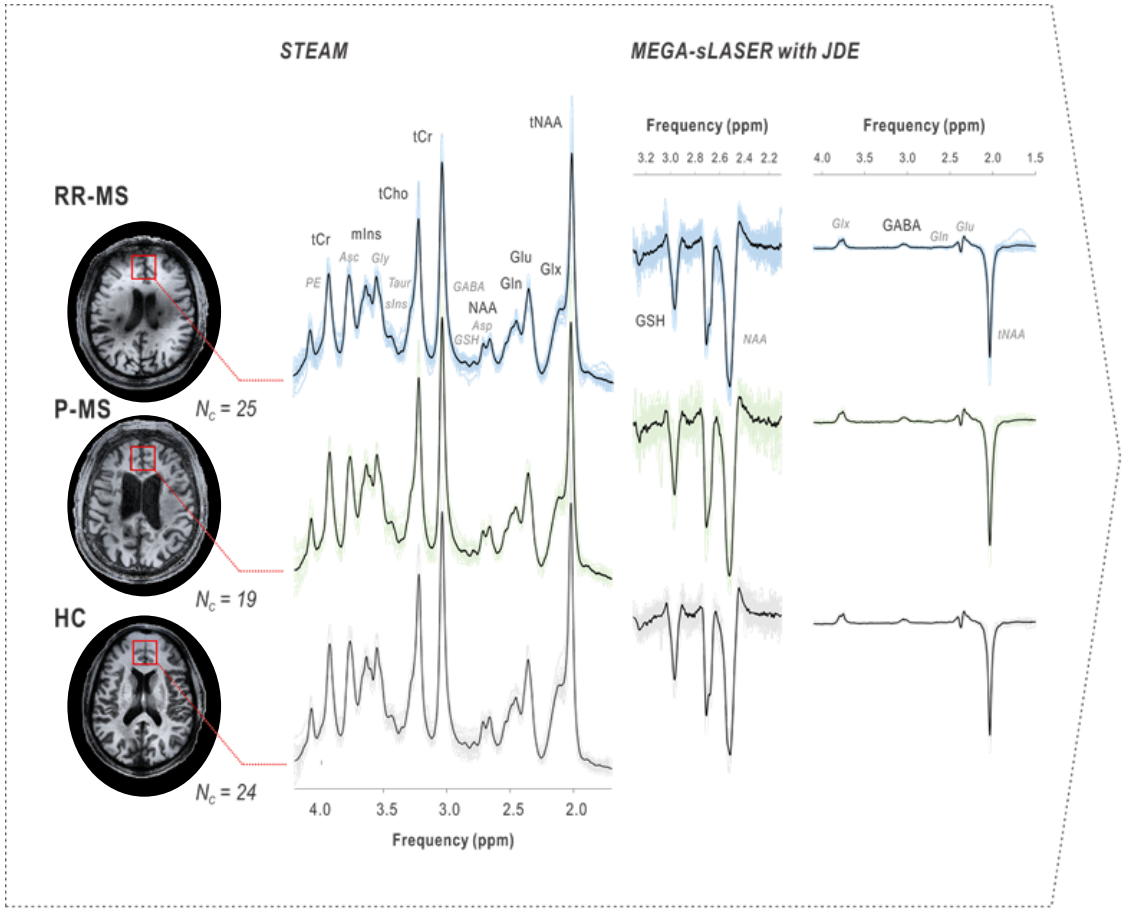


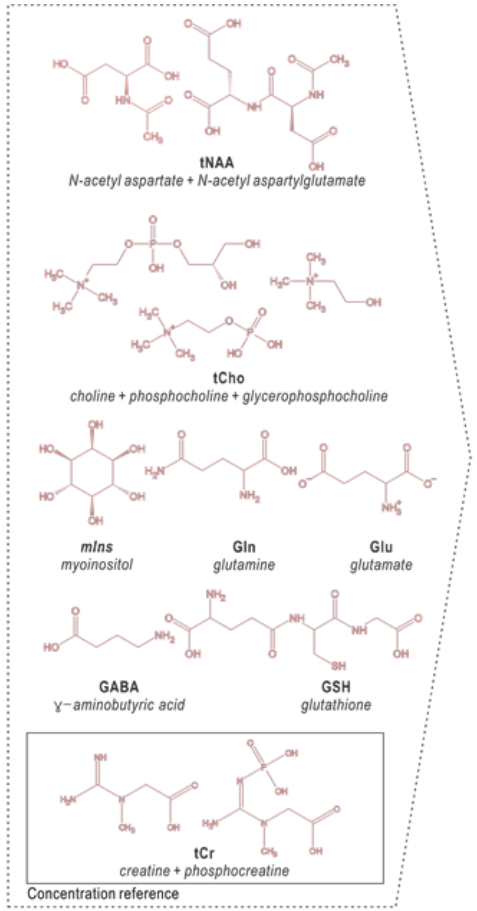


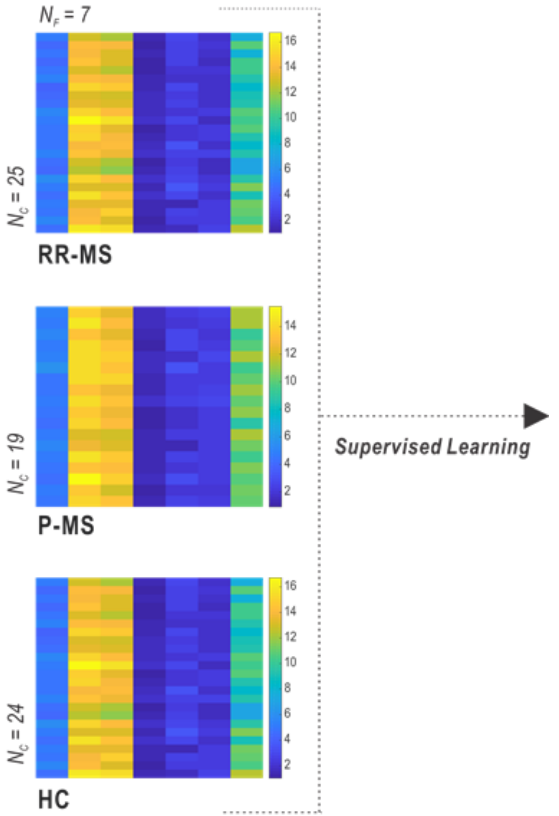


Swanberg, Kurada, Prinsen, and Juchem. Manuscript in review.

Since MS could not be identified one metabolite at a time, we used supervised learning to consider all of them at once.

## Chapter 4: Statistical Analysis

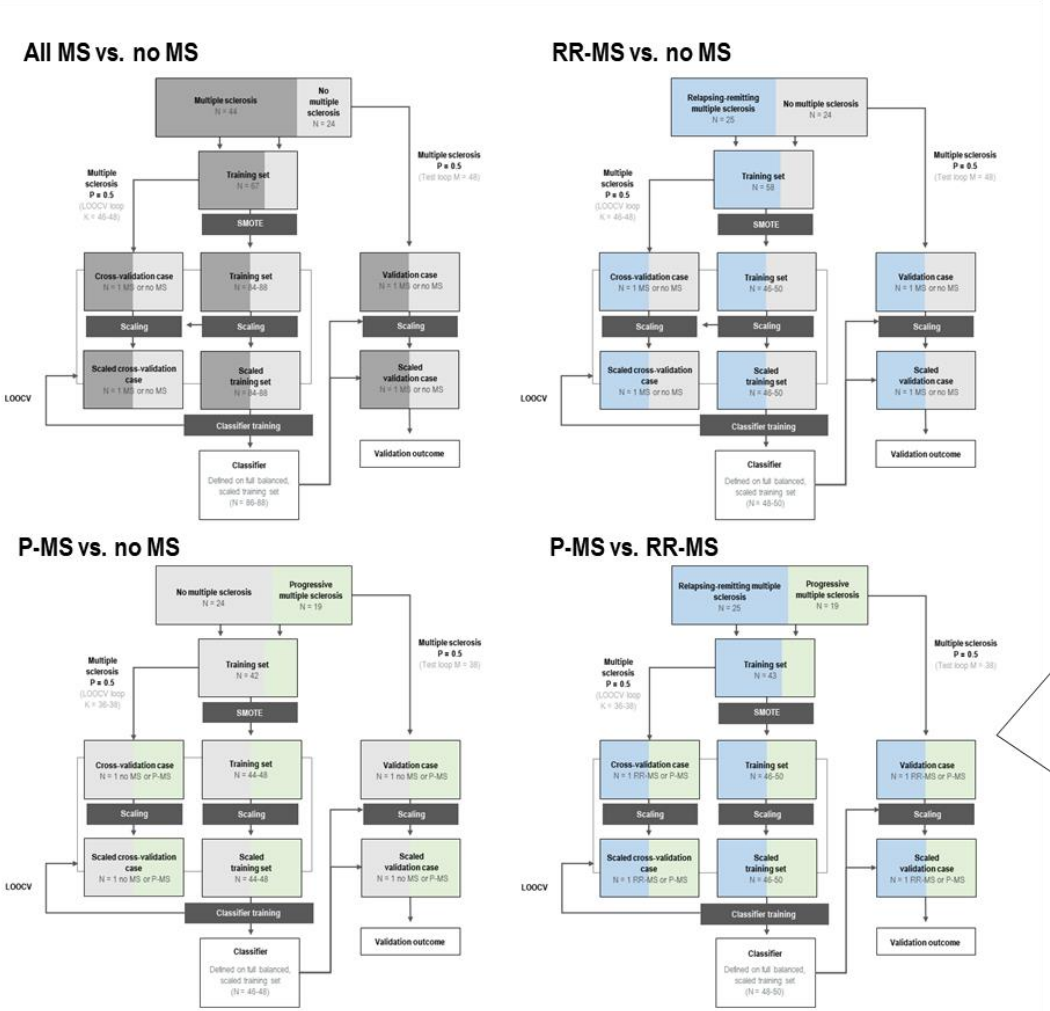


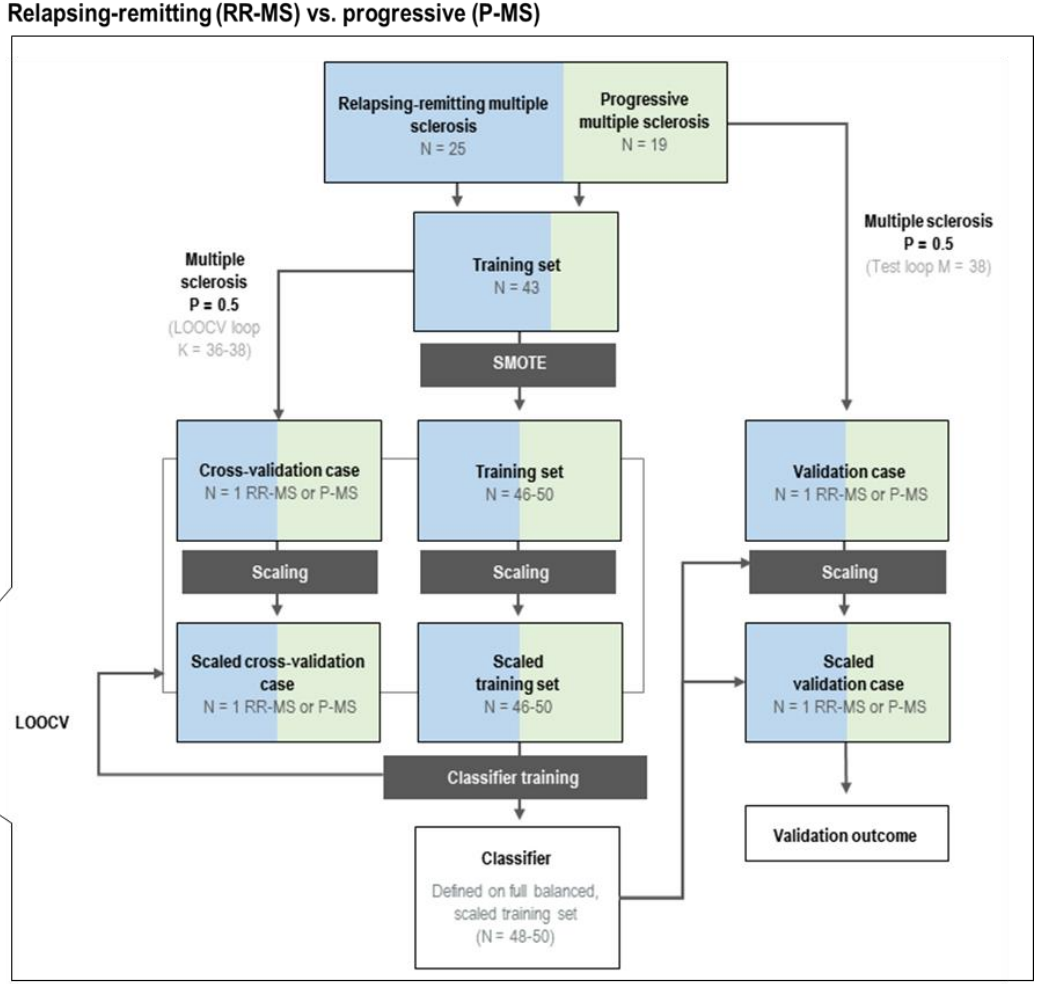


Swanberg, Kurada, Prinsen, and Juchem. Manuscript in review.

*In collaboration with Abhinav Kurada, B.Sc.*

We applied supervised learning to non-reduced feature sets of seven metabolites to perform one of four classifications.

**Control versus all multiple sclerosis**

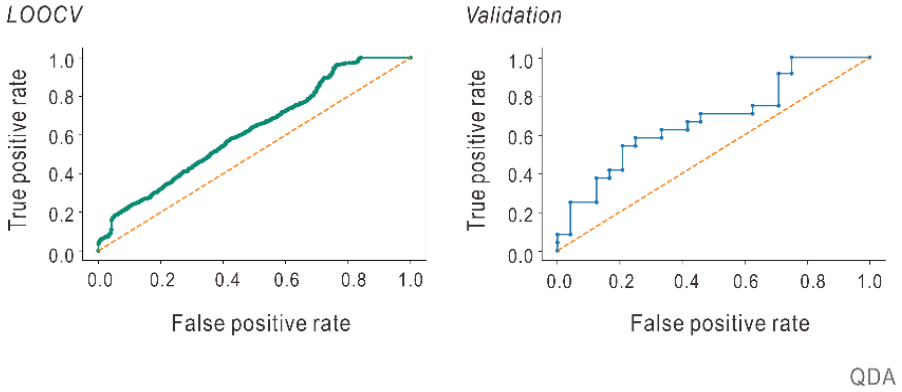


**Control versus relapsing-remitting multiple sclerosis**

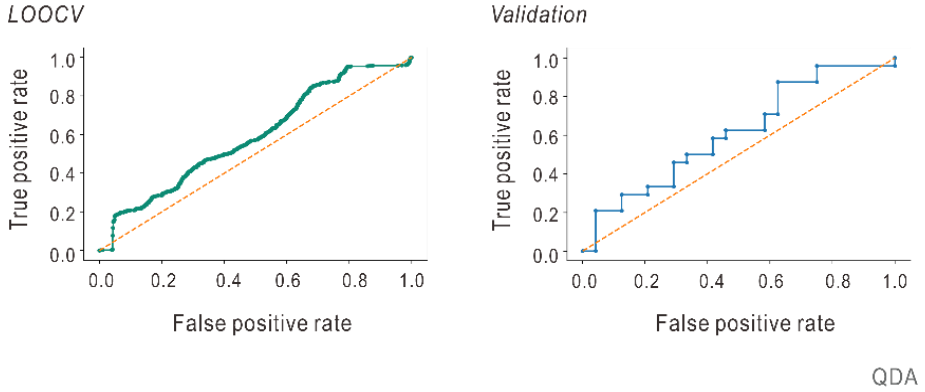


**Control versus progressive multiple sclerosis**

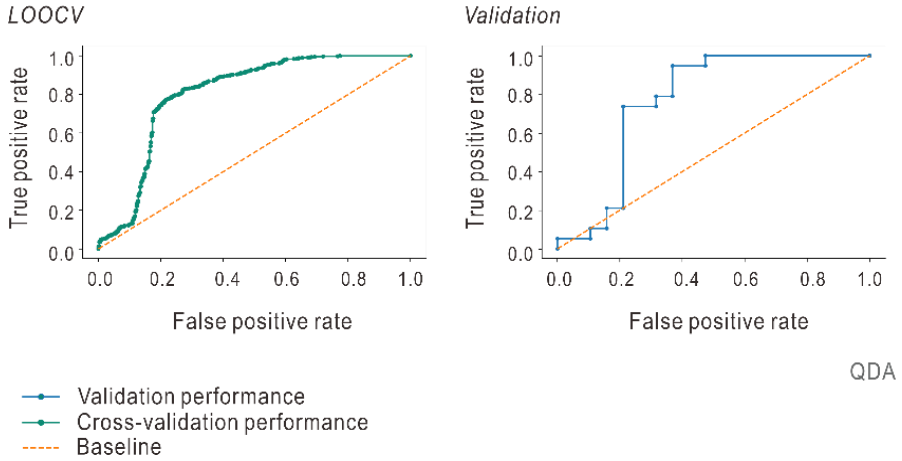


**Relapsing-remitting versus progressive multiple sclerosis**

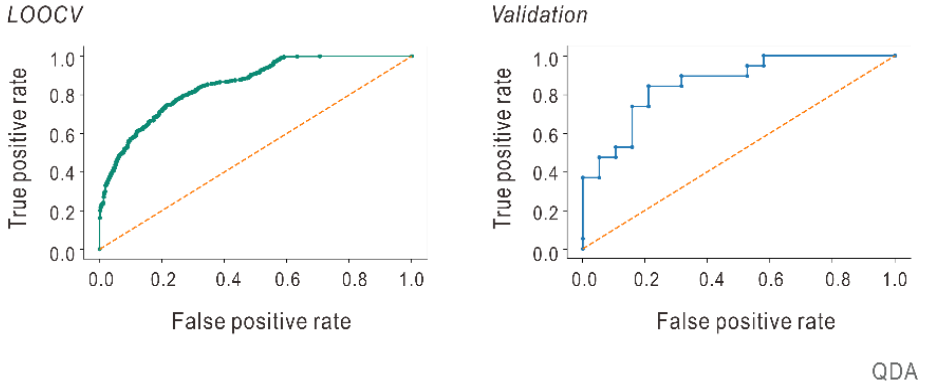


Swanberg, Kurada, Prinsen, and Juchem. Manuscript in review.

Models identifying progressive MS vs. control or relapsing-remitting MS outperformed those classifying only relapsing-remitting or all MS vs. control.

Chapter 4: Statistical Analysis

**Control vs. all multiple sclerosis (MS)**

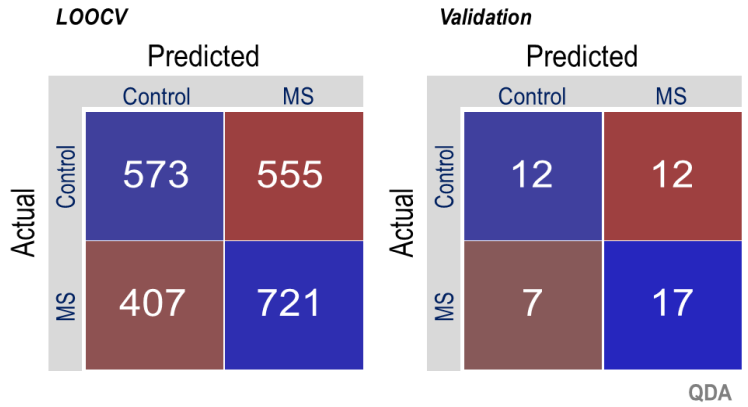


***Validation Performance***
60% accuracy
71% sensitivity
50% specificity

**Control vs. relapsing-remitting (RR-MS)**

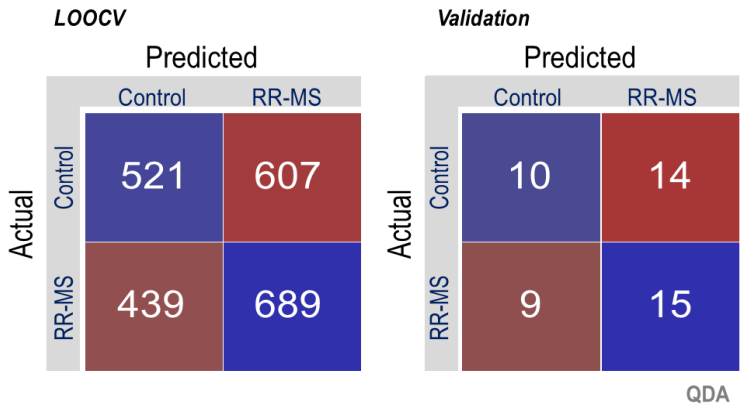


***Validation Performance***
52% accuracy
63% sensitivity
42% specificity

**Control vs. progressive (P-MS)**

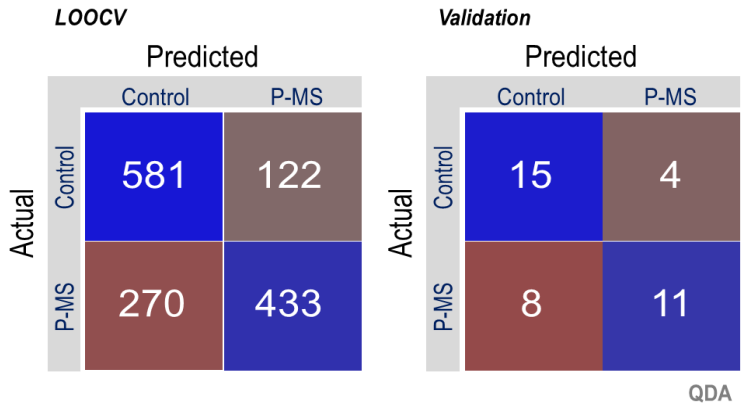


***Validation Performance***
68% accuracy
58% sensitivity
79% specificity

**Relapsing-remitting (RR-MS) vs. progressive (P-MS)**

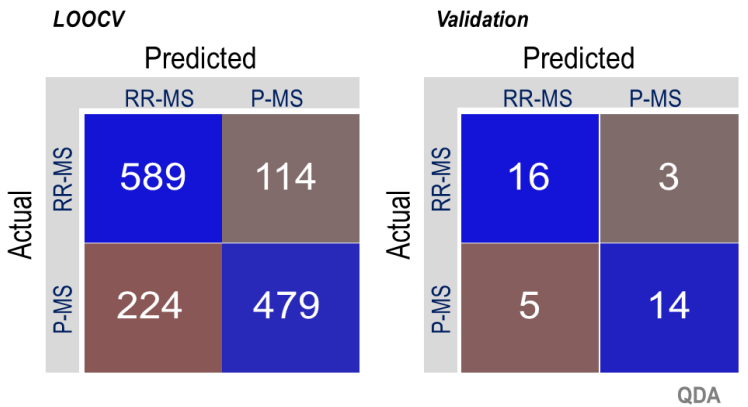


***Validation Performance***
79% accuracy
84% sensitivity
74% specificity

Swanberg, Kurada, Prinsen, and Juchem. Manuscript in review.

Models identifying progressive MS vs. control or relapsing-remitting MS outperformed those classifying only relapsing-remitting or all MS vs. control.

### Control vs. all multiple sclerosis (MS)

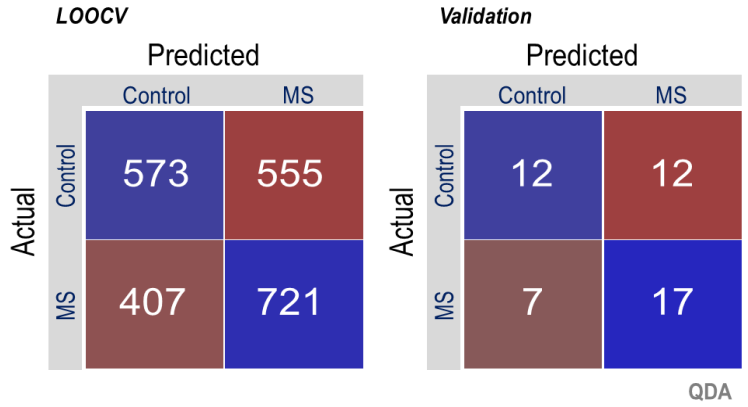


***Top 3 features***
Myoinositol (3/3)
Glutamate (3/3)
GABA (2/3)

### Control vs. relapsing-remitting (RR-MS)

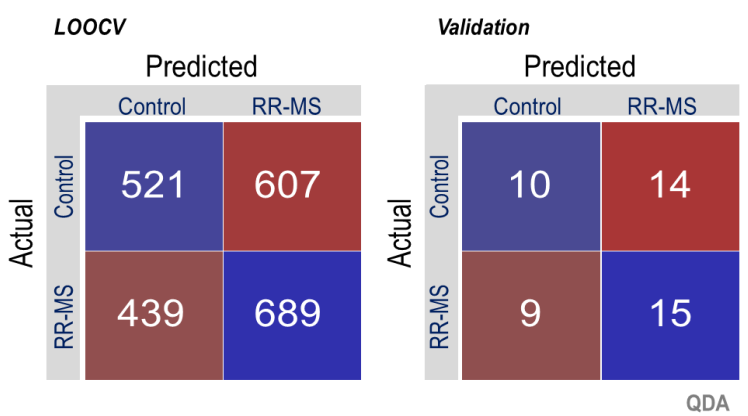


***Top 3 features***
Myoinositol (3/3)
Glutamate (3/3)
N-acetyl aspartate (2/3)

### Control vs. progressive (P-MS)

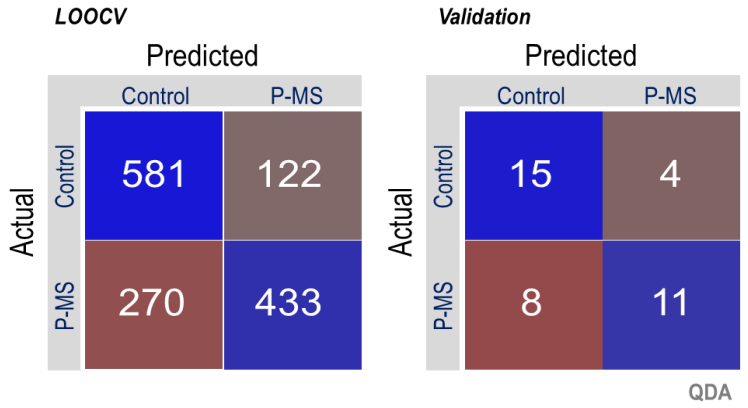


***Top 3 features***
Myoinositol (2/3)
Glutamate (3/3)
GABA (2/3)

### Relapsing-remitting (RR-MS) vs. progressive (P-MS)

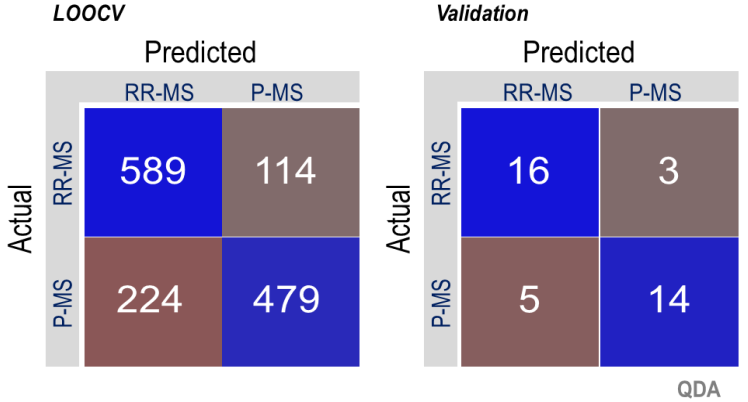


***Top 3 features***
Total choline (3/3)
Glutamine (2/3)
Glutathione (2/3)

Swanberg, Kurada, Prinsen, and Juchem. Manuscript in review.

Myoinositol, glutamate, and GABA were consistently important for identifying MS, while total choline, glutamine, and glutathione were consistently informative for differentiating MS phenotypes.

## The Big Picture:

$^1$H MRS is a potential but currently untapped source of clinical diagnostic biomarkers.

Chapter I

## Spectral Quantification:

Data quality (FWHM and SNR) interacts with spectral baselines to affect metabolite fit accuracy.

Fit residual can be misleading when deciding whether a spectral baseline model supports accurate metabolite estimates.

Incorporating baseline terms to the Fisher information matrix improves utility of CRLB as a proxy for metabolite fit precision.

Chapter II

## Absolute Quantification:

Water $T_2$ was shown to differ between individuals with and without progressive multiple sclerosis, emphasizing the utility of group-specific corrections for this variable when employed in cross-sectional $^1$H MRS studies of disease.

Chapter III

## Statistical Analysis:

Metabolite concentrations derived from $^1$H MRS were a viable means of characterizing progressive multiple sclerosis disease status relative to either relapsing-remitting or control.

Chapter IV

## Generalization:

Can a quantification and statistics pipeline optimized for classification of multiple sclerosis via $^1$H MRS-derived metabolite concentrations be generalized to identification of PTSD and MDD?

Chapter V

## Back to the Big Picture:

General conclusions and outlook

Chapter VI

*Exposure to trauma (A)*

Only 0.1%-19% conditional risk to develop PTSD depending on trauma*

*Intrusion (B)*
*Avoidance (C)*
*Negative cognition/mood (D)*
*Altered arousal/reactivity (E)*

*For at least one month (F)*
*Functional impairment (G)*
*Not from drugs or other illness (H)*

* Kessler et al. *Eur J Psychotraumatol* 8(S5): 1353383. (2017)

Table 1 | **DSM-5 criteria for PTSD**

| Criterion* | Description | Specific examples | Requirements | Compared with DSM-IV |
|---|---|---|---|---|
| Criterion A | Exposure to stressor | • Direct exposure<br>• Witnessing trauma<br>• Learning of a trauma<br>• Repeat or extreme indirect exposure to aversive details | DSM-5 recognizes that exposure to trauma can occur either by direct or indirect confrontation with extreme trauma | Specific definition of details of the stressor needed, including repeated experience or extreme exposure to details of events |
| Criterion B | Intrusion symptoms | • Recurrent memories<br>• Traumatic nightmares<br>• Dissociative reactions (flashbacks)<br>• Psychological distress at traumatic reminders<br>• Marked physiological reactivity to reminders | At least one of these five examples is required | No change, but further clarification of the dissociative quality of flashbacks needed |
| Criterion C | Persistent avoidance | • Trauma-related thoughts or feelings<br>• Trauma-related external reminders such as people, places or activities | At least one of these two examples is required | DSM-IV did not separate the avoidance criterion |
| Criterion D | Negative alterations in cognitions and mood | • Dissociative amnesia<br>• Persistent negative beliefs and expectations<br>• Persistent distorted blame of self or others for causing trauma<br>• Negative trauma-related emotions: fear, horror, guilt, shame and anger<br>• Diminished interest in activities<br>• Detachment or estrangement from others<br>• Inability to experience positive emotions | At least two of these seven examples are required | DSM-IV noted social estrangement and restricted the range of affect; numbing redefined to positive rather than all affects |
| Criterion E | Alterations in arousal and reactivity | • Irritable and aggressive behaviour<br>• Self-destructive and reckless behaviour<br>• Hypervigilance<br>• Exaggerated startle<br>• Problems concentrating<br>• Sleep disturbance | At least two of these six examples are required | Self-destructive and risk-taking behaviours were not defined in DSM-IV |
| Criterion F | Duration | Must experience criteria B, C, D and F for >1 month | Acute stress disorder is diagnosed for symptoms occurring for <1 month post trauma | No change |
| Criterion G | Functional significance | Impairment in social, occupational or other domains | Disability in at least one of these domains is required | No change |
| Criterion H | Exclusion | Not attributable to medication, substance use or other illness | Symptoms must not be secondary to other causes | Not stated in DSM-IV |
| Subtypes | • Dissociative subtype: used when depersonalization and derealization occur in tandem with other symptoms described above.<br>• Delayed subtype: used to describe the emergence of symptoms following a period post trauma in which symptoms were not present or were present at a subthreshold level. | | | |

DSM, Diagnostic and Statistical Manual of Mental Disorders; PTSD, post-traumatic stress disorder. *Criteria according to DSM-5 (REF. 1).

Yehuda et al. *Nat Rev* 1: 1. (2015).

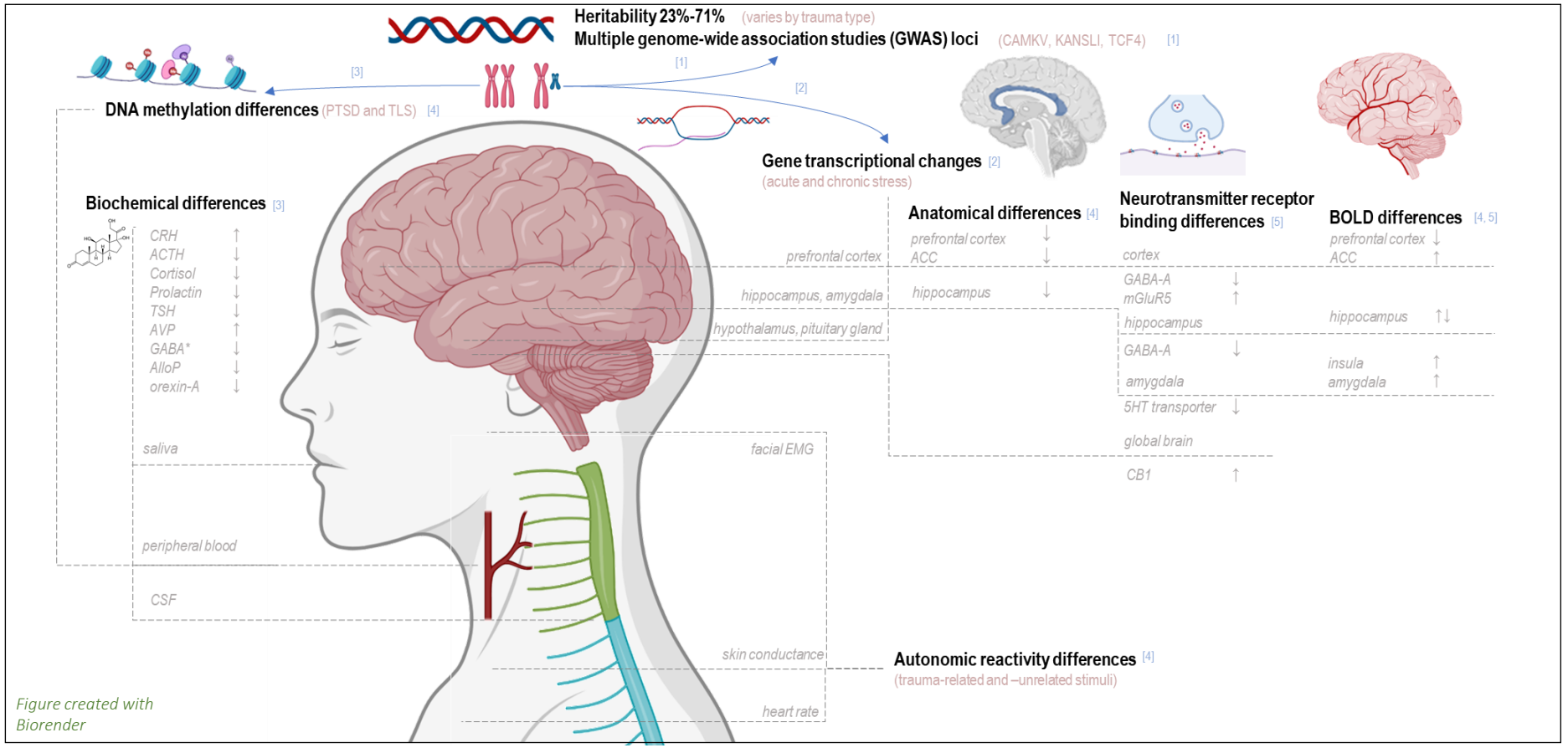


*Figure created with Biorender*

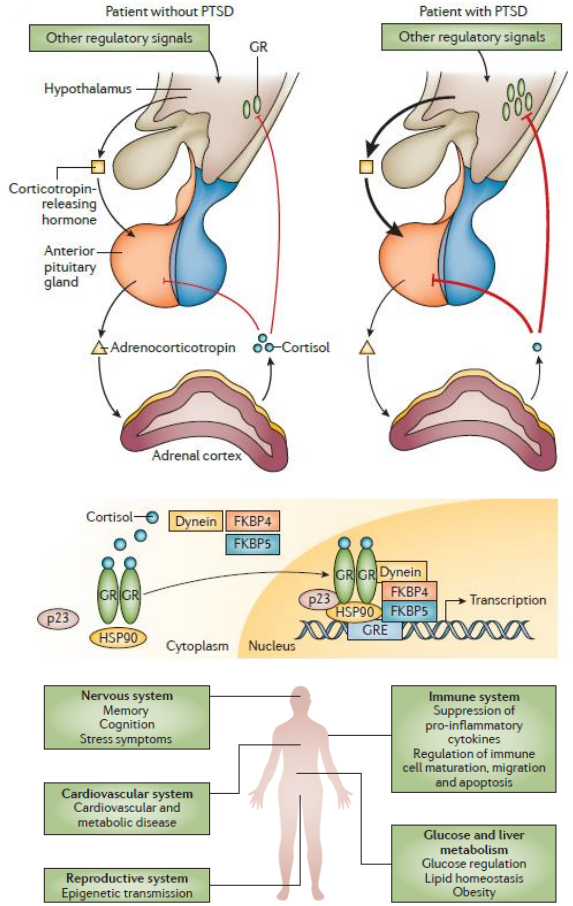


[1] Duncan et al. *Curr Psychiatry Rep* 20:115 (2018). [2] Brivio et al. *Genes Brain Behav* 19: e12643. (2020). [3] Malikowska-Racia et al. *Pharmacol Res* 142: 30-49. (2019). [4] Pitman et al. *Nat Rev* 13: 769. (2012). [5] Yehuda et al. *Nat Rev* 1: 1. (2015).

Swanberg, Campos, Abdallah, and Juchem. Manuscript in preparation.

Yehuda et al. *Nat Rev* 1: 1. (2015).

PTSD has been associated with a broad range of measurable signatures across the body.

# Optimizing $^1$H MRS: Generalization

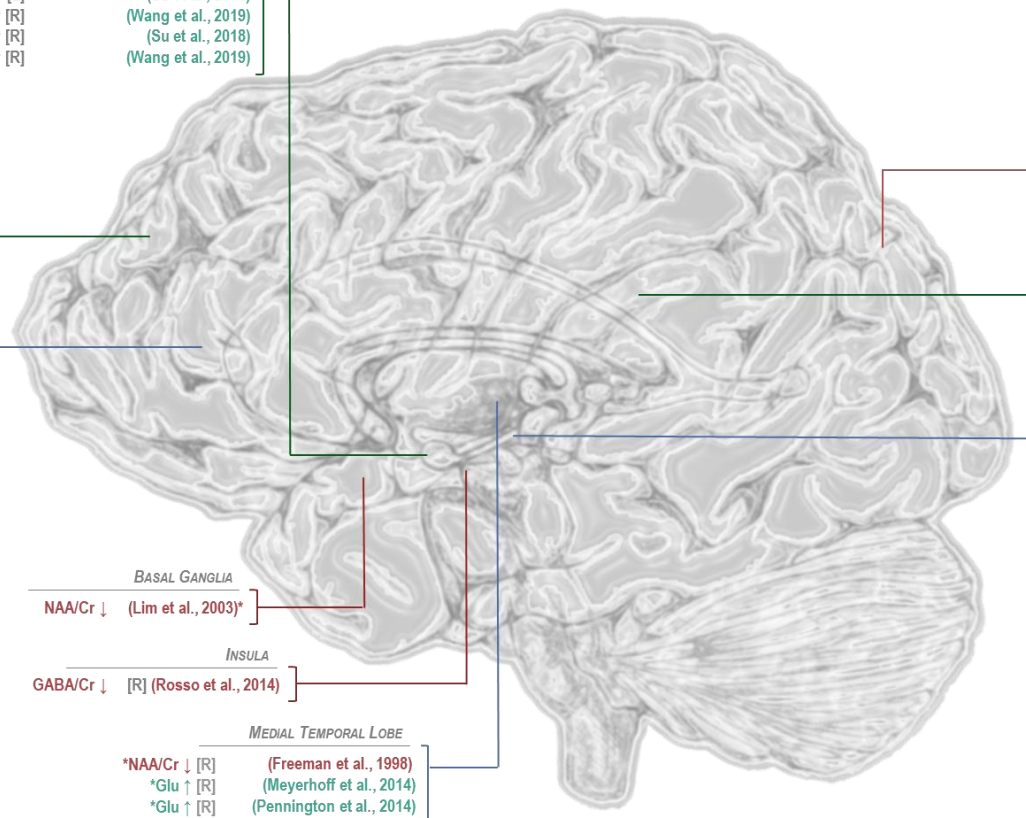

### Amygdala

| | |
|---|---|
| *NAA ↑ [R] | (Wang et al., 2019) |
| *Cr ↑ [L] | (Su et al., 2018) |
| *Cr ↑ [R] | (Wang et al., 2019) |
| *mIns ↑ [R] | (Su et al., 2018) |
| *mIns ↑ [R] | (Wang et al., 2019) |

### Dorsolateral PFC

| | |
|---|---|
| *GABA / Cr ↑ [L] | (Michels et al., 2014) |
| *GSH / Cr ↑ [L] | (Michels et al., 2014) |

### Anterior cingulate cortex

| | |
|---|---|
| NAA / Cr ↓ | (De Bellis et al., 2000) |
| NAA / Cr ↓ | (Mahmutyazicioğlu et al., 2014) |
| *NAA / Cr ↓ | (Schuff et al., 2008) |
| NAA / Cr ↓ | (Guo et al., 2012) |
| NAA ↓ | (Ham et al., 2007) |
| *NAA ↓ | (Meyerhoff et al., 2014) |
| *NAA ↓ | (Shin et al., 2017) |
| *NAA ↓ [R] | (Schuff et al., 2008) |
| *NAA ↑ | (Su et al., 2018) |
| Cho/Cr ↑ | (Guo et al., 2012) |
| *Cho/Cr ↑ | (Seedat et al., 2005) |
| *mIns/Cr ↑ | (Seedat et al., 2005) |
| *mIns ↑ | (Su et al., 2018) |
| *Glx/Cr ↓ | (Yang et al., 2015) |
| Gln ↓ | (Sheth et al., 2019) |
| *GABA/Cr ↑ | (Michels et al., 2014) |
| GABA ↓ | (Sheth et al., 2019) |
| *GSH/Cr ↑ | (Michels et al., 2014) |

### Basal Ganglia

| | |
|---|---|
| NAA/Cr ↓ | (Lim et al., 2003)* |

### Insula

| | |
|---|---|
| GABA/Cr ↓ | [R] (Rosso et al., 2014) |

### Medial Temporal Lobe

| | |
|---|---|
| *NAA/Cr ↓ [R] | (Freeman et al., 1998) |
| *Glu ↑ [R] | (Meyerhoff et al., 2014) |
| *Glu ↑ [R] | (Pennington et al., 2014) |
| *GABA↓ [R] | (Meyerhoff et al., 1998) |
| *Cho/Cr ↓ [L] | (Freeman et al., 1998) |

### Parieto-occipital cortex

| | |
|---|---|
| *Cr ↓ [WM] | (Lim et al., 2003) |
| *GABA ↓ | (Meyerhoff et al., 2014) |
| *GABA ↓ | (Pennington et al., 2014) |

### Posterior cingulate gyrus

| | |
|---|---|
| IMI-1 ↑ | (Quadrelli et al., 2019) |
| T-fucose ↑ | (Quadrelli et al., 2019) |
| Fucose IV | (Quadrelli et al., 2019) |
| Fucose V | (Quadrelli et al., 2019) |
| $HC{=}CH{-}CH_2{-}CH_2{-}CH_3$ | (Quadrelli et al., 2019) |

### Hippocampus

| | |
|---|---|
| NAA / Cr ↓ [R, L] | (Mahmutyazicioğlu et al., 2005) |
| NAA / Cr ↓ [R, L] | (Guo et al., 2012) |
| NAA / Cr ↓ [R, L] | (Shu et al., 2013) |
| *NAA / Cr ↓ [R+L] | (Schuff et al., 2008) |
| *NAA / Cr ↓ [L] | (Menon et al., 2003) |
| *NAA / Cr ↓ [L] | (Li et al., 2006) |
| *NAA / Cr ↓ [R] | (Rosso et al., 2017) |
| NAA ↓ [R, L] | (Neylan et al., 2003) |
| NAA ↓ [R, L] | (Ham et al., 2007) |
| NAA ↓ [R, L] | (Schuff et al., 2001) |
| NAA ↓ [L] | (Villarreal et al., 2017) |
| *NAA ↓ [R, L] | (Rosso et al., 2017) |
| Cr ↓ [R] | (Schuff et al., 2001) |
| Cho/Cr ↑ [R, L] | (Mahmutyazicioğlu et al., 2014) |
| *Glu/Cr ↑ [R] | (Rosso et al., 2017) |
| *Glu ↑ [R] | (Rosso et al., 2017) |

*PTSD vs. control groups that included trauma-exposed and/or military veteran individuals

PTSD: Post-Traumatic Stress Disorder; NAA: N-acetyl aspartate, Cr: total creatine; mIns: myoinositol; GABA: γ-aminobutyric acid; GSH: glutathione; Cho: total choline; Glx: glutamate + glutamine; Gln: glutamine; IMI-1: imidazole from histamine, histidine, and homocarnosine; Glu: glutamate

Swanberg, Campos, Abdallah, and Juchem. Manuscript in preparation.

So far the $^1$H-MRS-visible manifestation of PTSD appears unremarkable at first glance.

# Optimizing $^1$H MRS: Generalization

**A**

$^1$H MRS Studies of PTSD by Patient Group Mean Age

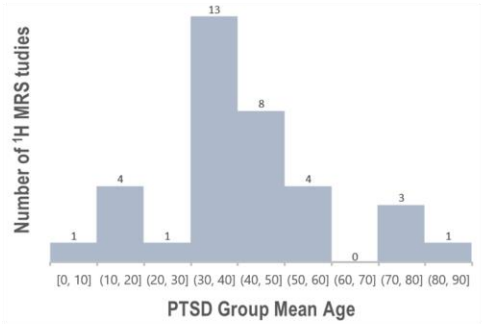


Between-Group Age Differences in $^1$H MRS Studies of PTSD

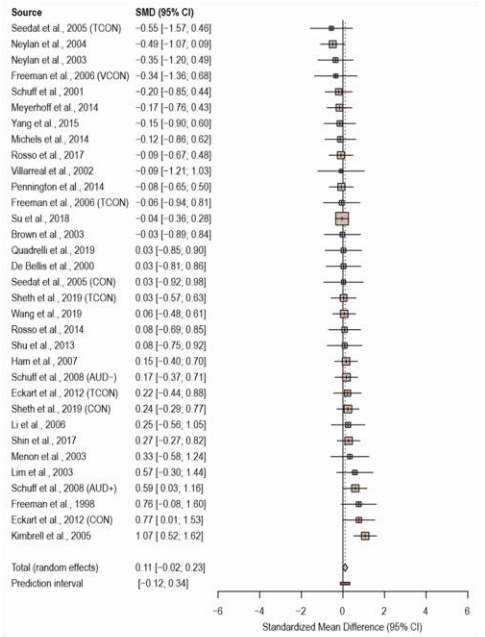


**B**

$^1$H MRS Studies of PTSD by Patient Group % Women

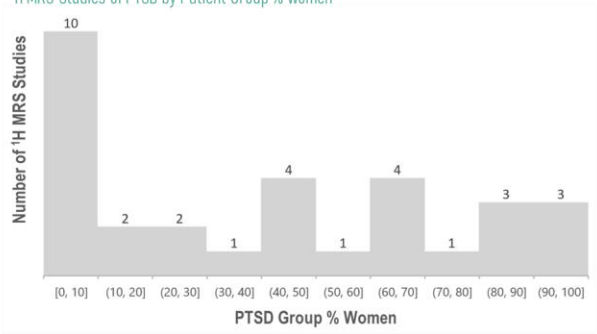


Between-Group Sex-Matching in Sex-Unmatched $^1$H MRS Studies of PTSD

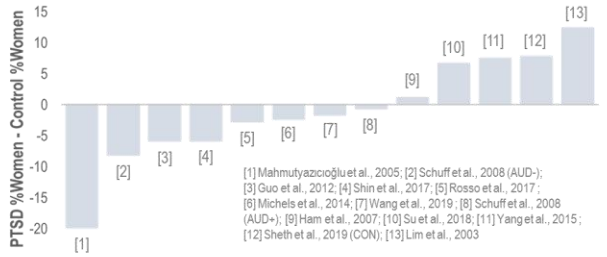


**C**

$^1$H MRS Studies of PTSD by Field Strength

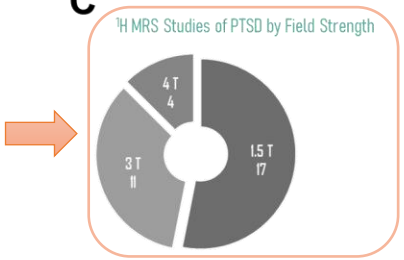


**D**

Metabolite Concentrations Reported by Unique $^1$H MRS Study Voxel

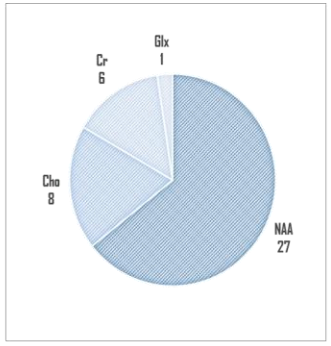


Hippocampus (N=27 voxels)

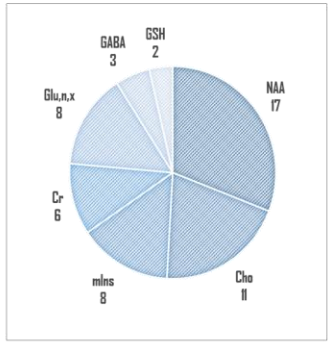


Frontal lobe, prefrontal cortex, or anterior cingulate cortex (N=19 voxels)

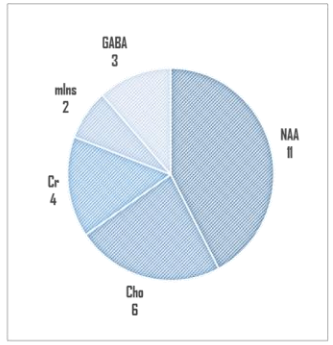


Insula or temporal lobe (N=13 voxels)

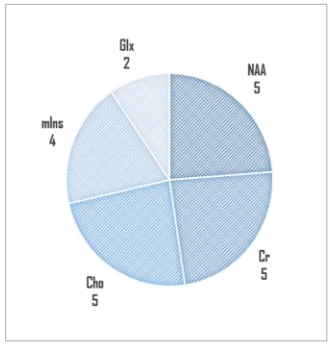


Amygdala (N=5 voxels)

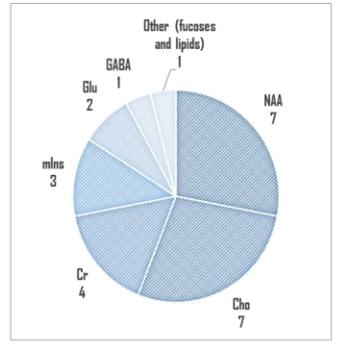


Other (occipital or parietal cortex, posterior cingulate gyrus, basal ganglia) (n=10 voxels)

Swanberg, Campos, Abdallah and Juchem. Manuscript in preparation.

# Optimizing $^1$H MRS: Generalization

| | |
|---|---|
| PTSD- MDD- | 5 F, 13 M; 34 ± 8 y.o. |
| PTSD- **MDD+** | 2 F, 7 M; 35 ± 15 y.o. |
| **PTSD+** MDD- | 2 F, 3 M; 37 ± 16 y.o. |
| **PTSD+ MDD+** | 1 F, 5 M; 39 ± 8 y.o. |

**Scan Participants**

| | | | |
|---|---|---|---|
| ***FOV*** | *x20 y22 z7.8 cm* | $T_R$ | *3s* |
| ***Matrix*** | *x256 y256 z39* | $T_E$ | *6 ms* |
| ***Resolution*** | *x0.78 y0.86 z2 mm* | $T_{ACQ}$ | *5 min* |
| $T_{INV}$ | *1 s* | | |

**Voxel Placement: IR-prepared $T_1$w MRI**

*In collaboration with:*


*Hetty Prinsen, Ph.D.*


*Chadi Abdallah, M.D.*


*Lynette Averill, Ph.D.*


*Christopher Averill, B.Sc.*

*STEAM (8 cm$^3$)* *JDE-GABA; JDE-GSH (27 cm$^3$)*

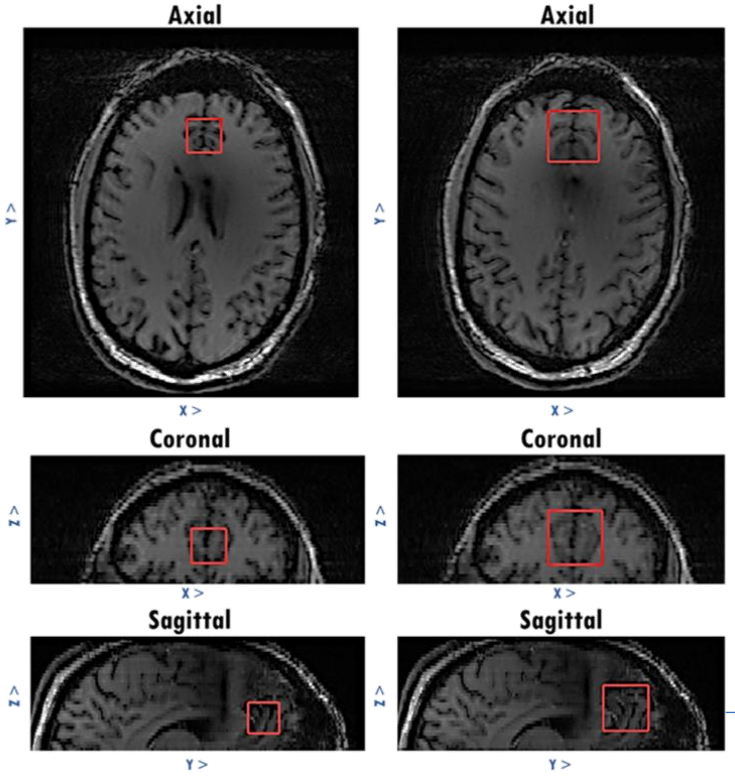


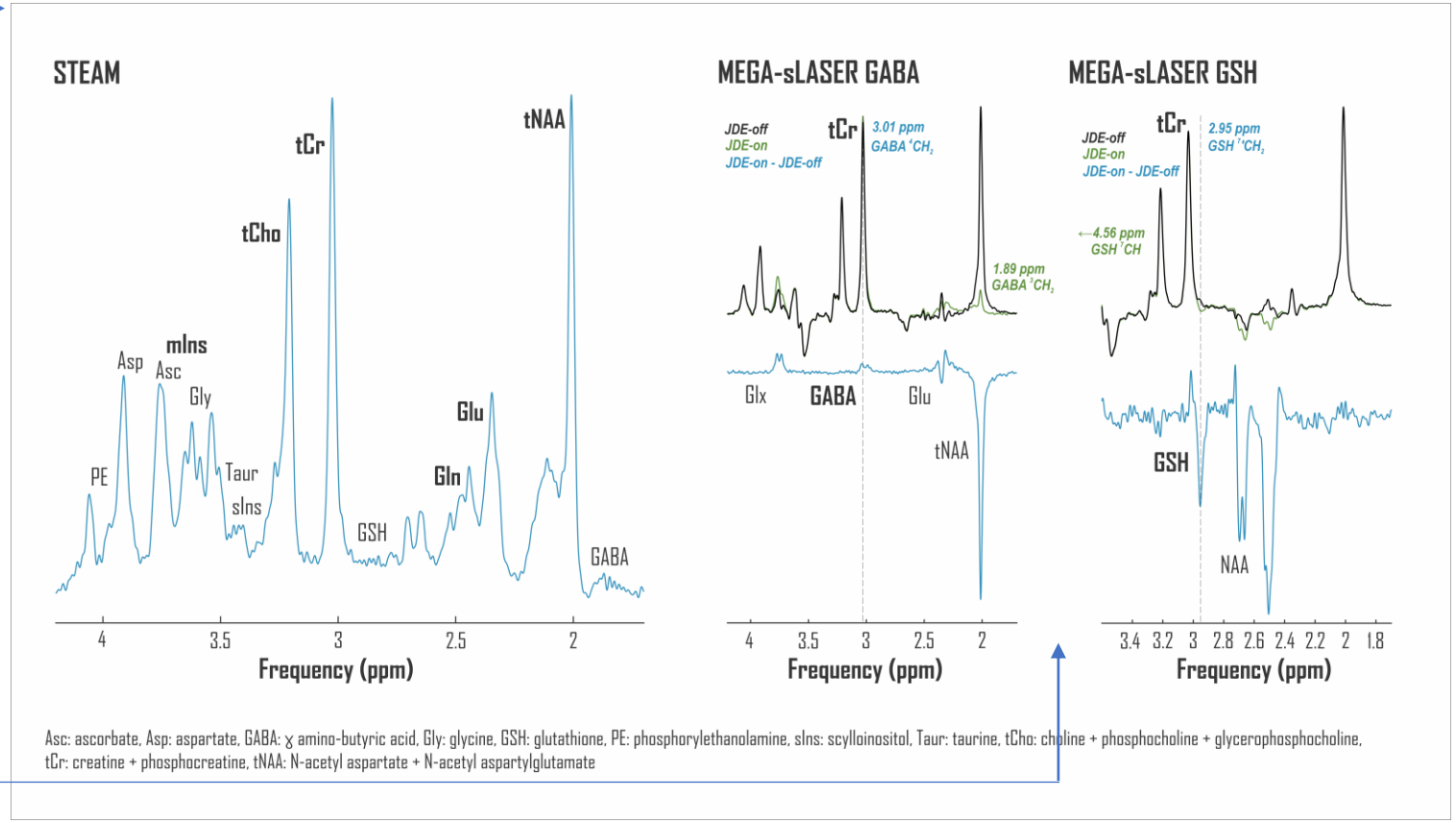


Asc: ascorbate, Asp: aspartate, GABA: γ amino-butyric acid, Gly: glycine, GSH: glutathione, PE: phosphorylethanolamine, sIns: scylloinositol, Taur: taurine, tCho: choline + phosphocholine + glycerophosphocholine, tCr: creatine + phosphocreatine, tNAA: N-acetyl aspartate + N-acetyl aspartylglutamate

**$^1$H MRS Acquisitions**

Swanberg, Prinsen, Averill C, Campos, Kurada, Krystal, Petrakis, Averill LA, Abdallah, and Juchem. Submitted to *Proc Intl Soc Mag Reson Med*. (2022).

# Optimizing $^1$H MRS: Generalization

*In collaboration with Leonardo Campos (B.Sc. '23)*

- Manually zero-order phase-corrected and frequency shift-calibrated
- JDE edit-off and –on aligned with cut, ZF, zero-order phase, frequency shift (x), offset (y)
- No ZF; 4096-pt spectra cut to 1024, 2048, or 4096 pts
- Cubic spline fit baseline
- Referenced to total creatine in $T_1$ , $T_2$ -uncorrected fashion

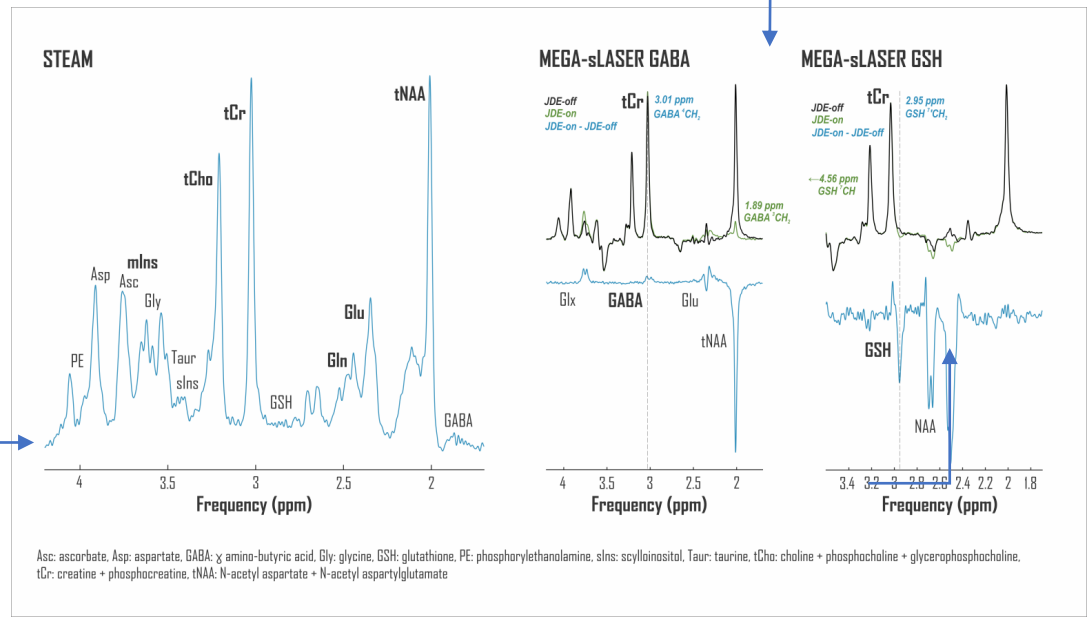


Asc: ascorbate, Asp: aspartate, GABA: γ amino-butyric acid, Gly: glycine, GSH: glutathione, PE: phosphorylethanolamine, sIns: scylloinositol, Taur: taurine, tCho: choline + phosphocholine + glycerophosphocholine, tCr: creatine + phosphocreatine, tNAA: N-acetyl aspartate + N-acetyl aspartylglutamate

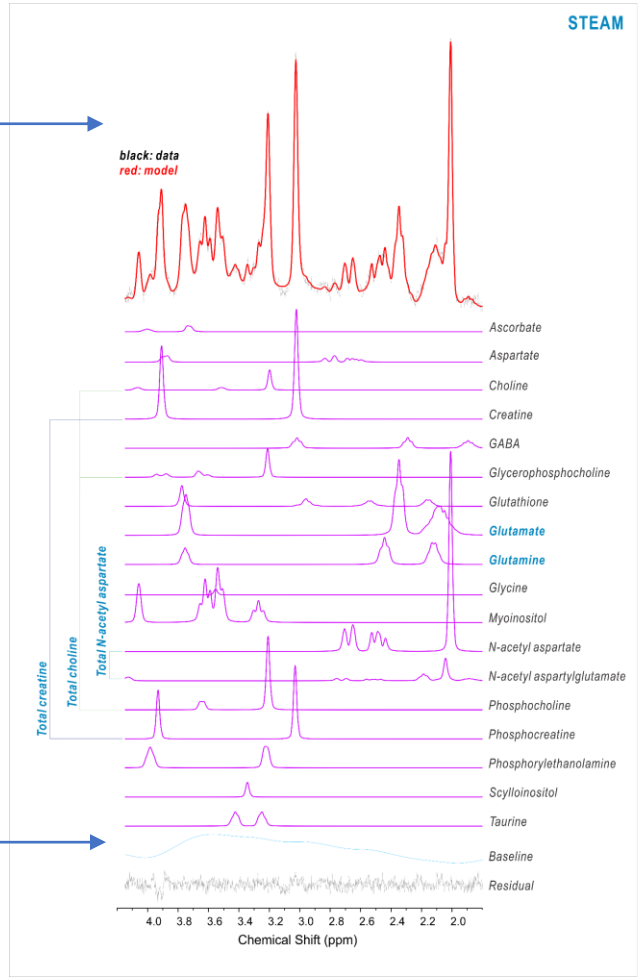


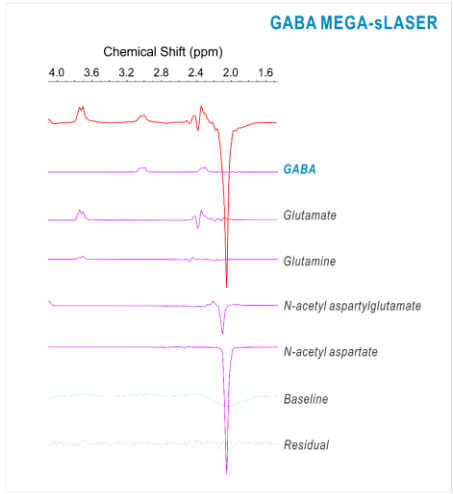


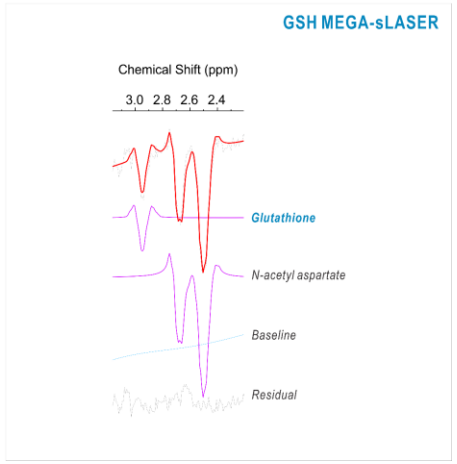


Swanberg, Prinsen, Averill C, Campos, Kurada, Krystal, Petrakis, Averill LA, Abdallah, and Juchem. Submitted to *Proc Intl Soc Mag Reson Med.* (2022).

# Optimizing $^1$H MRS: Generalization

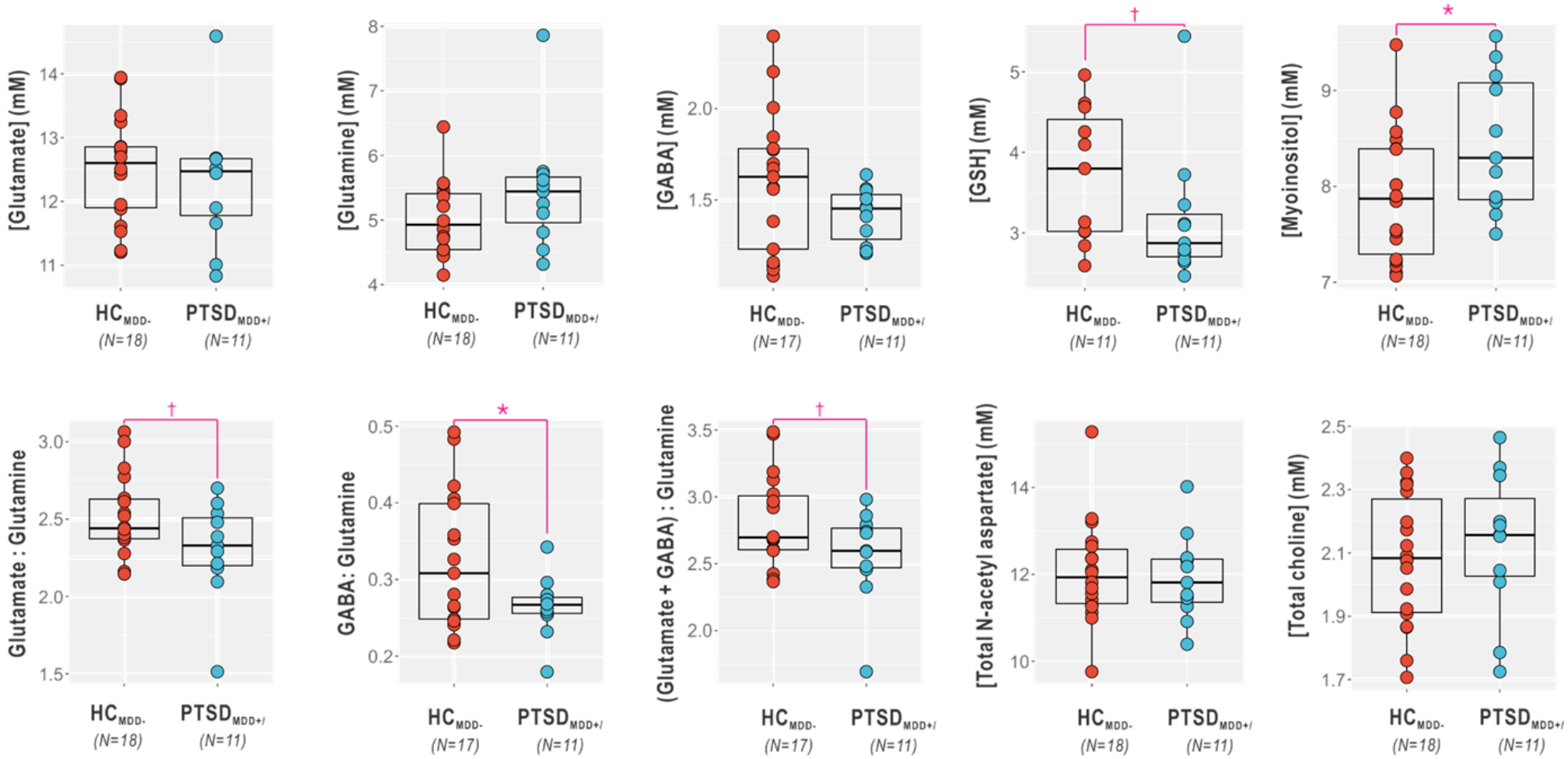


One-way ANOVA effect of fixed factor PTSD *$p$<0.05 †$p$<0.1

Swanberg, Prinsen, Averill C, Campos, Kurada, Krystal, Petrakis, Averill LA, Abdallah, and Juchem. Submitted to *Proc Intl Soc Mag Reson Med*. (2022).

# Optimizing $^1$H MRS: Generalization

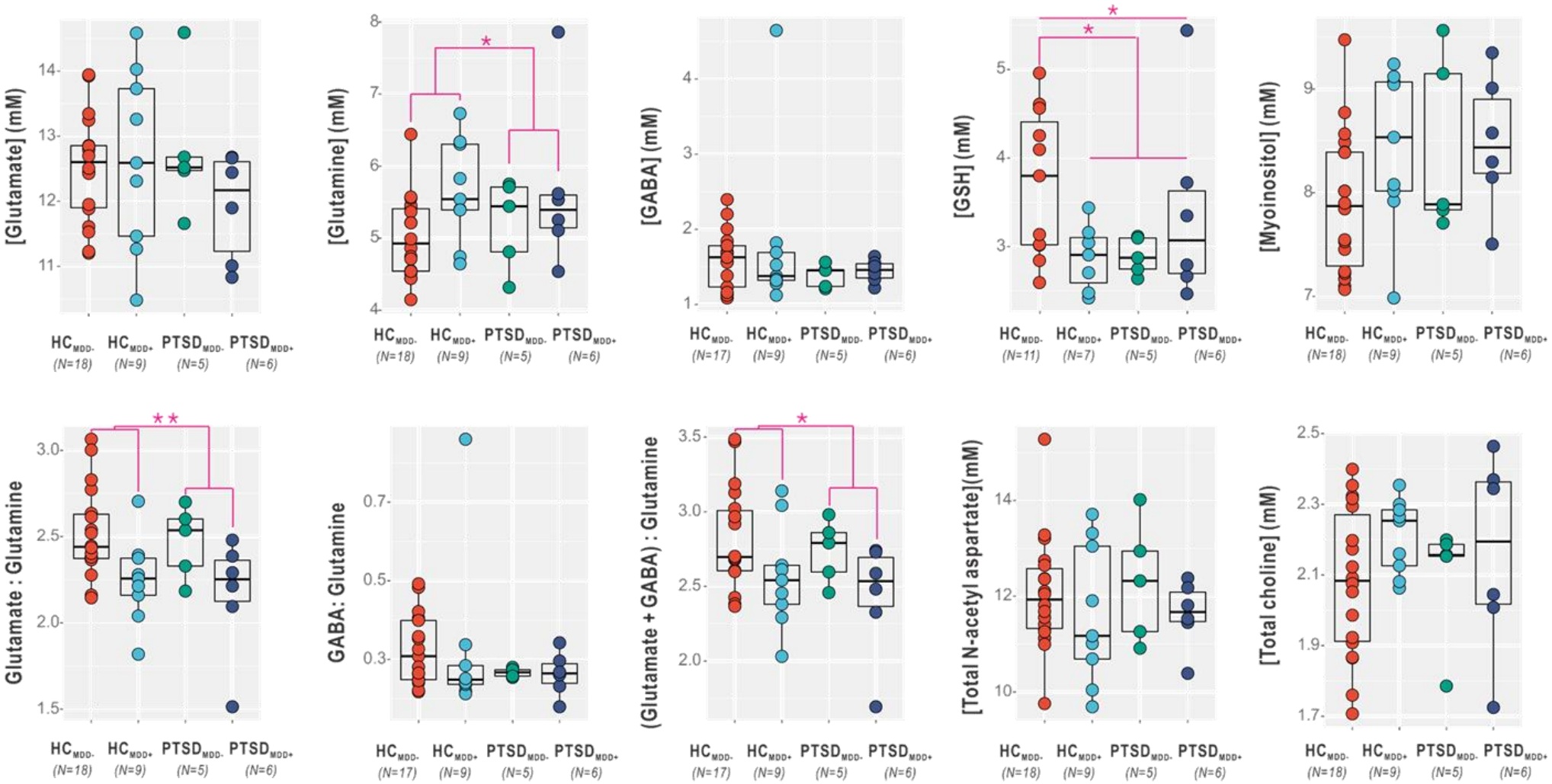


Two-way ANOVA effect of fixed factor MDD *$p$<0.05 **$p$<0.01, except GSH PTSD x MDD or W *$p$<0.05

Swanberg, Prinsen, Averill C, Campos, Kurada, Krystal, Petrakis, Averill LA, Abdallah, and Juchem. Submitted to *Proc Intl Soc Mag Reson Med*. (2022).

# Optimizing $^1$H MRS: Generalization

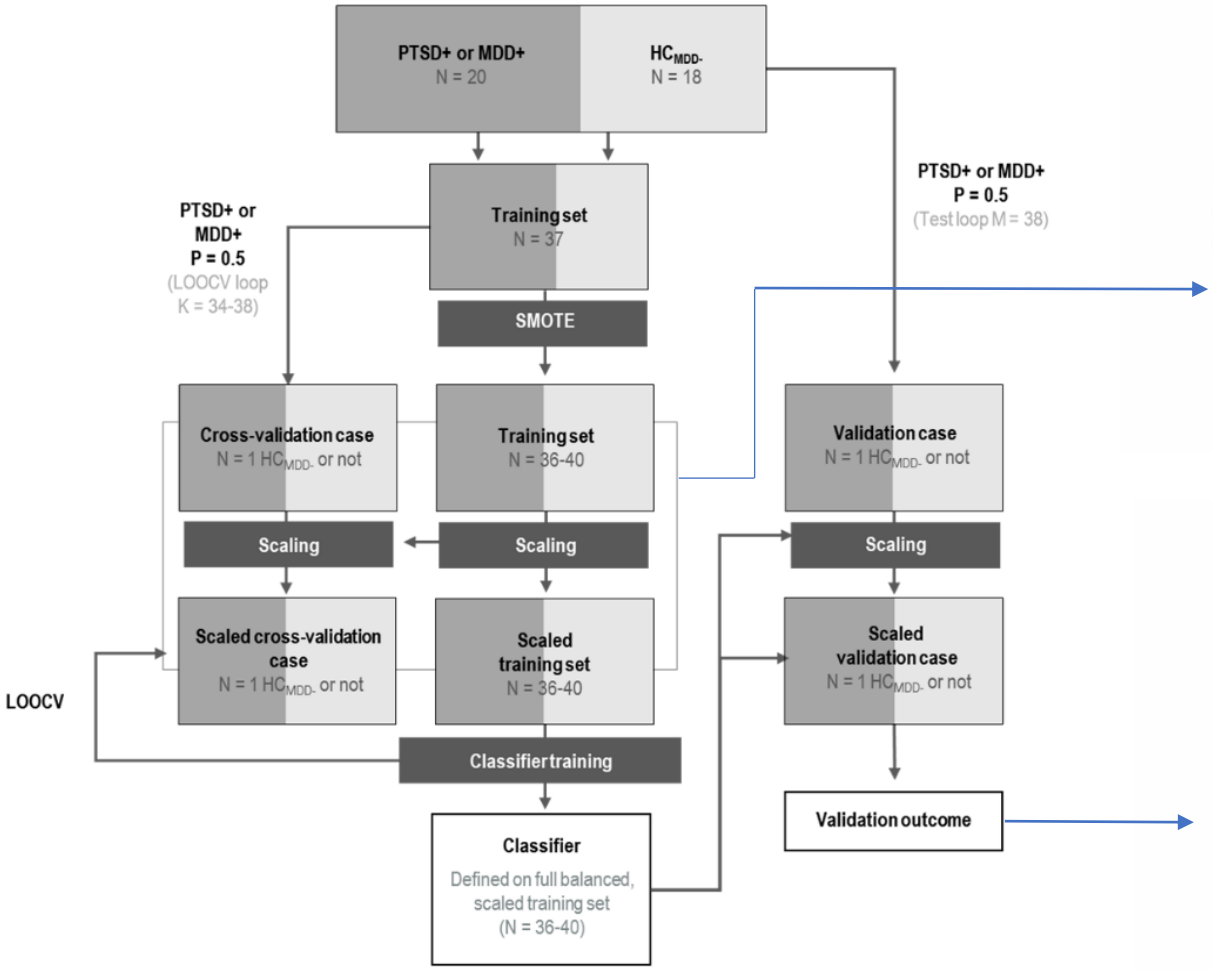


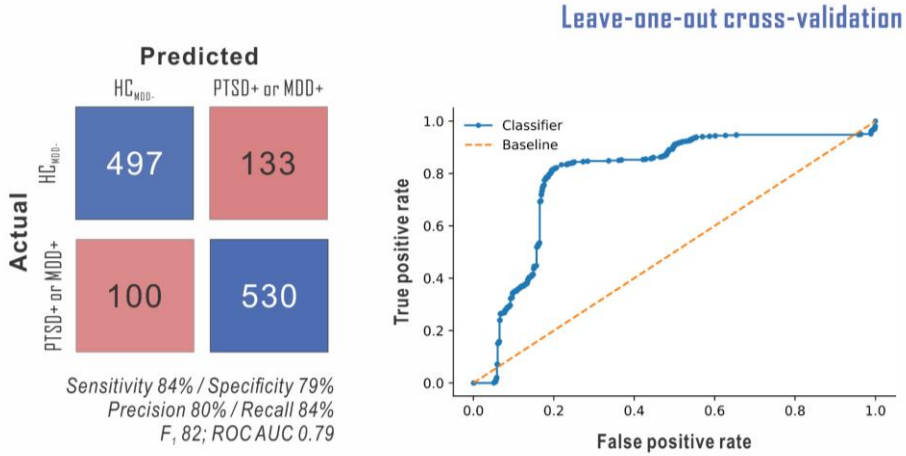


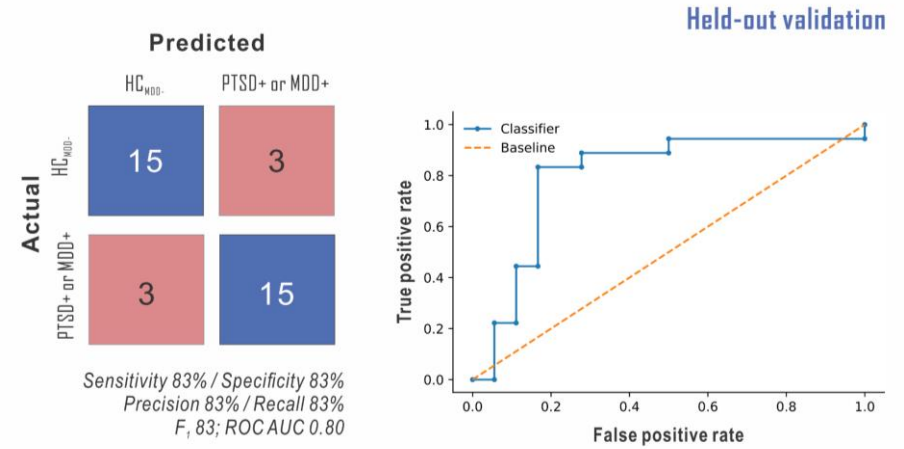


Swanberg, Prinsen, Averill C, Campos, Kurada, Krystal, Petrakis, Averill LA, Abdallah, and Juchem. Submitted to *Proc Intl Soc Mag Reson Med*. (2022).

## The Big Picture:

$^1$H MRS is a potential but currently untapped source of clinical diagnostic biomarkers.

Chapter I

## Spectral Quantification:

Data quality (FWHM and SNR) interacts with spectral baselines to affect metabolite fit accuracy.

Fit residual can be misleading when deciding whether a spectral baseline model supports accurate metabolite estimates.

Incorporating baseline terms to the Fisher information matrix improves utility of CRLB as a proxy for metabolite fit precision.

Chapter II

## Absolute Quantification:

Water $T_2$ was shown to differ between individuals with and without progressive multiple sclerosis, emphasizing the utility of group-specific corrections for this variable when employed in cross-sectional $^1$H MRS studies of disease.

Chapter III

## Statistical Analysis:

Metabolite concentrations derived from $^1$H MRS were a viable means of characterizing progressive multiple sclerosis disease status relative to either relapsing-remitting or control.

Chapter IV

## Generalization:

A quantification and statistics pipeline optimized for classification of multiple sclerosis via $^1$H MRS-derived metabolite concentrations can be generalized to comparably accurate identification of PTSD and MDD.

Chapter V

## Back to the Big Picture:

General conclusions and outlook

Chapter VI

# Conclusions and Outlook

- **$^1$H MRS processing pipelines** involve many opportunities for confound by **poorly defined or incorrect assumptions**.
- The relative effects of confounds like **spectral quality** and **spectral baseline model** on **metabolite concentration estimates** can be explicitly quantified using **simulated ground truth standards**. The **variance** of these effects can be indirectly estimated using **Cramer-Rao Lower Bound calculation considering baseline shapes**. These results can be used to inform decision-making about **how to process $^1$H MRS data** lacking a known ground truth.
- Conditions like **age** or **progressive multiple sclerosis** may influence water-referenced absolute metabolite estimates by **affecting signal relaxation via processes like $T_2$ decay**. These effects can be counteracted by **measured $T_2$** or **voxel composition** or **using another concentration reference**.
- Current understanding of both **MS** and **PTSD** implicates **multiple $^1$H-MR-visible metabolites**, but **no single metabolite finding in the brain** currently supports **sensitive** or **specific** identification of either condition.
- When processed and quantified according to **evidence from simulated validation of spectral quantification method** and **explicit measurement of reference $T_2$ behavior**, as well as **considered together by multivariate supervised classification model-building**, $^1$H-MRS metabolites measured in prefrontal cortex support **independent classification** of multiple **brain disorders** at **sensitivity and specificity near 80**%.
- Despite its limitations, **$^1$H MRS data** can still support identification of **clinically relevant biological phenotypes** and therefore potential utility as an auxiliary or mainstay of **clinical diagnostics** for **neurological** or **psychiatric disease**.

# Acknowledgements



Christoph Juchem, Ph.D.
Principal investigator

Sebastian Theilenberg, Ph.D.
Associate research scientist

Karl Landheer, Ph.D.
Postdoctoral alumnus

Martin Gajdošik, Ph.D.
Postdoctoral alumnus

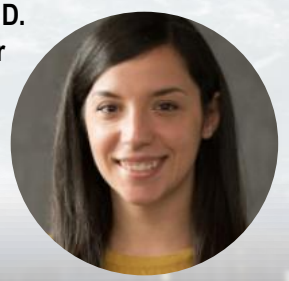

Carlotta Ianniello, Ph.D.
Postdoctoral research scientist

Yun Shang, M.Sc.
Ph.D. student, BME

Ronald Instrella, M.Sc.
Ph.D. student, BME

Kay Igwe, M.Sc.
Ph.D. student, BME

Abhinav Kurada, B.Sc.
Undergraduate alumnus, BME

Michael Treacy, B.A.
Undergraduate alumnus, physics

Leonardo Campos
Undergraduate, BME

Ian Dorian Macleod
Undergraduate, computer science

Catherine Medeiros
Undergraduate, BME

## In collaboration with:

Hetty Prinsen, Ph.D.
Yale School of Medicine

Lynette A. Averill, Ph.D.
Yale School of Medicine

Chris Averill, B.Sc.
Yale School of Medicine

Chadi Abdallah, M.D.
Yale School of Medicine

*A very special thank you to the 120+ human volunteers who dedicated their sometimes quite limited time and energy to participating in many of the studies presented today.*

Yale SCHOOL OF MEDICINE
Magnetic Resonance Research Center

COLUMBIA | Zuckerman Institute
MORTIMER B. ZUCKERMAN MIND BRAIN BEHAVIOR INSTITUTE

MS National Multiple Sclerosis Society
NMSS RG-5319

Yale Center for Clinical Investigation

COLUMBIA | ENGINEERING
The Fu Foundation School of Engineering and Applied Science